Observation of a new particle in the search for the Standard Model Higgs boson with the ATLAS detector at the LHC ☆

ATLAS Collaboration ★

This paper is dedicated to the memory of our ATLAS colleagues who did not live to see the full impact and significance of their contributions to the experiment.

ABSTRACT

A search for the Standard Model Higgs boson in proton–proton collisions with the ATLAS detector at the LHC is presented. The datasets used correspond to integrated luminosities of approximately 4.8 fb^{-1} collected at $\sqrt{s} = 7$ TeV in 2011 and 5.8 fb^{-1} at $\sqrt{s} = 8$ TeV in 2012. Individual searches in the channels $H \rightarrow ZZ^{(*)} \rightarrow 4\ell$, $H \rightarrow \gamma\gamma$ and $H \rightarrow WW^{(*)} \rightarrow e\nu\mu\nu$ in the 8 TeV data are combined with previously published results of searches for $H \rightarrow ZZ^{(*)}$, $WW^{(*)}$, $b\bar{b}$ and $\tau^{+}\tau^{-}$ in the 7 TeV data and results from improved analyses of the $H \rightarrow ZZ^{(*)} \rightarrow 4\ell$ and $H \rightarrow \gamma\gamma$ channels in the 7 TeV data. Clear evidence for the production of a neutral boson with a measured mass of 126.0 ± 0.4 (stat) ± 0.4 (sys) GeV is presented. This observation, which has a significance of 5.9 standard deviations, corresponding to a background fluctuation probability of 1.7×10^{-9}, is compatible with the production and decay of the Standard Model Higgs boson.

© 2012 CERN. Published by Elsevier B.V. All rights reserved.

1. Introduction

The Standard Model (SM) of particle physics [1–4] has been tested by many experiments over the last four decades and has been shown to successfully describe high energy particle interactions. However, the mechanism that breaks electroweak symmetry in the SM has not been verified experimentally. This mechanism [5–10], which gives mass to massive elementary particles, implies the existence of a scalar particle, the SM Higgs boson. The search for the Higgs boson, the only elementary particle in the SM that has not yet been observed, is one of the highlights of the Large Hadron Collider [11] (LHC) physics programme.

Indirect limits on the SM Higgs boson mass of $m_H < 158$ GeV at 95% confidence level (CL) have been set using global fits to precision electroweak results [12]. Direct searches at LEP [13], the Tevatron [14–16] and the LHC [17,18] have previously excluded, at 95% CL, a SM Higgs boson with mass below 600 GeV, apart from some mass regions between 116 GeV and 127 GeV.

Both the ATLAS and CMS Collaborations reported excesses of events in their 2011 datasets of proton–proton (pp) collisions at centre-of-mass energy $\sqrt{s} = 7$ TeV at the LHC, which were compatible with SM Higgs boson production and decay in the mass region 124–126 GeV, with significances of 2.9 and 3.1 standard deviations (σ), respectively [17,18]. The CDF and DØ experiments at the Tevatron have also recently reported a broad excess in the mass region

120–135 GeV; using the existing LHC constraints, the observed local significances for $m_H = 125$ GeV are 2.7σ for CDF [14], 1.1σ for DØ [15] and 2.8σ for their combination [16].

The previous ATLAS searches in 4.6–4.8 fb^{-1} of data at $\sqrt{s} = 7$ TeV are combined here with new searches for $H \rightarrow ZZ^{(*)} \rightarrow 4\ell$,[1] $H \rightarrow \gamma\gamma$ and $H \rightarrow WW^{(*)} \rightarrow e\nu\mu\nu$ in the 5.8–5.9 fb^{-1} of pp collision data taken at $\sqrt{s} = 8$ TeV between April and June 2012.

The data were recorded with instantaneous luminosities up to 6.8×10^{33} cm^{-2} s^{-1}; they are therefore affected by multiple pp collisions occurring in the same or neighbouring bunch crossings (pile-up). In the 7 TeV data, the average number of interactions per bunch crossing was approximately 10; the average increased to approximately 20 in the 8 TeV data. The reconstruction, identification and isolation criteria used for electrons and photons in the 8 TeV data are improved, making the $H \rightarrow ZZ^{(*)} \rightarrow 4\ell$ and $H \rightarrow \gamma\gamma$ searches more robust against the increased pile-up. These analyses were re-optimised with simulation and frozen before looking at the 8 TeV data.

In the $H \rightarrow WW^{(*)} \rightarrow \ell\nu\ell\nu$ channel, the increased pile-up deteriorates the event missing transverse momentum, E_T^{miss}, resolution, which results in significantly larger Drell–Yan background in the same-flavour final states. Since the $e\mu$ channel provides most of the sensitivity of the search, only this final state is used in the analysis of the 8 TeV data. The kinematic region in which a SM Higgs boson with a mass between 110 GeV and 140 GeV is

---

[1] The symbol ℓ stands for electron or muon.

searched for was kept blinded during the analysis optimisation, until satisfactory agreement was found between the observed and predicted numbers of events in control samples dominated by the principal backgrounds.

This Letter is organised as follows. The ATLAS detector is briefly described in Section 2. The simulation samples and the signal predictions are presented in Section 3. The analyses of the $H \rightarrow ZZ^{(*)} \rightarrow 4\ell$, $H \rightarrow \gamma\gamma$ and $H \rightarrow WW^{(*)} \rightarrow e\nu\mu\nu$ channels are described in Sections 4–6, respectively. The statistical procedure used to analyse the results is summarised in Section 7. The systematic uncertainties which are correlated between datasets and search channels are described in Section 8. The results of the combination of all channels are reported in Section 9, while Section 10 provides the conclusions.

2. The ATLAS detector

The ATLAS detector [19–21] is a multipurpose particle physics apparatus with forward-backward symmetric cylindrical geometry. The inner tracking detector (ID) consists of a silicon pixel detector, a silicon microstrip detector (SCT), and a straw-tube transition radiation tracker (TRT). The ID is surrounded by a thin superconducting solenoid which provides a 2 T magnetic field, and by high-granularity liquid-argon (LAr) sampling electromagnetic calorimetry. The electromagnetic calorimeter is divided into a central barrel (pseudorapidity[2] $|\eta| < 1.475$) and end-cap regions on either end of the detector ($1.375 < |\eta| < 2.5$ for the outer wheel and $2.5 < |\eta| < 3.2$ for the inner wheel). In the region matched to the ID ($|\eta| < 2.5$), it is radially segmented into three layers. The first layer has a fine segmentation in η to facilitate e/γ separation from π^0 and to improve the resolution of the shower position and direction measurements. In the region $|\eta| < 1.8$, the electromagnetic calorimeter is preceded by a presampler detector to correct for upstream energy losses. An iron-scintillator/tile calorimeter gives hadronic coverage in the central rapidity range ($|\eta| < 1.7$), while a LAr hadronic end-cap calorimeter provides coverage over $1.5 < |\eta| < 3.2$. The forward regions ($3.2 < |\eta| < 4.9$) are instrumented with LAr calorimeters for both electromagnetic and hadronic measurements. The muon spectrometer (MS) surrounds the calorimeters and consists of three large air-core superconducting magnets providing a toroidal field, each with eight coils, a system of precision tracking chambers, and fast detectors for triggering. The combination of all these systems provides charged particle measurements together with efficient and precise lepton and photon measurements in the pseudorapidity range $|\eta| < 2.5$. Jets and E_T^{miss} are reconstructed using energy deposits over the full coverage of the calorimeters, $|\eta| < 4.9$.

3. Signal and background simulation samples

The SM Higgs boson production processes considered in this analysis are the dominant gluon fusion ($gg \rightarrow H$, denoted ggF), vector-boson fusion ($qq' \rightarrow qq'H$, denoted VBF) and Higgs-strahlung ($qq' \rightarrow WH, ZH$, denoted WH/ZH). The small contribution from the associated production with a $t\bar{t}$ pair ($q\bar{q}/gg \rightarrow t\bar{t}H$, denoted $t\bar{t}H$) is taken into account only in the $H \rightarrow \gamma\gamma$ analysis.

For the ggF process, the signal cross section is computed at up to next-to-next-to-leading order (NNLO) in QCD [22–28]. Next-to-

Table 1

Event generators used to model the signal and background processes. "PYTHIA" indicates that PYTHIA6 and PYTHIA8 are used for simulations of $\sqrt{s} = 7$ TeV and $\sqrt{s} = 8$ TeV data, respectively.

Process	Generator
ggF, VBF	POWHEG [57,58] + PYTHIA
WH, ZH, $t\bar{t}H$	PYTHIA
W + jets, Z/γ^* + jets	ALPGEN [59] + HERWIG
$t\bar{t}$, tW, tb	MC@NLO [60] + HERWIG
tqb	AcerMC [61] + PYTHIA
$q\bar{q} \rightarrow WW$	MC@NLO + HERWIG
$gg \rightarrow WW$	gg2WW [62] + HERWIG
$q\bar{q} \rightarrow ZZ$	POWHEG [63] + PYTHIA
$gg \rightarrow ZZ$	gg2ZZ [64] + HERWIG
WZ	MadGraph + PYTHIA, HERWIG
$W\gamma$ + jets	ALPGEN + HERWIG
$W\gamma^*$ [65]	MadGraph + PYTHIA
$q\bar{q}/gg \rightarrow \gamma\gamma$	SHERPA

leading order (NLO) electroweak (EW) corrections are applied [29, 30], as well as QCD soft-gluon re-summations at up to next-to-next-to-leading logarithm (NNLL) [31]. These calculations, which are described in Refs. [32–35], assume factorisation between QCD and EW corrections. The transverse momentum, p_T, spectrum of the Higgs boson in the ggF process follows the HqT calculation [36], which includes QCD corrections at NLO and QCD soft-gluon re-summations up to NNLL; the effects of finite quark masses are also taken into account [37].

For the VBF process, full QCD and EW corrections up to NLO [38–41] and approximate NNLO QCD corrections [42] are used to calculate the cross section. Cross sections of the associated WH/ZH processes (VH) are calculated including QCD corrections up to NNLO [43–45] and EW corrections up to NLO [46]. The cross sections for the $t\bar{t}H$ process are estimated up to NLO QCD [47–51].

The total cross sections for SM Higgs boson production at the LHC with $m_H = 125$ GeV are predicted to be 17.5 pb for $\sqrt{s} = 7$ TeV and 22.3 pb for $\sqrt{s} = 8$ TeV [52,53].

The branching ratios of the SM Higgs boson as a function of m_H, as well as their uncertainties, are calculated using the HDECAY [54] and PROPHECY4F [55,56] programs and are taken from Refs. [52,53]. The interference in the $H \rightarrow ZZ^{(*)} \rightarrow 4\ell$ final states with identical leptons is taken into account [55,56,53].

The event generators used to model signal and background processes in samples of Monte Carlo (MC) simulated events are listed in Table 1. The normalisations of the generated samples are obtained from the state of the art calculations described above. Several different programs are used to generate the hard-scattering processes. To generate parton showers and their hadronisation, and to simulate the underlying event [66–68], PYTHIA6 [69] (for 7 TeV samples and 8 TeV samples produced with MadGraph [70,71] or AcerMC) or PYTHIA8 [72] (for other 8 TeV samples) are used. Alternatively, HERWIG [73] or SHERPA [74] are used to generate and hadronise parton showers, with the HERWIG underlying event simulation performed using JIMMY [75]. When PYTHIA6 or HERWIG are used, TAUOLA [76] and PHOTOS [77] are employed to describe tau lepton decays and additional photon radiation from charged leptons, respectively.

The following parton distribution function (PDF) sets are used: CT10 [78] for the POWHEG, MC@NLO, gg2WW and gg2ZZ samples; CTEQ6L1 [79] for the PYTHIA8, ALPGEN, AcerMC, MadGraph, HERWIG and SHERPA samples; and MRSTMCal [80] for the PYTHIA6 samples.

Acceptances and efficiencies are obtained mostly from full simulations of the ATLAS detector [81] using GEANT4 [82]. These simulations include a realistic modelling of the pile-up conditions observed in the data. Corrections obtained from measurements in

---

[2] ATLAS uses a right-handed coordinate system with its origin at the nominal interaction point (IP) in the centre of the detector, and the z-axis along the beam line. The x-axis points from the IP to the centre of the LHC ring, and the y-axis points upwards. Cylindrical coordinates (r, ϕ) are used in the transverse plane, ϕ being the azimuthal angle around the beam line. Observables labelled "transverse" are projected into the x–y plane. The pseudorapidity is defined in terms of the polar angle θ as $\eta = -\ln\tan(\theta/2)$.

data are applied to account for small differences between data and simulation (e.g. large samples of W, Z and J/ψ decays are used to derive scale factors for lepton reconstruction and identification efficiencies).

4. $H \to ZZ^{(*)} \to 4\ell$ channel

The search for the SM Higgs boson through the decay $H \to ZZ^{(*)} \to 4\ell$, where $\ell = e$ or μ, provides good sensitivity over a wide mass range (110–600 GeV), largely due to the excellent momentum resolution of the ATLAS detector. This analysis searches for Higgs boson candidates by selecting two pairs of isolated leptons, each of which is comprised of two leptons with the same flavour and opposite charge. The expected cross section times branching ratio for the process $H \to ZZ^{(*)} \to 4\ell$ with $m_H = 125$ GeV is 2.2 fb for $\sqrt{s} = 7$ TeV and 2.8 fb for $\sqrt{s} = 8$ TeV.

The largest background comes from continuum $(Z^{(*)}/\gamma^*)(Z^{(*)}/\gamma^*)$ production, referred to hereafter as $ZZ^{(*)}$. For low masses there are also important background contributions from $Z + $ jets and $t\bar{t}$ production, where charged lepton candidates arise either from decays of hadrons with b- or c-quark content or from misidentification of jets.

The 7 TeV data have been re-analysed and combined with the 8 TeV data. The analysis is improved in several aspects with respect to Ref. [83] to enhance the sensitivity to a low-mass Higgs boson. In particular, the kinematic selections are revised, and the 8 TeV data analysis benefits from improvements in the electron reconstruction and identification. The expected signal significances for a Higgs boson with $m_H = 125$ GeV are 1.6σ for the 7 TeV data (to be compared with 1.25σ in Ref. [83]) and 2.1σ for the 8 TeV data.

4.1. Event selection

The data are selected using single-lepton or dilepton triggers. For the single-muon trigger, the p_T threshold is 18 GeV for the 7 TeV data and 24 GeV for the 8 TeV data, while for the single-electron trigger the transverse energy, E_T, threshold varies from 20 GeV to 22 GeV for the 7 TeV data and is 24 GeV for the 8 TeV data. For the dielectron triggers, the thresholds are 12 GeV for both electrons. For the dimuon triggers, the thresholds for the 7 TeV data are 10 GeV for each muon, while for the 8 TeV data the thresholds are 13 GeV. An additional asymmetric dimuon trigger is used in the 8 TeV data with thresholds 18 GeV and 8 GeV for the leading and sub-leading muon, respectively.

Muon candidates are formed by matching reconstructed ID tracks with either a complete track or a track-segment reconstructed in the MS [84]. The muon acceptance is extended with respect to Ref. [83] using tracks reconstructed in the forward region of the MS ($2.5 < |\eta| < 2.7$), which is outside the ID coverage. If both an ID and a complete MS track are present, the two independent momentum measurements are combined; otherwise the information of the ID or the MS is used alone. Electron candidates must have a well-reconstructed ID track pointing to an electromagnetic calorimeter cluster and the cluster should satisfy a set of identification criteria [85] that require the longitudinal and transverse shower profiles to be consistent with those expected for electromagnetic showers. Tracks associated with electromagnetic clusters are fitted using a Gaussian-Sum Filter [86], which allows for bremsstrahlung energy losses to be taken into account.

Each electron (muon) must satisfy $p_T > 7$ GeV ($p_T > 6$ GeV) and be measured in the pseudorapidity range $|\eta| < 2.47$ ($|\eta| < 2.7$). All possible quadruplet combinations with same-flavour opposite-charge lepton pairs are then formed. The most energetic lepton in the quadruplet must satisfy $p_T > 20$ GeV, and the second (third

lepton in p_T order must satisfy $p_T > 15$ GeV ($p_T > 10$ GeV). At least one of the leptons must satisfy the single-lepton trigger or one pair must satisfy the dilepton trigger requirements. The leptons are required to be separated from each other by $\Delta R = \sqrt{(\Delta\eta)^2 + (\Delta\phi)^2} > 0.1$ if they are of the same flavour and by $\Delta R > 0.2$ otherwise. The longitudinal impact parameters of the leptons along the beam axis are required to be within 10 mm of the reconstructed primary vertex. The primary vertex used for the event is defined as the reconstructed vertex with the highest $\sum p_T^2$ of associated tracks and is required to have at least three tracks with $p_T > 0.4$ GeV. To reject cosmic rays, muon tracks are required to have a transverse impact parameter, defined as the distance of closest approach to the primary vertex in the transverse plane, of less than 1 mm.

The same-flavour and opposite-charge lepton pair with an invariant mass closest to the Z boson mass (m_Z) in the quadruplet is referred to as the leading lepton pair. Its invariant mass, denoted by m_{12}, is required to be between 50 GeV and 106 GeV. The remaining same-flavour, opposite-charge lepton pair is the sub-leading lepton pair. Its invariant mass, m_{34}, is required to be in the range $m_{min} < m_{34} < 115$ GeV, where the value of m_{min} depends on the reconstructed four-lepton invariant mass, $m_{4\ell}$. The value of m_{min} varies monotonically from 17.5 GeV at $m_{4\ell} = 120$ GeV to 50 GeV at $m_{4\ell} = 190$ GeV [87] and is constant above this value. All possible lepton pairs in the quadruplet that have the same flavour and opposite charge must satisfy $m_{\ell\ell} > 5$ GeV in order to reject backgrounds involving the production and decay of J/ψ mesons. If two or more quadruplets satisfy the above selection, the one with the highest value of m_{34} is selected. Four different analysis sub-channels, $4e$, $2e2\mu$, $2\mu2e$ and 4μ, arranged by the flavour of the leading lepton pair, are defined.

Non-prompt leptons from heavy flavour decays, electrons from photon conversions and jets mis-identified as electrons have broader transverse impact parameter distributions than prompt leptons from Z boson decays and/or are non-isolated. Thus, the $Z + $ jets and $t\bar{t}$ background contributions are reduced by applying a cut on the transverse impact parameter significance, defined as the transverse impact parameter divided by its uncertainty, d_0/σ_{d_0}. This is required to be less than 3.5 (6.5) for muons (electrons). The electron impact parameter is affected by bremsstrahlung and thus has a broader distribution.

In addition, leptons must satisfy isolation requirements based on tracking and calorimetric information. The normalised track isolation discriminant is defined as the sum of the transverse momenta of tracks inside a cone of size $\Delta R = 0.2$ around the lepton direction, excluding the lepton track, divided by the lepton p_T. The tracks considered in the sum are those compatible with the lepton vertex and have $p_T > 0.4$ GeV ($p_T > 1$ GeV) in the case of electron (muon) candidates. Each lepton is required to have a normalised track isolation smaller than 0.15. The normalised calorimetric isolation for electrons is computed as the sum of the E_T of positive-energy topological clusters [88] with a reconstructed barycentre falling within a cone of size $\Delta R = 0.2$ around the candidate electron cluster, divided by the electron E_T. The algorithm for topological clustering suppresses noise by keeping cells with a significant energy deposit and their neighbours. The summed energy of the cells assigned to the electron cluster is excluded, while a correction is applied to account for the electron energy deposited outside the cluster. The ambient energy deposition in the event from pile-up and the underlying event is accounted for using a calculation of the median transverse energy density from low-p_T jets [89,90]. The normalised calorimetric isolation for electrons is required to be less than 0.20. The normalised calorimetric isolation discriminant for muons is defined by the ratio to the p_T of the muon of the E_T sum of the calorimeter cells inside a cone of size

$\Delta R = 0.2$ around the muon direction minus the energy deposited by the muon. Muons are required to have a normalised calorimetric isolation less than 0.30 (0.15 for muons without an associated ID track). For both the track- and calorimeter-based isolation, any contributions arising from other leptons of the quadruplet are subtracted.

The combined signal reconstruction and selection efficiencies for a SM Higgs with $m_H = 125$ GeV for the 7 TeV (8 TeV) data are 37% (36%) for the 4μ channel, 20% (22%) for the $2e2\mu/2\mu2e$ channels and 15% (20%) for the $4e$ channel.

The 4ℓ invariant mass resolution is improved by applying a Z-mass constrained kinematic fit to the leading lepton pair for $m_{4\ell} < 190$ GeV and to both lepton pairs for higher masses. The expected width of the reconstructed mass distribution is dominated by the experimental resolution for $m_H < 350$ GeV, and by the natural width of the Higgs boson for higher masses (30 GeV at $m_H = 400$ GeV). The typical mass resolutions for $m_H = 125$ GeV are 1.7 GeV, 1.7 GeV/2.2 GeV and 2.3 GeV for the 4μ, $2e2\mu/2\mu2e$ and $4e$ sub-channels, respectively.

4.2. Background estimation

The expected background yield and composition are estimated using the MC simulation normalised to the theoretical cross section for $ZZ^{(*)}$ production and by methods using control regions from data for the Z + jets and $t\bar{t}$ processes. Since the background composition depends on the flavour of the sub-leading lepton pair, different approaches are taken for the $\ell\ell + \mu\mu$ and the $\ell\ell + ee$ final states. The transfer factors needed to extrapolate the background yields from the control regions defined below to the signal region are obtained from the MC simulation. The MC description of the selection efficiencies for the different background components has been verified with data.

The reducible $\ell\ell + \mu\mu$ background is dominated by $t\bar{t}$ and Z + jets (mostly $Zb\bar{b}$) events. A control region is defined by removing the isolation requirement on the leptons in the sub-leading pair, and by requiring that at least one of the sub-leading muons fails the transverse impact parameter significance selection. These modifications remove $ZZ^{(*)}$ contributions, and allow both the $t\bar{t}$ and Z + jets backgrounds to be estimated simultaneously using a fit to the m_{12} distribution. The $t\bar{t}$ background contribution is cross-checked by selecting a control sample of events with an opposite charge $e\mu$ pair with an invariant mass between 50 GeV and 106 GeV, accompanied by an opposite-charge muon pair. Events with a Z candidate decaying to a pair of electrons or muons in the aforementioned mass range are excluded. Isolation and transverse impact parameter significance requirements are applied only to the leptons of the $e\mu$ pair.

In order to estimate the reducible $\ell\ell + ee$ background, a control region is formed by relaxing the selection criteria for the electrons of the sub-leading pair. The different sources of electron background are then separated into categories consisting of non-prompt leptons from heavy flavour decays, electrons from photon conversions and jets mis-identified as electrons, using appropriate discriminating variables [91]. This method allows the sum of the Z + jets and $t\bar{t}$ background contributions to be estimated. As a cross-check, the same method is also applied to a similar control region containing same-charge sub-leading electron pairs. An additional cross-check of the $\ell\ell + ee$ background estimation is performed by using a control region with same-charge sub-leading electron pairs, where the three highest p_T leptons satisfy all the analysis criteria whereas the selection cuts are relaxed for the remaining electrons. All the cross-checks yield consistent results.

The data-driven background estimates are summarised in Table 2. The distribution of m_{34}, for events selected by the analysis

Table 2

Summary of the estimated numbers of Z + jets and $t\bar{t}$ background events, for the $\sqrt{s} = 7$ TeV and $\sqrt{s} = 8$ TeV data in the entire phase-space of the analysis after the kinematic selections described in the text. The backgrounds are combined for the $2\mu2e$ and $4e$ channels, as discussed in the text. The first uncertainty is statistical, while the second is systematic.

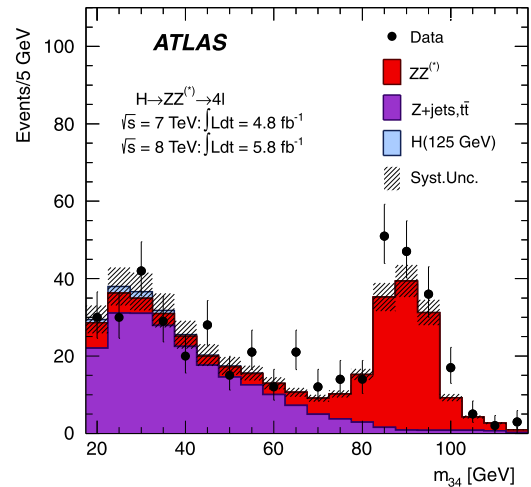| Background	Estimated numbers of events	
	$\sqrt{s} = 7$ TeV	$\sqrt{s} = 8$ TeV
4μ		
Z + jets	$0.3 \pm 0.1 \pm 0.1$	$0.5 \pm 0.1 \pm 0.2$
$t\bar{t}$	$0.02 \pm 0.02 \pm 0.01$	$0.04 \pm 0.02 \pm 0.02$
$2e2\mu$		
Z + jets	$0.2 \pm 0.1 \pm 0.1$	$0.4 \pm 0.1 \pm 0.1$
$t\bar{t}$	$0.02 \pm 0.01 \pm 0.01$	$0.04 \pm 0.01 \pm 0.01$
$2\mu2e$		
Z + jets, $t\bar{t}$	$2.6 \pm 0.4 \pm 0.4$	$4.9 \pm 0.8 \pm 0.7$
$4e$		
Z + jets, $t\bar{t}$	$3.1 \pm 0.6 \pm 0.5$	$3.9 \pm 0.7 \pm 0.8$

Fig. 1. Invariant mass distribution of the sub-leading lepton pair (m_{34}) for a sample defined by the presence of a Z boson candidate and an additional same-flavour electron or muon pair, for the combination of $\sqrt{s} = 7$ TeV and $\sqrt{s} = 8$ TeV data in the entire phase-space of the analysis after the kinematic selections described in the text. Isolation and transverse impact parameter significance requirements are applied to the leading lepton pair only. The MC is normalised to the data-driven background estimations. The relatively small contribution of a SM Higgs with $m_H = 125$ GeV in this sample is also shown.

except that the isolation and transverse impact parameter requirements for the sub-leading lepton pair are removed, is presented in Fig. 1.

4.3. Systematic uncertainties

The uncertainties on the integrated luminosities are determined to be 1.8% for the 7 TeV data and 3.6% for the 8 TeV data using the techniques described in Ref. [92].

The uncertainties on the lepton reconstruction and identification efficiencies and on the momentum scale and resolution are determined using samples of W, Z and J/ψ decays [85, 84]. The relative uncertainty on the signal acceptance due to the uncertainty on the muon reconstruction and identification efficiency is $\pm0.7\%$ ($\pm0.5\%/\pm0.5\%$) for the 4μ ($2e2\mu/2\mu2e$) channel for $m_{4\ell} = 600$ GeV and increases to $\pm0.9\%$ ($\pm0.8\%/\pm0.5\%$) for $m_{4\ell} = 115$ GeV. Similarly, the relative uncertainty on the signal acceptance due to the uncertainty on the electron reconstruction and identification efficiency is $\pm2.6\%$ ($\pm1.7\%/\pm1.8\%$) for the $4e$ ($2e2\mu/2\mu2e$) channel for $m_{4\ell} = 600$ GeV and reaches $\pm8.0\%$
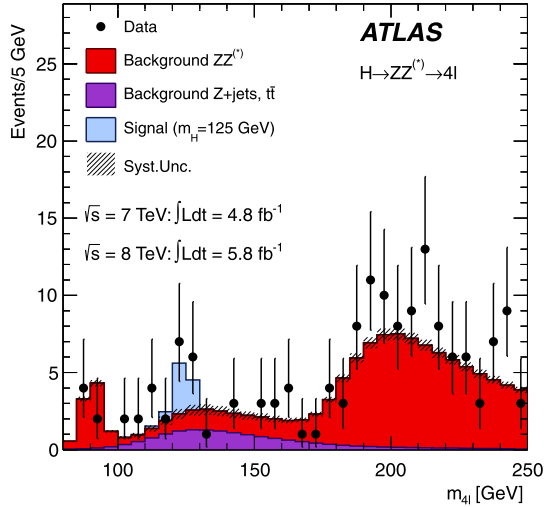
Fig. 2. The distribution of the four-lepton invariant mass, $m_{4\ell}$, for the selected candidates, compared to the background expectation in the 80–250 GeV mass range, for the combination of the $\sqrt{s} = 7$ TeV and $\sqrt{s} = 8$ TeV data. The signal expectation for a SM Higgs with $m_H = 125$ GeV is also shown.

Table 3
The numbers of expected signal ($m_H = 125$ GeV) and background events, together with the numbers of observed events in the data, in a window of size ± 5 GeV around 125 GeV, for the combined $\sqrt{s} = 7$ TeV and $\sqrt{s} = 8$ TeV data.

	Signal	$ZZ^{(*)}$	$Z + $ jets, $t\bar{t}$	Observed
4μ	2.09 ± 0.30	1.12 ± 0.05	0.13 ± 0.04	6
$2e2\mu/2\mu2e$	2.29 ± 0.33	0.80 ± 0.05	1.27 ± 0.19	5
$4e$	0.90 ± 0.14	0.44 ± 0.04	1.09 ± 0.20	2

($\pm 2.3\%/\pm 7.6\%$) for $m_{4\ell} = 115$ GeV. The uncertainty on the electron energy scale results in an uncertainty of $\pm 0.7\%$ ($\pm 0.5\%/\pm 0.2\%$) on the mass scale of the $m_{4\ell}$ distribution for the $4e$ ($2e2\mu/2\mu2e$) channel. The impact of the uncertainties on the electron energy resolution and on the muon momentum resolution and scale are found to be negligible.

The theoretical uncertainties associated with the signal are described in detail in Section 8. For the SM $ZZ^{(*)}$ background, which is estimated from MC simulation, the uncertainty on the total yield due to the QCD scale uncertainty is $\pm 5\%$, while the effect of the PDF and α_s uncertainties is $\pm 4\%$ ($\pm 8\%$) for processes initiated by quarks (gluons) [53]. In addition, the dependence of these uncertainties on the four-lepton invariant mass spectrum has been taken into account as discussed in Ref. [53]. Though a small excess of events is observed for $m_{4l} > 160$ GeV, the measured $ZZ^{(*)} \to 4\ell$ cross section [93] is consistent with the SM theoretical prediction. The impact of not using the theoretical constraints on the $ZZ^{(*)}$ yield on the search for a Higgs boson with $m_H < 2m_Z$ has been studied in Ref. [87] and has been found to be negligible. The impact of the interference between a Higgs signal and the non-resonant $gg \to ZZ^{(*)}$ background is small and becomes negligible for $m_H < 2m_Z$ [94].

4.4. Results

The expected distributions of $m_{4\ell}$ for the background and for a Higgs boson signal with $m_H = 125$ GeV are compared to the data in Fig. 2. The numbers of observed and expected events in a window of ± 5 GeV around $m_H = 125$ GeV are presented for the combined 7 TeV and 8 TeV data in Table 3. The distribution of the m_{34} versus m_{12} invariant mass is shown in Fig. 3. The statistical interpretation of the excess of events near $m_{4\ell} = 125$ GeV in Fig. 2 is presented in Section 9.
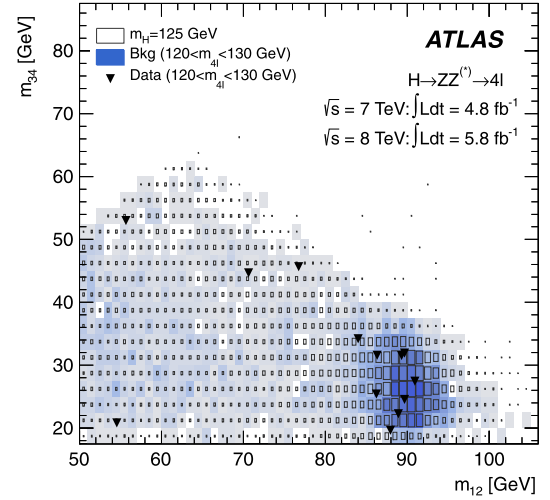

Fig. 3. Distribution of the m_{34} versus the m_{12} invariant mass, before the application of the Z-mass constrained kinematic fit, for the selected candidates in the $m_{4\ell}$ range 120–130 GeV. The expected distributions for a SM Higgs with $m_H = 125$ GeV (the sizes of the boxes indicate the relative density) and for the total background (the intensity of the shading indicates the relative density) are also shown.

5. $H \to \gamma\gamma$ channel

The search for the SM Higgs boson through the decay $H \to \gamma\gamma$ is performed in the mass range between 110 GeV and 150 GeV. The dominant background is SM diphoton production ($\gamma\gamma$); contributions also come from $\gamma + $ jet and jet $+$ jet production with one or two jets mis-identified as photons (γj and jj) and from the Drell–Yan process. The 7 TeV data have been re-analysed and the results combined with those from the 8 TeV data. Among other changes to the analysis, a new category of events with two jets is introduced, which enhances the sensitivity to the VBF process. Higgs boson events produced by the VBF process have two forward jets, originating from the two scattered quarks, and tend to be devoid of jets in the central region. Overall, the sensitivity of the analysis has been improved by about 20% with respect to that described in Ref. [95].

5.1. Event selection

The data used in this channel are selected using a diphoton trigger [96], which requires two clusters formed from energy depositions in the electromagnetic calorimeter. An E_T threshold of 20 GeV is applied to each cluster for the 7 TeV data, while for the 8 TeV data the thresholds are increased to 35 GeV on the leading (the highest E_T) cluster and to 25 GeV on the sub-leading (the next-highest E_T) cluster. In addition, loose criteria are applied to the shapes of the clusters to match the expectations for electromagnetic showers initiated by photons. The efficiency of the trigger is greater than 99% for events passing the final event selection.

Events are required to contain at least one reconstructed vertex with at least two associated tracks with $p_T > 0.4$ GeV, as well as two photon candidates. Photon candidates are reconstructed in the fiducial region $|\eta| < 2.37$, excluding the calorimeter barrel/endcap transition region $1.37 \leqslant |\eta| < 1.52$. Photons that convert to electron–positron pairs in the ID material can have one or two reconstructed tracks matched to the clusters in the calorimeter. The photon reconstruction efficiency is about 97% for $E_T > 30$ GeV.

In order to account for energy losses upstream of the calorimeter and energy leakage outside of the cluster, MC simulation results are used to calibrate the energies of the photon candidates; there are separate calibrations for unconverted and converted

candidates. The calibration is refined by applying η-dependent correction factors, which are of the order of $\pm 1\%$, determined from measured $Z \to e^+e^-$ events. The leading (sub-leading) photon candidate is required to have $E_T > 40$ GeV (30 GeV).

Photon candidates are required to pass identification criteria based on shower shapes in the electromagnetic calorimeter and on energy leakage into the hadronic calorimeter [97]. For the 7 TeV data, this information is combined in a neural network, tuned to achieve a similar jet rejection as the cut-based selection described in Ref. [95], but with higher photon efficiency. For the 8 TeV data, cut-based criteria are used to ensure reliable photon performance for recently-recorded data. This cut-based selection has been tuned to be robust against pile-up by relaxing requirements on shower shape criteria more susceptible to pile-up, and tightening others. The photon identification efficiencies, averaged over η, range from 85% to above 95% for the E_T range under consideration.

To further suppress the jet background, an isolation requirement is applied. The isolation transverse energy is defined as the sum of the transverse energy of positive-energy topological clusters, as described in Section 4, within a cone of size $\Delta R = 0.4$ around the photon candidate, excluding the region within 0.125×0.175 in $\Delta\eta \times \Delta\phi$ around the photon barycentre. The distributions of the isolation transverse energy in data and simulation have been found to be in good agreement using electrons from $Z \to e^+e^-$ events and photons from $Z \to \ell^+\ell^-\gamma$ events. Remaining small differences are taken into account as a systematic uncertainty. Photon candidates are required to have an isolation transverse energy of less than 4 GeV.

5.2. Invariant mass reconstruction

The invariant mass of the two photons is evaluated using the photon energies measured in the calorimeter, the azimuthal angle ϕ between the photons as determined from the positions of the photons in the calorimeter, and the values of η calculated from the position of the identified primary vertex and the impact points of the photons in the calorimeter.

The primary vertex of the hard interaction is identified by combining the following information in a global likelihood: the directions of flight of the photons as determined using the longitudinal segmentation of the electromagnetic calorimeter (calorimeter pointing), the parameters of the beam spot, and the $\sum p_T^2$ of the tracks associated with each reconstructed vertex. In addition, for the 7 TeV data analysis, the reconstructed conversion vertex is used in the likelihood for converted photons with tracks containing hits in the silicon layers of the ID. The calorimeter pointing is sufficient to ensure that the contribution of the opening angle between the photons to the mass resolution is negligible. Using the calorimeter pointing alone, the resolution of the vertex z coordinate is ~ 15 mm, improving to ~ 6 mm for events with two reconstructed converted photons. The tracking information from the ID improves the identification of the vertex of the hard interaction, which is needed for the jet selection in the 2-jet category.

With the selection described in Section 5.1, in the diphoton invariant mass range between 100 GeV and 160 GeV, 23 788 and 35 251 diphoton candidates are observed in the 7 TeV and 8 TeV data samples, respectively.

Data-driven techniques [98] are used to estimate the numbers of $\gamma\gamma$, γj and jj events in the selected sample. The contribution from the Drell–Yan background is determined from a sample of $Z \to e^+e^-$ decays in data where either one or both electrons pass the photon selection. The measured composition of the selected sample is approximately 74%, 22%, 3% and 1% for the $\gamma\gamma$, γj, jj and Drell–Yan processes, respectively, demonstrating the dominance of the irreducible diphoton production. This decomposition

is not directly used in the signal search; however, it is used to study the parameterisation of the background modelling.

5.3. Event categorisation

To increase the sensitivity to a Higgs boson signal, the events are separated into ten mutually exclusive categories having different mass resolutions and signal-to-background ratios. An exclusive category of events containing two jets improves the sensitivity to VBF. The other nine categories are defined by the presence or not of converted photons, η of the selected photons, and p_{Tt}, the component[3] of the diphoton p_T that is orthogonal to the axis defined by the difference between the two photon momenta [99,100].

Jets are reconstructed [101] using the anti-k_t algorithm [102] with radius parameter $R = 0.4$. At least two jets with $|\eta| < 4.5$ and $p_T > 25$ GeV are required in the 2-jet selection. In the analysis of the 8 TeV data, the p_T threshold is raised to 30 GeV for jets with $2.5 < |\eta| < 4.5$. For jets in the ID acceptance ($|\eta| < 2.5$), the fraction of the sum of the p_T of tracks, associated with the jet and matched to the selected primary vertex, with respect to the sum of the p_T of tracks associated with the jet (jet vertex fraction, JVF) is required to be at least 0.75. This requirement on the JVF reduces the number of jets from proton–proton interactions not associated with the primary vertex. Motivated by the VBF topology, three additional cuts are applied in the 2-jet selection: the difference of the pseudorapidity between the leading and sub-leading jets (tag jets) is required to be larger than 2.8, the invariant mass of the tag jets has to be larger than 400 GeV, and the azimuthal angle difference between the diphoton system and the system of the tag jets has to be larger than 2.6. About 70% of the signal events in the 2-jet category come from the VBF process.

The other nine categories are defined as follows: events with two unconverted photons are separated into *unconverted central* ($|\eta| < 0.75$ for both candidates) and *unconverted rest* (all other events), events with at least one converted photon are separated into *converted central* ($|\eta| < 0.75$ for both candidates), *converted transition* (at least one photon with $1.3 < |\eta| < 1.75$) and *converted rest* (all other events). Except for the *converted transition* category, each category is further divided by a cut at $p_{Tt} = 60$ GeV into two categories, *low p_{Tt}* and *high p_{Tt}*. MC studies show that signal events, particularly those produced via VBF or associated production (WH/ZH and $t\bar{t}H$), have on average larger p_{Tt} than background events. The number of data events in each category, as well as the sum of all the categories, which is denoted *inclusive*, are given in Table 4.

5.4. Signal modelling

The description of the Higgs boson signal is obtained from MC, as described in Section 3. The cross sections multiplied by the branching ratio into two photons are given in Table 4 for $m_H = 126.5$ GeV. The number of signal events produced via the ggF process is rescaled to take into account the expected destructive interference between the $gg \to \gamma\gamma$ continuum background and ggF [103], leading to a reduction of the production rate by 2–5% depending on m_H and the event category. For both the 7 TeV and 8 TeV MC samples, the fractions of ggF, VBF, WH, ZH and $t\bar{t}H$ production are approximately 88%, 7%, 3%, 2% and 0.5%, respectively, for $m_H = 126.5$ GeV.

In the simulation, the shower shape distributions are shifted slightly to improve the agreement with the data [97], and the

---

[3] $p_{Tt} = |(\mathbf{p}_T^{\gamma 1} + \mathbf{p}_T^{\gamma 2}) \times (\mathbf{p}_T^{\gamma 1} - \mathbf{p}_T^{\gamma 2})|/|\mathbf{p}_T^{\gamma 1} - \mathbf{p}_T^{\gamma 2}|$, where $\mathbf{p}_T^{\gamma 1}$ and $\mathbf{p}_T^{\gamma 2}$ are the transverse momenta of the two photons.

Table 4

Number of events in the data (N_D) and expected number of signal events (N_S) for $m_H = 126.5$ GeV from the $H \to \gamma\gamma$ analysis, for each category in the mass range 100–160 GeV. The mass resolution FWHM (see text) is also given for the 8 TeV data. The Higgs boson production cross section multiplied by the branching ratio into two photons ($\sigma \times B(H \to \gamma\gamma)$) is listed for $m_H = 126.5$ GeV. The statistical uncertainties on N_S and FWHM are less than 1%.

$\sqrt{s}$	7 TeV		8 TeV		
$\sigma \times B(H \to \gamma\gamma)$ [fb]	39		50		FWHM
Category	N_D	N_S	N_D	N_S	[GeV]
Unconv. central, low p_{Tt}	2054	10.5	2945	14.2	3.4
Unconv. central, high p_{Tt}	97	1.5	173	2.5	3.2
Unconv. rest, low p_{Tt}	7129	21.6	12 136	30.9	3.7
Unconv. rest, high p_{Tt}	444	2.8	785	5.2	3.6
Conv. central, low p_{Tt}	1493	6.7	2015	8.9	3.9
Conv. central, high p_{Tt}	77	1.0	113	1.6	3.5
Conv. rest, low p_{Tt}	8313	21.1	11 099	26.9	4.5
Conv. rest, high p_{Tt}	501	2.7	706	4.5	3.9
Conv. transition	3591	9.5	5140	12.8	6.1
2-jet	89	2.2	139	3.0	3.7
All categories (inclusive)	23 788	79.6	35 251	110.5	3.9

photon energy resolution is broadened (by approximately 1% in the barrel calorimeter and 1.2–2.1% in the end-cap regions) to account for small differences observed between $Z \to e^+e^-$ data and MC events. The signal yields expected for the 7 TeV and 8 TeV data samples are given in Table 4. The overall selection efficiency is about 40%.

The shape of the invariant mass of the signal in each category is modelled by the sum of a Crystal Ball function [104], describing the core of the distribution with a width σ_{CB}, and a Gaussian contribution describing the tails (amounting to $< 10\%$) of the mass distribution. The expected full-width-at-half-maximum (FWHM) is 3.9 GeV and σ_{CB} is 1.6 GeV for the inclusive sample. The resolution varies with event category (see Table 4); the FWHM is typically a factor 2.3 larger than σ_{CB}.

5.5. Background modelling

The background in each category is estimated from data by fitting the diphoton mass spectrum in the mass range 100–160 GeV with a selected model with free parameters of shape and normalisation. Different models are chosen for the different categories to achieve a good compromise between limiting the size of a potential bias while retaining good statistical power. A fourth-order Bernstein polynomial function [105] is used for the *unconverted rest* (*low p_{Tt}*), *converted rest* (*low p_{Tt}*) and *inclusive* categories, an exponential function of a second-order polynomial for the *unconverted central* (*low p_{Tt}*), *converted central* (*low p_{Tt}*) and *converted transition* categories, and an exponential function for all others.

Studies to determine the potential bias have been performed using large samples of simulated background events complemented by data-driven estimates. The background shapes in the simulation have been cross-checked using data from control regions. The potential bias for a given model is estimated, separately for each category, by performing a maximum likelihood fit to large samples of simulated background events in the mass range 100–160 GeV, of the sum of a signal plus the given background model. The signal shape is taken to follow the expectation for a SM Higgs boson; the signal yield is a free parameter of the fit. The potential bias is defined by the largest absolute signal yield obtained from the likelihood fit to the simulated background samples for hypothesised Higgs boson masses in the range 110–150 GeV. A pre-selection of background parameterisations is made by requiring that the potential bias, as defined above, is less than 20% of the statistical uncertainty on the fitted signal yield. The pre-

selected parameterisation in each category with the best expected sensitivity for $m_H = 125$ GeV is selected as the background model.

The largest absolute signal yield as defined above is taken as the systematic uncertainty on the background model. It amounts to $\pm(0.2$–$4.6)$ and $\pm(0.3$–$6.8)$ events, depending on the category for the 7 TeV and 8 TeV data samples, respectively. In the final fit to the data (see Section 5.7) a signal-like term is included in the likelihood function for each category. This term incorporates the estimated potential bias, thus providing a conservative estimate of the uncertainty due to the background modelling.

5.6. Systematic uncertainties

Hereafter, in cases where two uncertainties are quoted, they refer to the 7 TeV and 8 TeV data, respectively. The dominant experimental uncertainty on the signal yield ($\pm 8\%$, $\pm 11\%$) comes from the photon reconstruction and identification efficiency, which is estimated with data using electrons from Z decays and photons from $Z \to \ell^+\ell^-\gamma$ events. Pile-up modelling also affects the expected yields and contributes to the uncertainty ($\pm 4\%$). Further uncertainties on the signal yield are related to the trigger ($\pm 1\%$), photon isolation ($\pm 0.4\%$, $\pm 0.5\%$) and luminosity ($\pm 1.8\%$, $\pm 3.6\%$). Uncertainties due to the modelling of the underlying event are $\pm 6\%$ for VBF and $\pm 30\%$ for other production processes in the 2-jet category. Uncertainties on the predicted cross sections and branching ratio are summarised in Section 8.

The uncertainty on the expected fractions of signal events in each category is described in the following. The uncertainty on the knowledge of the material in front of the calorimeter is used to derive the amount of possible event migration between the converted and unconverted categories ($\pm 4\%$). The uncertainty from pile-up on the population of the converted and unconverted categories is $\pm 2\%$. The uncertainty from the jet energy scale (JES) amounts to up to $\pm 19\%$ for the 2-jet category, and up to $\pm 4\%$ for the other categories. Uncertainties from the JVF modelling are $\pm 12\%$ (for the 8 TeV data) for the 2-jet category, estimated from $Z + 2$-jets events by comparing data and MC. Different PDFs and scale variations in the HqT calculations are used to derive possible event migration among categories ($\pm 9\%$) due to the modelling of the Higgs boson kinematics.

The total uncertainty on the mass resolution is $\pm 14\%$. The dominant contribution ($\pm 12\%$) comes from the uncertainty on the energy resolution of the calorimeter, which is determined from $Z \to e^+e^-$ events. Smaller contributions come from the imperfect knowledge of the material in front of the calorimeter, which affects the extrapolation of the calibration from electrons to photons ($\pm 6\%$), and from pile-up ($\pm 4\%$).

5.7. Results

The distributions of the invariant mass, $m_{\gamma\gamma}$, of the diphoton events, summed over all categories, are shown in Fig. 4(a) and (b). The result of a fit including a signal component fixed to $m_H = 126.5$ GeV and a background component described by a fourth-order Bernstein polynomial is superimposed.

The statistical analysis of the data employs an unbinned likelihood function constructed from those of the ten categories of the 7 TeV and 8 TeV data samples. To demonstrate the sensitivity of this likelihood analysis, Figs. 4(c) and (d) also show the mass spectrum obtained after weighting events with category-dependent factors reflecting the signal-to-background ratios. The weight w_i for events in category $i \in [1, 10]$ for the 7 TeV and 8 TeV data samples is defined to be $\ln(1 + S_i/B_i)$, where S_i is 90% of the expected signal for $m_H = 126.5$ GeV, and B_i is the integral, in
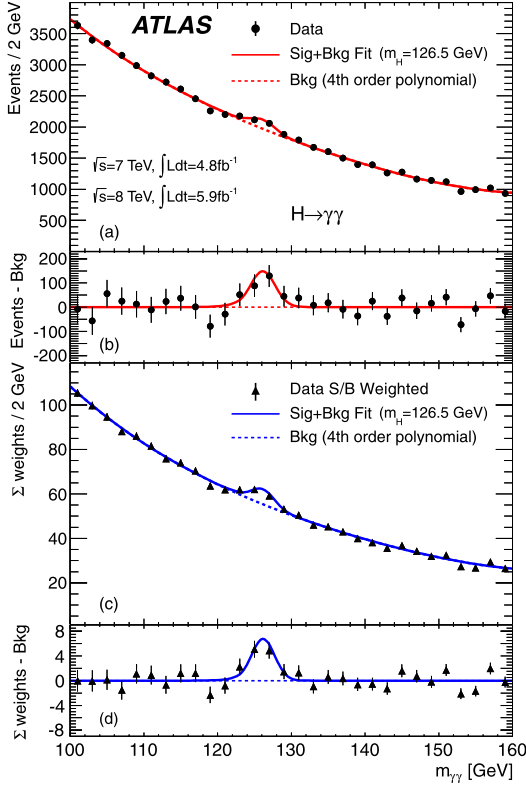
Fig. 4. The distributions of the invariant mass of diphoton candidates after all selections for the combined 7 TeV and 8 TeV data sample. The inclusive sample is shown in (a) and a weighted version of the same sample in (c); the weights are explained in the text. The result of a fit to the data of the sum of a signal component fixed to $m_H = 126.5$ GeV and a background component described by a fourth-order Bernstein polynomial is superimposed. The residuals of the data and weighted data with respect to the respective fitted background component are displayed in (b) and (d).

a window containing S_i, of a background-only fit to the data. The values S_i/B_i have only a mild dependence on m_H.

The statistical interpretation of the excess of events near $m_{\gamma\gamma} = 126.5$ GeV in Fig. 4 is presented in Section 9.

6. $H \rightarrow WW^{(*)} \rightarrow e\nu\mu\nu$ channel

The signature for this channel is two opposite-charge leptons with large transverse momentum and a large momentum imbalance in the event due to the escaping neutrinos. The dominant backgrounds are non-resonant WW, $t\bar{t}$, and Wt production, all of which have real W pairs in the final state. Other important backgrounds include Drell–Yan events ($pp \rightarrow Z/\gamma^{(*)} \rightarrow \ell\ell$) with E_T^{miss} that may arise from mismeasurement, W + jets events in which a jet produces an object reconstructed as the second electron or muon, and $W\gamma$ events in which the photon undergoes a conversion. Boson pair production ($W\gamma^*/WZ^{(*)}$ and $ZZ^{(*)}$) can also produce opposite-charge lepton pairs with additional leptons that are not detected.

The analysis of the 8 TeV data presented here is focused on the mass range $110 < m_H < 200$ GeV. It follows the procedure used for the 7 TeV data, described in Ref. [106], except that more stringent criteria are applied to reduce the W + jets background and some selections have been modified to mitigate the impact of the higher instantaneous luminosity at the LHC in 2012. In particular, the higher luminosity results in a larger Drell–Yan background to the same-flavour final states, due to the deterioration of the missing transverse momentum resolution. For this reason, and the fact that the $e\mu$ final state provides more than 85% of the sensitivity of

the search, the same-flavour final states have not been used in the analysis described here.

6.1. Event selection

For the 8 TeV $H \rightarrow WW^{(*)} \rightarrow e\nu\mu\nu$ search, the data are selected using inclusive single-muon and single-electron triggers. Both triggers require an isolated lepton with $p_T > 24$ GeV. Quality criteria are applied to suppress non-collision backgrounds such as cosmic-ray muons, beam-related backgrounds, and noise in the calorimeters. The primary vertex selection follows that described in Section 4. Candidates for the $H \rightarrow WW^{(*)} \rightarrow e\nu\mu\nu$ search are pre-selected by requiring exactly two opposite-charge leptons of different flavours, with p_T thresholds of 25 GeV for the leading lepton and 15 GeV for the sub-leading lepton. Events are classified into two exclusive lepton channels depending on the flavour of the leading lepton, where $e\mu$ (μe) refers to events with a leading electron (muon). The dilepton invariant mass is required to be greater than 10 GeV.

The lepton selection and isolation have more stringent requirements than those used for the $H \rightarrow ZZ^{(*)} \rightarrow 4\ell$ analysis (see Section 4), to reduce the larger background from non-prompt leptons in the $\ell\nu\ell\nu$ final state. Electron candidates are selected using a combination of tracking and calorimetric information [85]; the criteria are optimised for background rejection, at the expense of some reduced efficiency. Muon candidates are restricted to those with matching MS and ID tracks [84], and therefore are reconstructed over $|\eta| < 2.5$. The isolation criteria require the scalar sums of the p_T of charged particles and of calorimeter topological clusters within $\Delta R = 0.3$ of the lepton direction (excluding the lepton itself) each to be less than 0.12–0.20 times the lepton p_T. The exact value differs between the criteria for tracks and calorimeter clusters, for both electrons and muons, and depends on the lepton p_T. Jet selections follow those described in Section 5.3, except that the JVF is required to be greater than 0.5.

Since two neutrinos are present in the signal final state, events are required to have large E_T^{miss}. $\mathbf{E}_T^{miss}$ is the negative vector sum of the transverse momenta of the reconstructed objects, including muons, electrons, photons, jets, and clusters of calorimeter cells not associated with these objects. The quantity $E_{T,rel}^{miss}$ used in this analysis is required to be greater than 25 GeV and is defined as: $E_{T,rel}^{miss} = E_T^{miss} \sin \Delta\phi_{min}$, where $\Delta\phi_{min}$ is $\min(\Delta\phi, \frac{\pi}{2})$, and E_T^{miss} is the magnitude of the vector $\mathbf{E}_T^{miss}$. Here, $\Delta\phi$ is the angle between $\mathbf{E}_T^{miss}$ and the transverse momentum of the nearest lepton or jet with $p_T > 25$ GeV. Compared to E_T^{miss}, $E_{T,rel}^{miss}$ has increased rejection power for events in which the E_T^{miss} is generated by a neutrino in a jet or the mismeasurement of an object, since in those events the $\mathbf{E}_T^{miss}$ tends to point in the direction of the object. After the lepton isolation and $E_{T,rel}^{miss}$ requirements that define the pre-selected sample, the multijet background is negligible and the Drell–Yan background is much reduced. The Drell–Yan contribution becomes very small after the topological selections, described below, are applied.

The background rate and composition depend significantly on the jet multiplicity, as does the signal topology. Without accompanying jets, the signal originates almost entirely from the ggF process and the background is dominated by WW events. In contrast, when produced in association with two or more jets, the signal contains a much larger contribution from the VBF process compared to the ggF process, and the background is dominated by $t\bar{t}$ production. Therefore, to maximise the sensitivity to SM Higgs events, further selection criteria depending on the jet multiplicity are applied to the pre-selected sample. The data are subdivided into 0-jet, 1-jet and 2-jet search channels according to the number

of jets in the final state, with the 2-jet channel also including higher jet multiplicities.

Owing to spin correlations in the $WW^{(*)}$ system arising from the spin-0 nature of the SM Higgs boson and the V-A structure of the W boson decay vertex, the charged leptons tend to emerge from the primary vertex pointing in the same direction [107]. This kinematic feature is exploited for all jet multiplicities by requiring that $|\Delta\phi_{\ell\ell}| < 1.8$, and the dilepton invariant mass, $m_{\ell\ell}$, be less than 50 GeV for the 0-jet and 1-jet channels. For the 2-jet channel, the $m_{\ell\ell}$ upper bound is increased to 80 GeV.

In the 0-jet channel, the magnitude $p_T^{\ell\ell}$ of the transverse momentum of the dilepton system, $\mathbf{p}_T^{\ell\ell} = \mathbf{p}_T^{\ell1} + \mathbf{p}_T^{\ell2}$, is required to be greater than 30 GeV. This improves the rejection of the Drell–Yan background.

In the 1-jet channel, backgrounds from top quark production are suppressed by rejecting events containing a b-tagged jet, as determined using a b-tagging algorithm that uses a neural network and exploits the topology of weak decays of b- and c-hadrons [108]. The total transverse momentum, p_T^{tot}, defined as the magnitude of the vector sum $\mathbf{p}_T^{\text{tot}} = \mathbf{p}_T^{\ell1} + \mathbf{p}_T^{\ell2} + \mathbf{p}_T^{j} + \mathbf{E}_T^{\text{miss}}$, is required to be smaller than 30 GeV to suppress top background events that have jets with p_T below the threshold defined for jet counting. In order to reject the background from $Z \to \tau\tau$, the $\tau\tau$ invariant mass, $m_{\tau\tau}$, is computed under the assumptions that the reconstructed leptons are τ lepton decay products. In addition the neutrinos produced in these decays are assumed to be the only source of E_T^{miss} and to be collinear with the leptons [109]. Events with $|m_{\tau\tau} - m_Z| < 25$ GeV are rejected if the collinear approximation yields a physical solution.

The 2-jet selection follows the 1-jet selection described above, with the p_T^{tot} definition modified to include all selected jets. Motivated by the VBF topology, several additional criteria are applied to the tag jets, defined as the two highest-p_T jets in the event. These are required to be separated in rapidity by a distance $|\Delta y_{jj}| > 3.8$ and to have an invariant mass, m_{jj}, larger than 500 GeV. Events with an additional jet with $p_T > 20$ GeV between the tag jets ($y_{j1} < y < y_{j2}$) are rejected.

A transverse mass variable, m_T [110], is used to test for the presence of a signal for all jet multiplicities. This variable is defined as:

$$m_T = \sqrt{\left(E_T^{\ell\ell} + E_T^{\text{miss}}\right)^2 - \left|\mathbf{p}_T^{\ell\ell} + \mathbf{E}_T^{\text{miss}}\right|^2},$$

where $E_T^{\ell\ell} = \sqrt{|\mathbf{p}_T^{\ell\ell}|^2 + m_{\ell\ell}^2}$. The statistical analysis of the data uses a fit to the m_T distribution in the signal region after the $\Delta\phi_{\ell\ell}$ requirement (see Section 6.4), which results in increased sensitivity compared to the analysis described in Ref. [111].

For a SM Higgs boson with $m_H = 125$ GeV, the cross section times branching ratio to the $e\nu\mu\nu$ final state is 88 fb for $\sqrt{s} = 7$ TeV, increasing to 112 fb at $\sqrt{s} = 8$ TeV. The combined acceptance times efficiency of the 8 TeV 0-jet and 1-jet selection relative to the ggF production cross section times branching ratio is about 7.4%. The acceptance times efficiency of the 8 TeV 2-jet selection relative to the VBF production cross section times branching ratio is about 14%. Both of these figures are based on the number of events selected before the final m_T criterion is applied (as described in Section 6.4).

6.2. Background normalisation and control samples

The leading backgrounds from SM processes producing two isolated high-p_T leptons are WW and top (in this section, "top" background always includes both $t\bar{t}$ and single top, unless otherwise noted). These are estimated using partially data-driven techniques based on normalising the MC predictions to the data in control regions dominated by the relevant background source. The W + jets background is estimated from data for all jet multiplicities. Only the small backgrounds from Drell–Yan and diboson processes other than WW, as well as the WW background for the 2-jet analysis, are estimated using MC simulation.

The control and validation regions are defined by selections similar to those used for the signal region but with some criteria reversed or modified to obtain signal-depleted samples enriched in a particular background. The term "validation region" distinguishes these regions from the control regions that are used to directly normalise the backgrounds. Some control regions have significant contributions from backgrounds other than the targeted one, which introduces dependencies among the background estimates. These correlations are fully incorporated in the fit to the m_T distribution. In the following sections, each background estimate is described after any others on which it depends. Hence, the largest background (WW) is described last.

6.2.1. W + jets background estimation

The W + jets background contribution is estimated using a control sample of events where one of the two leptons satisfies the identification and isolation criteria described in Section 6.1, and the other lepton fails these criteria but satisfies a loosened selection (denoted "anti-identified"). Otherwise, events in this sample are required to pass all the signal selections. The dominant contribution to this sample comes from W + jets events in which a jet produces an object that is reconstructed as a lepton. This object may be either a true electron or muon from the decay of a heavy quark, or else a product of the fragmentation identified as a lepton candidate.

The contamination in the signal region is obtained by scaling the number of events in the data control sample by a transfer factor. The transfer factor is defined here as the ratio of the number of identified lepton candidates passing all selections to the number of anti-identified leptons. It is calculated as a function of the anti-identified lepton p_T using a data sample dominated by QCD jet production (dijet sample) after subtracting the residual contributions from leptons produced by leptonic W and Z decays, as estimated from data. The small remaining lepton contamination, which includes $W\gamma^{(*)}/WZ^{(*)}$ events, is subtracted using MC simulation.

The processes producing the majority of same-charge dilepton events, W + jets, $W\gamma^{(*)}/WZ^{(*)}$ and $Z^{(*)}Z^{(*)}$, are all backgrounds in the opposite-charge signal region. W + jets and $W\gamma^{(*)}$ backgrounds are particularly important in a search optimised for a low Higgs boson mass hypothesis. Therefore, the normalisation and kinematic features of same-charge dilepton events are used to validate the predictions of these backgrounds. The predicted number of same-charge events after the $E_{T,\text{rel}}^{\text{miss}}$ and zero-jet requirements is 216 ± 7 (stat) ± 42 (syst), while 182 events are observed in the data. Satisfactory agreement between data and simulation is observed in various kinematic distributions, including those of $\Delta\phi_{\ell\ell}$ (see Fig. 5(a)) and the transverse mass.

6.2.2. Top control sample

In the 0-jet channel, the top quark background prediction is first normalised using events satisfying the pre-selection criteria described in Section 6.1. This sample is selected without jet multiplicity or b-tagging requirements, and the majority of events contain top quarks. Non-top contributions are subtracted using predictions from simulation, except for W + jets, which is estimated using data. After this normalisation is performed, the fraction of events with zero jets that pass all selections is evaluated. This fraction is small (about 3%), since the top quark decay $t \to Wb$
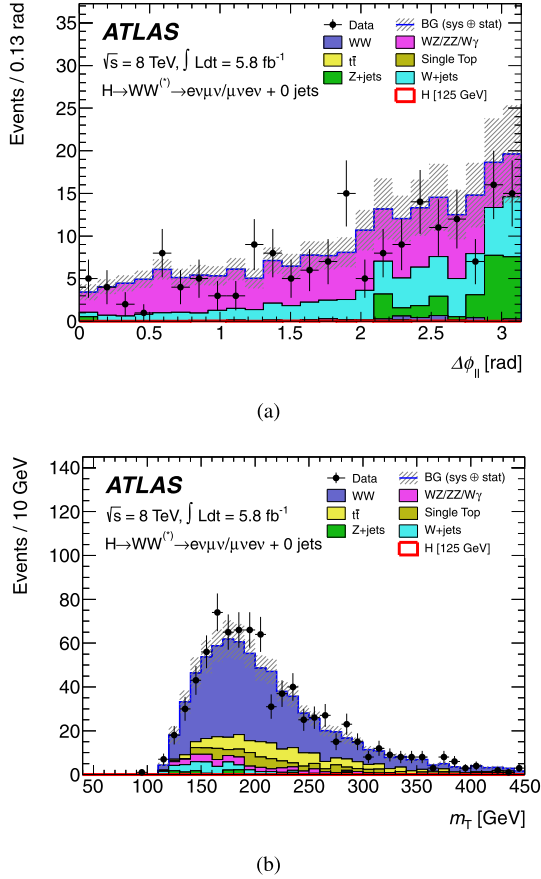
(a)

(b)

Fig. 5. Validation and control distributions for the $H \to WW^{(*)} \to e\nu\mu\nu$ analysis. (a) $\Delta\phi_{\ell\ell}$ distribution in the same-charge validation region after the $E_{\mathrm{T,rel}}^{\mathrm{miss}}$ and zero-jet requirements. (b) m_{T} distribution in the WW control region for the 0-jet channel. The $e\mu$ and μe final states are combined. The hashed area indicates the total uncertainty on the background prediction. The expected signal for $m_H = 125$ GeV is negligible and therefore not visible.

has a branching ratio of nearly 1. Predictions of this fraction from MC simulation are sensitive to theoretical uncertainties such as the modelling of initial- and final-state radiation, as well as experimental uncertainties, especially that on the jet energy scale. To reduce the impact of these uncertainties, the top quark background determination uses data from a b-tagged control region in which the one-to-two jet ratio is compared to the MC simulation [112]. The resulting correction factor to a purely MC-based background estimate after all selections amounts to 1.11 ± 0.06 (stat).

In the 1-jet and 2-jet analyses, the top quark background predictions are normalised to the data using control samples defined by reversing the b-jet veto and removing the requirements on $\Delta\phi_{\ell\ell}$ and $m_{\ell\ell}$. The $|\Delta y_{\mathrm{jj}}|$ and m_{jj} requirements are included in the definition of the 2-jet control region. The resulting samples are dominated by top quark events. The small contributions from other sources are taken into account using MC simulation and the data-driven $W + $ jets estimate. Good agreement between data and MC simulation is observed for the total numbers of events and the shapes of the m_{T} distributions. The resulting normalisation factors are 1.11 ± 0.05 for the 1-jet control region and 1.01 ± 0.26 for the 2-jet control region. Only the statistical uncertainties are quoted.

6.2.3. WW control sample

The MC predictions of the WW background in the 0-jet and 1-jet analyses, summed over lepton flavours, are normalised using control regions defined with the same selections as for the signal

region except that the $\Delta\phi_{\ell\ell}$ requirement is removed and the upper bound on $m_{\ell\ell}$ is replaced with a lower bound: $m_{\ell\ell} > 80$ GeV. The numbers of events and the shape of the m_{T} distribution in the control regions are in good agreement between data and MC, as shown in Fig. 5(b). WW production contributes about 70% of the events in the 0-jet control region and about 45% in the 1-jet region. Contaminations from sources other than WW are derived as for the signal region, including the data-driven $W + $ jets and top estimates. The resulting normalisation factors with their associated statistical uncertainties are 1.06 ± 0.06 for the 0-jet control region and 0.99 ± 0.15 for the 1-jet control region.

6.3. Systematic uncertainties

The systematic uncertainties that have the largest impact on the sensitivity of the search are the theoretical uncertainties associated with the signal. These are described in Section 9. The main experimental uncertainties are associated with the JES, the jet energy resolution (JER), pile-up, $E_{\mathrm{T}}^{\mathrm{miss}}$, the b-tagging efficiency, the $W + $ jets transfer factor, and the integrated luminosity. The largest uncertainties on the backgrounds include WW normalisation and modelling, top normalisation, and $W\gamma^{(*)}$ normalisation. The 2-jet systematic uncertainties are dominated by the statistical uncertainties in the data and the MC simulation, and are therefore not discussed further.

Variations of the jet energy scale within the systematic uncertainties can cause events to migrate between the jet bins. The uncertainty on the JES varies from $\pm 2\%$ to $\pm 9\%$ as a function of jet p_{T} and η for jets with $p_{\mathrm{T}} > 25$ GeV and $|\eta| < 4.5$ [101]. The largest impact of this uncertainty on the total signal (background) yield amounts to 7% (4%) in the 0-jet (1-jet) bin. The uncertainty on the JER is estimated from *in situ* measurements and it impacts mostly the 1-jet channel, where its effect on the total signal and background yields is 4% and 2%, respectively. An additional contribution to the JES uncertainty arises from pile-up, and is estimated to vary between $\pm 1\%$ and $\pm 5\%$ for multiple pp collisions in the same bunch crossing and up to $\pm 10\%$ for neighbouring bunch crossings. This uncertainty affects mainly the 1-jet channel, where its impact on the signal and background yields is 4% and 2%, respectively. JES and lepton momentum scale uncertainties are propagated to the $E_{\mathrm{T}}^{\mathrm{miss}}$ measurement. Additional contributions to the $E_{\mathrm{T}}^{\mathrm{miss}}$ uncertainties arise from jets with $p_{\mathrm{T}} < 20$ GeV and from low-energy calorimeter deposits not associated with reconstructed physics objects [113]. The impact of the $E_{\mathrm{T}}^{\mathrm{miss}}$ uncertainty on the total signal and background yields is $\sim 3\%$. The efficiency of the b-tagging algorithm is calibrated using samples containing muons reconstructed in the vicinity of jets [114]. The uncertainty on the b-jet tagging efficiency varies between $\pm 5\%$ and $\pm 18\%$ as a function of the jet p_{T}, and its impact on the total background yield is 10% for the 1-jet channel. The uncertainty in the $W + $ jets transfer factor is dominated by differences in jet properties between dijet and $W + $ jets events as observed in MC simulations. The total uncertainty on this background is approximately $\pm 40\%$, resulting in an uncertainty on the total background yield of 5%. The uncertainty on the integrated luminosity is $\pm 3.6\%$.

A fit to the distribution of m_{T} is performed in order to obtain the signal yield for each mass hypothesis (see Section 6.4). Most theoretical and experimental uncertainties do not produce statistically significant changes to the m_{T} distribution. The uncertainties that do produce significant changes of the distribution of m_{T} have no appreciable effect on the final results, with the exception of those associated with the WW background. In this case, an uncertainty is included to take into account differences in the distribution of m_{T} and normalisation observed between the MCFM [115], MC@NLO + HERWIG and POWHEG + PYTHIA

Table 5

The expected numbers of signal ($m_H = 125$ GeV) and background events after all selections, including a cut on the transverse mass of $0.75\,m_H < m_T < m_H$ for $m_H = 125$ GeV. The observed numbers of events in data are also displayed. The $e\mu$ and μe channels are combined. The uncertainties shown are the combination of the statistical and all systematic uncertainties, taking into account the constraints from control samples. For the 2-jet analysis, backgrounds with fewer than 0.01 expected events are marked with '–'.

	0-jet	1-jet	2-jet
Signal	20 ± 4	5 ± 2	0.34 ± 0.07
WW	101 ± 13	12 ± 5	0.10 ± 0.14
$WZ^{(*)}/ZZ/W\gamma^{(*)}$	12 ± 3	1.9 ± 1.1	0.10 ± 0.10
$t\bar{t}$	8 ± 2	6 ± 2	0.15 ± 0.10
$tW/tb/tqb$	3.4 ± 1.5	3.7 ± 1.6	–
$Z/\gamma^* + \text{jets}$	1.9 ± 1.3	0.10 ± 0.10	–
$W + \text{jets}$	15 ± 7	2 ± 1	–
Total background	142 ± 16	26 ± 6	0.35 ± 0.18
Observed	185	38	0

generators. The potential impact of interference between resonant (Higgs-mediated) and non-resonant $gg \to WW$ diagrams [116] for $m_T > m_H$ was investigated and found to be negligible. The effect of the WW normalisation, modelling, and shape systematics on the total background yield is 9% for the 0-jet channel and 19% for the 1-jet channel. The uncertainty on the shape of the total background is dominated by the uncertainties on the normalisations of the individual backgrounds. The main uncertainties on the top background in the 0-jet analysis include those associated with interference effects between $t\bar{t}$ and single top, initial state an final state radiation, b-tagging, and JER. The impact on the total background yield in the 0-jet bin is 3%. For the 1-jet analysis, the impact of the top background on the total yield is 14%. Theoretical uncertainties on the $W\gamma$ background normalisation are evaluated for each jet bin using the procedure described in Ref. [117]. They are ± 11% for the 0-jet bin and ± 50% for the 1-jet bin. For $W\gamma^*$ with $m_{\ell\ell} < 7$ GeV, a k-factor of 1.3 ± 0.3 is applied to the MadGraph LO prediction based on the comparison with the MCFM NLO calculation. The k-factor for $W\gamma^*/WZ^{(*)}$ with $m_{\ell\ell} > 7$ GeV is 1.5 ± 0.5. These uncertainties affect mostly the 1-jet channel, where their impact on the total background yield is approximately 4%.

6.4. Results

Table 5 shows the numbers of events expected from a SM Higgs boson with $m_H = 125$ GeV and from the backgrounds, as well as the numbers of candidates observed in data, after application of all selection criteria plus an additional cut on m_T of $0.75\,m_H < m_T < m_H$. The uncertainties shown in Table 5 include the systematic uncertainties discussed in Section 6.3, constrained by the use of the control regions discussed in Section 6.2. An excess of events relative to the background expectation is observed in the data.

Fig. 6 shows the distribution of the transverse mass after all selection criteria in the 0-jet and 1-jet channels combined, and for both lepton channels together.

The statistical analysis of the data employs a binned likelihood function constructed as the product of Poisson probability terms for the $e\mu$ channel and the μe channel. The mass-dependent cuts on m_T described above are not used. Instead, the 0-jet (1-jet) signal regions are subdivided into five (three) m_T bins. For the 2-jet signal region, only the results integrated over m_T are used, due to the small number of events in the final sample. The statistical interpretation of the observed excess of events is presented in Section 9.
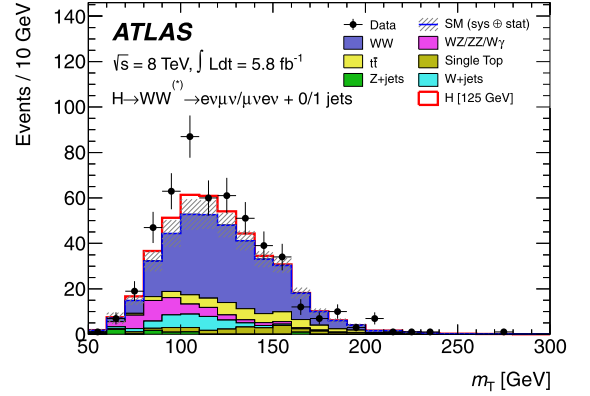

Fig. 6. Distribution of the transverse mass, m_T, in the 0-jet and 1-jet analyses with both $e\mu$ and μe channels combined, for events satisfying all selection criteria. The expected signal for $m_H = 125$ GeV is shown stacked on top of the background prediction. The $W + \text{jets}$ background is estimated from data, and WW and top background MC predictions are normalised to the data using control regions. The hashed area indicates the total uncertainty on the background prediction.

7. Statistical procedure

The statistical procedure used to interpret the data is described in Refs. [17,118–121]. The parameter of interest is the global signal strength factor μ, which acts as a scale factor on the total number of events predicted by the Standard Model for the Higgs boson signal. This factor is defined such that $\mu = 0$ corresponds to the background-only hypothesis and $\mu = 1$ corresponds to the SM Higgs boson signal in addition to the background. Hypothesised values of μ are tested with a statistic $\lambda(\mu)$ based on the profile likelihood ratio [122]. This test statistic extracts the information on the signal strength from a full likelihood fit to the data. The likelihood function includes all the parameters that describe the systematic uncertainties and their correlations.

Exclusion limits are based on the CL_s prescription [123]; a value of μ is regarded as excluded at 95% CL when CL_s is less than 5%. A SM Higgs boson with mass m_H is considered excluded at 95% confidence level (CL) when $\mu = 1$ is excluded at that mass. The significance of an excess in the data is first quantified with the local p_0, the probability that the background can produce a fluctuation greater than or equal to the excess observed in data. The equivalent formulation in terms of number of standard deviations, Z_l, is referred to as the local significance. The global probability for the most significant excess to be observed anywhere in a given search region is estimated with the method described in Ref. [124]. The ratio of the global to the local probabilities, the trials factor used to correct for the "look elsewhere" effect, increases with the range of Higgs boson mass hypotheses considered, the mass resolutions of the channels involved in the combination, and the significance of the excess.

The statistical tests are performed in steps of values of the hypothesised Higgs boson mass m_H. The asymptotic approximation [122] upon which the results are based has been validated with the method described in Ref. [17].

The combination of individual search sub-channels for a specific Higgs boson decay, and the full combination of all search channels, are based on the global signal strength factor μ and on the identification of the nuisance parameters that correspond to the correlated sources of systematic uncertainty described in Section 8.

8. Correlated systematic uncertainties

The individual search channels that enter the combination are summarised in Table 6.

Table 6

Summary of the individual channels entering the combination. The transition points between separately optimised m_H regions are indicated where applicable. In channels sensitive to associated production of the Higgs boson, V indicates a W or Z boson. The symbols $\otimes$ and $\oplus$ represent direct products and sums over sets of selection requirements, respectively.

Higgs boson decay	Subsequent decay	Sub-channels	m_H range [GeV]	$\int L dt$ [fb^{-1}]	Ref.
2011 $\sqrt{s} = 7$ TeV					
$H \to ZZ^{(*)}$	4ℓ	$\{4e, 2e2\mu, 2\mu 2e, 4\mu\}$	110–600	4.8	[87]
	$\ell\ell\nu\bar{\nu}$	$\{ee, \mu\mu\} \otimes \{\text{low, high pile-up}\}$	200–280–600	4.7	[125]
	$\ell\ell q\bar{q}$	$\{b\text{-tagged, untagged}\}$	200–300–600	4.7	[126]
$H \to \gamma\gamma$	–	10 categories $\{p_{\text{Tt}} \otimes \eta_\gamma \otimes \text{conversion}\} \oplus \{2\text{-jet}\}$	110–150	4.8	[127]
$H \to WW^{(*)}$	$\ell\nu\ell\nu$	$\{ee, e\mu/\mu e, \mu\mu\} \otimes \{0\text{-jet, }1\text{-jet, }2\text{-jet}\} \otimes \{\text{low, high pile-up}\}$	110–200–300–600	4.7	[106]
	$\ell\nu qq'$	$\{e, \mu\} \otimes \{0\text{-jet, }1\text{-jet, }2\text{-jet}\}$	300–600	4.7	[128]
$H \to \tau\tau$	$\tau_{\text{lep}}\tau_{\text{lep}}$	$\{e\mu\} \otimes \{0\text{-jet}\} \oplus \{\ell\ell\} \otimes \{1\text{-jet, }2\text{-jet, }VH\}$	110–150	4.7	[129]
	$\tau_{\text{lep}}\tau_{\text{had}}$	$\{e, \mu\} \otimes \{0\text{-jet}\} \otimes \{E_{\text{T}}^{\text{miss}} < 20 \text{ GeV}, E_{\text{T}}^{\text{miss}} \geqslant 20 \text{ GeV}\}$ $\oplus \{e, \mu\} \otimes \{1\text{-jet}\} \oplus \{\ell\} \otimes \{2\text{-jet}\}$	110–150	4.7	
	$\tau_{\text{had}}\tau_{\text{had}}$	$\{1\text{-jet}\}$	110–150	4.7	
$VH \to Vbb$	$Z \to \nu\nu$	$E_{\text{T}}^{\text{miss}} \in \{120\text{–}160, 160\text{–}200, \geqslant 200 \text{ GeV}\}$	110–130	4.6	[130]
	$W \to \ell\nu$	$p_{\text{T}}^W \in \{< 50, 50\text{–}100, 100\text{–}200, \geqslant 200 \text{ GeV}\}$	110–130	4.7	
	$Z \to \ell\ell$	$p_{\text{T}}^Z \in \{< 50, 50\text{–}100, 100\text{–}200, \geqslant 200 \text{ GeV}\}$	110–130	4.7	
2012 $\sqrt{s} = 8$ TeV					
$H \to ZZ^{(*)}$	4ℓ	$\{4e, 2e2\mu, 2\mu 2e, 4\mu\}$	110–600	5.8	[87]
$H \to \gamma\gamma$	–	10 categories $\{p_{\text{Tt}} \otimes \eta_\gamma \otimes \text{conversion}\} \oplus \{2\text{-jet}\}$	110–150	5.9	[127]
$H \to WW^{(*)}$	$e\nu\mu\nu$	$\{e\mu, \mu e\} \otimes \{0\text{-jet, }1\text{-jet, }2\text{-jet}\}$	110–200	5.8	[131]

The main uncorrelated systematic uncertainties are described in Sections 4–6 for the $H \to ZZ^{(*)} \to 4\ell$, $H \to \gamma\gamma$ and $H \to WW^{(*)} \to \ell\nu\ell\nu$ channels and in Ref. [17] for the other channels. They include the background normalisations or background model parameters from control regions or sidebands, the Monte Carlo simulation statistical uncertainties and the theoretical uncertainties affecting the background processes.

The main sources of correlated systematic uncertainties are the following.

1. *Integrated luminosity*: The uncertainty on the integrated luminosity is considered as fully correlated among channels and amounts to $\pm 3.9\%$ for the 7 TeV data [132,133], except for the $H \to ZZ^{(*)} \to 4\ell$ and $H \to \gamma\gamma$ channels which were re-analysed; the uncertainty is $\pm 1.8\%$ [92] for these channels. The uncertainty is $\pm 3.6\%$ for the 8 TeV data.

2. *Electron and photon trigger identification*: The uncertainties in the trigger and identification efficiencies are treated as fully correlated for electrons and photons.

3. *Electron and photon energy scales*: The electron and photon energy scales in the $H \to ZZ^{(*)} \to 4\ell$ and $H \to \gamma\gamma$ channels are described by five parameters, which provide a detailed account of the sources of systematic uncertainty. They are related to the calibration method, the presampler energy scale in the barrel and end-cap calorimeters, and the material description upstream of the calorimeters.

4. *Muon reconstruction*: The uncertainties affecting muons are separated into those related to the ID and MS, in order to obtain a better description of the correlated effects among channels using different muon identification criteria and different ranges of muon p_T.

5. *Jet energy scale and missing transverse energy*: The jet energy scale and jet energy resolution are affected by uncertainties which depend on the p_T, η, and flavour of the jet. A simplified scheme is used in which independent JES and JER nuisance parameters are associated with final states with significantly different kinematic selections and sensitivity to scattering processes with different kinematic distributions or flavour composition. This scheme includes a specific treatment for b-jets. The sensitivity of the results to various assumptions about the correlation between these sources of uncertainty has been found to be negligible. An uncorrelated component of the uncertainty on $E_{\text{T}}^{\text{miss}}$ is included, in addition to the JES uncertainty, which is due to low energy jet activity not associated with reconstructed physics objects.

6. *Theory uncertainties*: Correlated theoretical uncertainties affect mostly the signal predictions. The QCD scale uncertainties for $m_H = 125$ GeV amount to $^{+7\%}_{-8\%}$ for the ggF process, $\pm 1\%$ for the VBF and WH/ZH processes, and $^{+4\%}_{-9\%}$ for the $t\bar{t}H$ process [52,53]; the small dependence of these uncertainties on m_H is taken into account. The uncertainties on the predicted branching ratios amount to $\pm 5\%$. The uncertainties related to the parton distribution functions amount to $\pm 8\%$ for the predominantly gluon-initiated ggF and $t\bar{t}H$ processes, and $\pm 4\%$ for the predominantly quark-initiated VBF and WH/ZH processes [78,134–136]. The theoretical uncertainty associated with the exclusive Higgs boson production process with additional jets in the $H \to \gamma\gamma$, $H \to WW^{(*)} \to \ell\nu\ell\nu$ and $H \to \tau^+\tau^-$ channels is estimated using the prescription of Refs. [53,117,118], with the noticeable difference that an explicit calculation of the gluon-fusion process at NLO using MCFM [137] in the 2-jet category reduces the uncertainty on this non-negligible contribution to 25%. An additional theoretical uncertainty on the signal normalisation of $\pm 150\% \times (m_H/\text{TeV})^3$ (e.g. $\pm 4\%$ for $m_H = 300$ GeV) accounts for effects related to off-shell Higgs boson production and interference with other SM processes [53].

Sources of systematic uncertainty that affect both the 7 TeV and the 8 TeV data are taken as fully correlated. The uncertainties on background estimates based on control samples in the data are considered uncorrelated between the 7 TeV and 8 TeV data.

9. Results

The addition of the 8 TeV data for the $H \to ZZ^{(*)} \to 4\ell$, $H \to \gamma\gamma$ and $H \to WW^{(*)} \to e\nu\mu\nu$ channels, as well as the improvements to the analyses of the 7 TeV data in the first two of these channels, bring a significant gain in sensitivity in the low-mass region with respect to the previous combined search [17].

9.1. Excluded mass regions

The combined 95% CL exclusion limits on the production of the SM Higgs boson, expressed in terms of the signal strength parameter μ, are shown in Fig. 7(a) as a function of m_H. The expected 95% CL exclusion region covers the m_H range from 110 GeV to
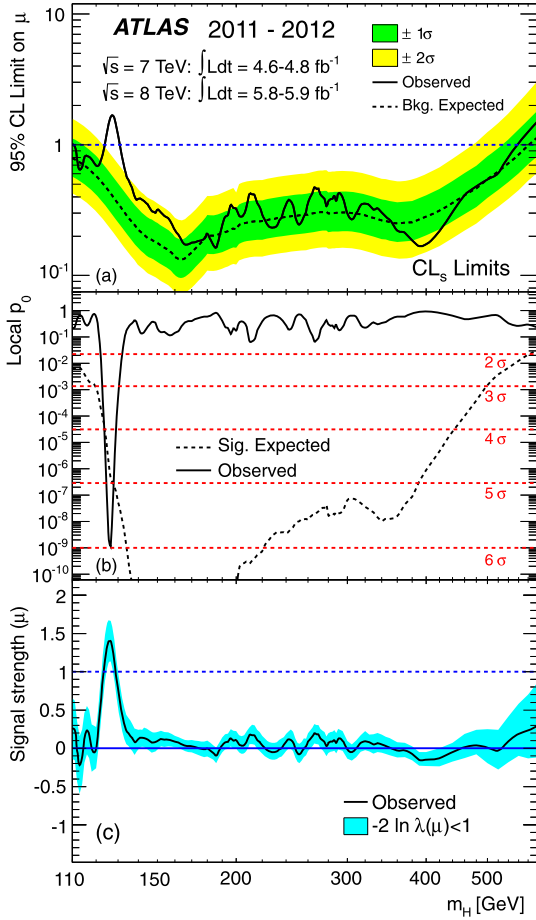
Fig. 7. Combined search results: (a) The observed (solid) 95% CL limits on the signal strength as a function of m_H and the expectation (dashed) under the background-only hypothesis. The dark and light shaded bands show the $\pm 1\sigma$ and $\pm 2\sigma$ uncertainties on the background-only expectation. (b) The observed (solid) local p_0 as a function of m_H and the expectation (dashed) for a SM Higgs boson signal hypothesis ($\mu = 1$) at the given mass. (c) The best-fit signal strength $\hat{\mu}$ as a function of m_H. The band indicates the approximate 68% CL interval around the fitted value.

Fig. 8. The observed local p_0 as a function of the hypothesised Higgs boson mass for the (a) $H \to ZZ^{(*)} \to 4\ell$, (b) $H \to \gamma\gamma$ and (c) $H \to WW^{(*)} \to \ell\nu\ell\nu$ channels. The dashed curves show the expected local p_0 under the hypothesis of a SM Higgs boson signal at that mass. Results are shown separately for the $\sqrt{s} = 7$ TeV data (dark, blue in the web version), the $\sqrt{s} = 8$ TeV data (light, red in the web version), and their combination (black).

582 GeV. The observed 95% CL exclusion regions are 111–122 GeV and 131–559 GeV. Three mass regions are excluded at 99% CL, 113–114, 117–121 and 132–527 GeV, while the expected exclusion range at 99% CL is 113–532 GeV.

9.2. Observation of an excess of events

An excess of events is observed near $m_H = 126$ GeV in the $H \to ZZ^{(*)} \to 4\ell$ and $H \to \gamma\gamma$ channels, both of which provide fully reconstructed candidates with high resolution in invariant mass, as shown in Figs. 8(a) and 8(b). These excesses are confirmed by the highly sensitive but low-resolution $H \to WW^{(*)} \to \ell\nu\ell\nu$ channel, as shown in Fig. 8(c).

The observed local p_0 values from the combination of channels, using the asymptotic approximation, are shown as a function of m_H in Fig. 7(b) for the full mass range and in Fig. 9 for the low mass range.

The largest local significance for the combination of the 7 and 8 TeV data is found for a SM Higgs boson mass hypothesis of $m_H = 126.5$ GeV, where it reaches 6.0σ, with an expected value in the presence of a SM Higgs boson signal at that mass of 4.9σ (see also Table 7). For the 2012 data alone, the maximum local significance for the $H \to ZZ^{(*)} \to 4\ell$, $H \to \gamma\gamma$ and $H \to WW^{(*)} \to$

Fig. 9. The observed (solid) local p_0 as a function of m_H in the low mass range. The dashed curve shows the expected local p_0 under the hypothesis of a SM Higgs boson signal at that mass with its $\pm 1\sigma$ band. The horizontal dashed lines indicate the p-values corresponding to significances of 1 to 6 σ.

$e\nu\mu\nu$ channels combined is 4.9σ, and occurs at $m_H = 126.5$ GeV (3.8σ expected).

The significance of the excess is mildly sensitive to uncertainties in the energy resolutions and energy scale systematic uncertainties for photons and electrons; the effect of the muon energy scale systematic uncertainties is negligible. The presence of these

Table 7

Characterisation of the excess in the $H \to ZZ^{(*)} \to 4\ell$, $H \to \gamma\gamma$ and $H \to WW^{(*)} \to \ell\nu\ell\nu$ channels and the combination of all channels listed in Table 6. The mass value m_{max} for which the local significance is maximum, the maximum observed local significance Z_l and the expected local significance $E(Z_l)$ in the presence of a SM Higgs boson signal at m_{max} are given. The best fit value of the signal strength parameter $\hat{\mu}$ at $m_H = 126$ GeV is shown with the total uncertainty. The expected and observed mass ranges excluded at 95% CL (99% CL, indicated by a *) are also given, for the combined $\sqrt{s} = 7$ TeV and $\sqrt{s} = 8$ TeV data.

Search channel	Dataset	m_{max} [GeV]	Z_l [σ]	$E(Z_l)$ [σ]	$\hat{\mu}(m_H = 126$ GeV$)$	Expected exclusion [GeV]	Observed exclusion [GeV]
$H \to ZZ^{(*)} \to 4\ell$	7 TeV	125.0	2.5	1.6	1.4 ± 1.1		
	8 TeV	125.5	2.6	2.1	1.1 ± 0.8		
	7 & 8 TeV	125.0	3.6	2.7	1.2 ± 0.6	124–164, 176–500	131–162, 170–460
$H \to \gamma\gamma$	7 TeV	126.0	3.4	1.6	2.2 ± 0.7		
	8 TeV	127.0	3.2	1.9	1.5 ± 0.6		
	7 & 8 TeV	126.5	4.5	2.5	1.8 ± 0.5	110–140	112–123, 132–143
$H \to WW^{(*)} \to \ell\nu\ell\nu$	7 TeV	135.0	1.1	3.4	0.5 ± 0.6		
	8 TeV	120.0	3.3	1.0	1.9 ± 0.7		
	7 & 8 TeV	125.0	2.8	2.3	1.3 ± 0.5	124–233	137–261
Combined	7 TeV	126.5	3.6	3.2	1.2 ± 0.4		
	8 TeV	126.5	4.9	3.8	1.5 ± 0.4		
	7 & 8 TeV	126.5	6.0	4.9	1.4 ± 0.3	110–582 113–532 (*)	111–122, 131–559 113–114, 117–121, 132–527 (*)

uncertainties, evaluated as described in Ref. [138], reduces the local significance to 5.9σ.

The global significance of a local 5.9σ excess anywhere in the mass range 110–600 GeV is estimated to be approximately 5.1σ, increasing to 5.3σ in the range 110–150 GeV, which is approximately the mass range not excluded at the 99% CL by the LHC combined SM Higgs boson search [139] and the indirect constraints from the global fit to precision electroweak measurements [12].

9.3. Characterising the excess

The mass of the observed new particle is estimated using the profile likelihood ratio $\lambda(m_H)$ for $H \to ZZ^{(*)} \to 4\ell$ and $H \to \gamma\gamma$, the two channels with the highest mass resolution. The signal strength is allowed to vary independently in the two channels, although the result is essentially unchanged when restricted to the SM hypothesis $\mu = 1$. The leading sources of systematic uncertainty come from the electron and photon energy scales and resolutions. The resulting estimate for the mass of the observed particle is 126.0 ± 0.4 (stat) ± 0.4 (sys) GeV.

The best-fit signal strength $\hat{\mu}$ is shown in Fig. 7(c) as a function of m_H. The observed excess corresponds to $\hat{\mu} = 1.4 \pm 0.3$ for $m_H = 126$ GeV, which is consistent with the SM Higgs boson hypothesis $\mu = 1$. A summary of the individual and combined best-fit values of the strength parameter for a SM Higgs boson mass hypothesis of 126 GeV is shown in Fig. 10, while more information about the three main channels is provided in Table 7.

In order to test which values of the strength and mass of a signal hypothesis are simultaneously consistent with the data, the profile likelihood ratio $\lambda(\mu, m_H)$ is used. In the presence of a strong signal, it will produce closed contours around the best-fit point $(\hat{\mu}, \hat{m}_H)$, while in the absence of a signal the contours will be upper limits on μ for all values of m_H.

Asymptotically, the test statistic $-2\ln\lambda(\mu, m_H)$ is distributed as a χ^2 distribution with two degrees of freedom. The resulting 68% and 95% CL contours for the $H \to \gamma\gamma$ and $H \to WW^{(*)} \to \ell\nu\ell\nu$ channels are shown in Fig. 11, where the asymptotic approximations have been validated with ensembles of pseudo-experiments. Similar contours for the $H \to ZZ^{(*)} \to 4\ell$ channel are also shown in Fig. 11, although they are only approximate confidence intervals due to the smaller number of candidates in this channel. These contours in the (μ, m_H) plane take into account uncertainties in the energy scale and resolution.

The probability for a single Higgs boson-like particle to produce resonant mass peaks in the $H \to ZZ^{(*)} \to 4\ell$ and $H \to \gamma\gamma$

Fig. 10. Measurements of the signal strength parameter μ for $m_H = 126$ GeV for the individual channels and their combination.

Fig. 11. Confidence intervals in the (μ, m_H) plane for the $H \to ZZ^{(*)} \to 4\ell$, $H \to \gamma\gamma$, and $H \to WW^{(*)} \to \ell\nu\ell\nu$ channels, including all systematic uncertainties. The markers indicate the maximum likelihood estimates $(\hat{\mu}, \hat{m}_H)$ in the corresponding channels (the maximum likelihood estimates for $H \to ZZ^{(*)} \to 4\ell$ and $H \to WW^{(*)} \to \ell\nu\ell\nu$ coincide).

channels separated by more than the observed mass difference, allowing the signal strengths to vary independently, is about 8%.

The contributions from the different production modes in the $H \to \gamma\gamma$ channel have been studied in order to assess any tension between the data and the ratios of the production cross

Fig. 12. Likelihood contours for the $H \to \gamma\gamma$ channel in the $(\mu_{\mathrm{ggF}+t\bar{t}H}, \mu_{\mathrm{VBF}+VH})$ plane including the branching ratio factor B/B_{SM}. The quantity $\mu_{\mathrm{ggF}+t\bar{t}H}$ ($\mu_{\mathrm{VBF}+VH}$) is a common scale factor for the ggF and $t\bar{t}H$ (VBF and VH) production cross-sections. The best fit to the data $(+)$ and 68% (full) and 95% (dashed) CL contours are also indicated, as well as the SM expectation $(\times)$.

sections predicted in the Standard Model. A new signal strength parameter μ_i is introduced for each production mode, defined by $\mu_i = \sigma_i/\sigma_{i,\mathrm{SM}}$. In order to determine the values of (μ_i, μ_j) that are simultaneously consistent with the data, the profile likelihood ratio $\lambda(\mu_i, \mu_j)$ is used with the measured mass treated as a nuisance parameter.

Since there are four Higgs boson production modes at the LHC, two-dimensional contours require either some μ_i to be fixed, or multiple μ_i to be related in some way. Here, μ_{ggF} and $\mu_{t\bar{t}H}$ have been grouped together as they scale with the $t\bar{t}H$ coupling in the SM, and are denoted by the common parameter $\mu_{\mathrm{ggF}+t\bar{t}H}$. Similarly, μ_{VBF} and μ_{VH} have been grouped together as they scale with the WWH/ZZH coupling in the SM, and are denoted by the common parameter $\mu_{\mathrm{VBF}+VH}$. Since the distribution of signal events among the 10 categories of the $H \to \gamma\gamma$ search is sensitive to these factors, constraints in the plane of $\mu_{\mathrm{ggF}+t\bar{t}H} \times B/B_{\mathrm{SM}}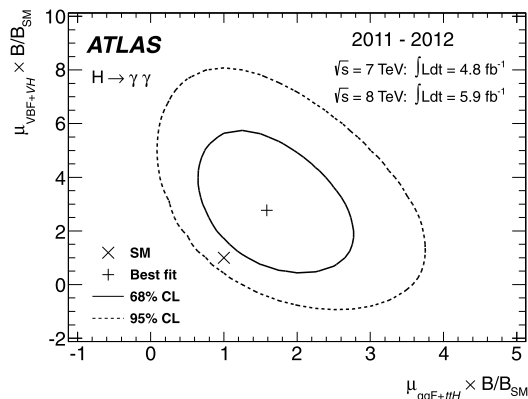$ and $\mu_{\mathrm{VBF}+VH} \times B/B_{\mathrm{SM}}$, where B is the branching ratio for $H \to \gamma\gamma$, can be obtained (Fig. 12). Theoretical uncertainties are included so that the consistency with the SM expectation can be quantified. The data are compatible with the SM expectation at the $1.5\,\sigma$ level.

10. Conclusion

Searches for the Standard Model Higgs boson have been performed in the $H \to ZZ^{(*)} \to 4\ell$, $H \to \gamma\gamma$ and $H \to WW^{(*)} \to e\nu\mu\nu$ channels with the ATLAS experiment at the LHC using 5.8–5.9 fb^{-1} of pp collision data recorded during April to June 2012 at a centre-of-mass energy of 8 TeV. These results are combined with earlier results [17], which are based on an integrated luminosity of 4.6–4.8 fb^{-1} recorded in 2011 at a centre-of-mass energy of 7 TeV, except for the $H \to ZZ^{(*)} \to 4\ell$ and $H \to \gamma\gamma$ channels, which have been updated with the improved analyses presented here.

The Standard Model Higgs boson is excluded at 95% CL in the mass range 111–559 GeV, except for the narrow region 122–131 GeV. In this region, an excess of events with significance 5.9σ, corresponding to $p_0 = 1.7 \times 10^{-9}$, is observed. The excess is driven by the two channels with the highest mass resolution, $H \to ZZ^{(*)} \to 4\ell$ and $H \to \gamma\gamma$, and the equally sensitive but low-resolution $H \to WW^{(*)} \to \ell\nu\ell\nu$ channel. Taking into account the entire mass range of the search, 110–600 GeV, the global significance of the excess is 5.1σ, which corresponds to $p_0 = 1.7 \times 10^{-7}$.

These results provide conclusive evidence for the discovery of a new particle with mass 126.0 ± 0.4 (stat) ± 0.4 (sys) GeV. The signal strength parameter μ has the value 1.4 ± 0.3 at the fitted mass,

which is consistent with the SM Higgs boson hypothesis $\mu = 1$. The decays to pairs of vector bosons whose net electric charge is zero identify the new particle as a neutral boson. The observation in the diphoton channel disfavours the spin-1 hypothesis [140, 141]. Although these results are compatible with the hypothesis that the new particle is the Standard Model Higgs boson, more data are needed to assess its nature in detail.

Open access

References

[1] S.L. Glashow, Nucl. Phys. 22 (4) (1961) 579.
[2] S. Weinberg, Phys. Rev. Lett. 19 (1967) 1264.
[3] A. Salam, in: N. Svartholm (Ed.), Proceedings of the Eighth Nobel Symposium, Almqvist & Wiksell, 1968, p. 367.
[4] G. 't Hooft, M. Veltman, Nucl. Phys. B 44 (1972) 189.
[5] F. Englert, R. Brout, Phys. Rev. Lett. 13 (1964) 321.
[6] P.W. Higgs, Phys. Lett. 12 (1964) 132.
[7] P.W. Higgs, Phys. Rev. Lett. 13 (1964) 508.
[8] G.S. Guralnik, C.R. Hagen, T.W.B. Kibble, Phys. Rev. Lett. 13 (1964) 585.
[9] P.W. Higgs, Phys. Rev. 145 (1966) 1156.
[10] T.W.B. Kibble, Phys. Rev. 155 (1967) 1554.
[11] L. Evans, P. Bryant (Eds.), LHC Machine, JINST, vol. 3, 2008, p. S08001.
[12] ALEPH, CDF, DØ, DELPHI, L3, OPAL, SLD Collaborations, the LEP Electroweak Working Group, the Tevatron Electroweak Working Group,

the SLD Electroweak and Heavy Flavour Groups, CERN-PH-EP-2010-095, arXiv:1012.2367 [hep-ex], 2010.

[13] ALEPH, DELPHI, L3 and OPAL Collaborations, Phys. Lett. B 565 (2003) 61.

[14] CDF Collaboration, T. Aaltonen, et al. Phys. Rev. Lett. (2012), in press, arXiv:1207.1707 [hep-ex].

[15] DØ Collaboration, V.M. Abazov, et al. Phys. Rev. Lett. (2012), submitted for publication, arXiv:1207.6631 [hep-ex].

[16] CDF Collaboration, DØ Collaboration, Phys. Rev. Lett. (2012), submitted for publication, arXiv:1207.6436 [hep-ex].

[17] ATLAS Collaboration, Phys. Rev. D 86 (2012) 032003.

[18] CMS Collaboration, Phys. Lett. B 710 (2012) 26.

[19] ATLAS Collaboration, ATLAS: Letter of intent for a general-purpose pp experiment at the large hadron collider at CERN, CERN-LHCC-92-004 (1992).

[20] ATLAS Collaboration, The ATLAS Collaboration, ATLAS Technical Proposal for a General-Purpose pp Experiment at the Large Hadron Collider at CERN, CERN-LHCC-94-43 (1994).

[21] ATLAS Collaboration, JINST 3 (2008) S08003.

[22] H. Georgi, S. Glashow, M. Machacek, D.V. Nanopoulos, Phys. Rev. Lett. 40 (1978) 692.

[23] A. Djouadi, M. Spira, P.M. Zerwas, Phys. Lett. B 264 (1991) 440.

[24] S. Dawson, Nucl. Phys. B 359 (1991) 283.

[25] M. Spira, A. Djouadi, D. Graudenz, P.M. Zerwas, Nucl. Phys. B 453 (1995) 17.

[26] R. Harlander, W.B. Kilgore, Phys. Rev. Lett. 88 (2002) 201801.

[27] C. Anastasiou, K. Melnikov, Nucl. Phys. B 646 (2002) 220.

[28] V. Ravindran, J. Smith, W.L. van Neerven, Nucl. Phys. B 665 (2003) 325.

[29] U. Aglietti, R. Bonciani, G. Degrassi, A. Vicini, Phys. Lett. B 595 (2004) 432.

[30] S. Actis, G. Passarino, C. Sturm, S. Uccirati, Phys. Lett. B 670 (2008) 12.

[31] S. Catani, D. de Florian, M. Grazzini, P. Nason, JHEP 0307 (2003) 028.

[32] C. Anastasiou, R. Boughezal, F. Petriello, JHEP 0904 (2009) 003.

[33] D. de Florian, M. Grazzini, Higgs production at the LHC: Updated cross sections at $\sqrt{s}$ = 8 TeV, arXiv:1206.4133 [hep-ph].

[34] C. Anastasiou, S. Buehler, F. Herzog, A. Lazopoulos, JHEP 1204 (2012) 004.

[35] J. Baglio, A. Djouadi, JHEP 1103 (2011) 055.

[36] D. de Florian, G. Ferrera, M. Grazzini, D. Tommasini, JHEP 1111 (2011) 064.

[37] P.S.E. Bagnaschi, G. Degrassi, A. Vicini, JHEP 1202 (2012) 88.

[38] R. Cahn, S. Dawson, Phys. Lett. B 136 (1984) 196;
R. Cahn, S. Dawson, Phys. Lett. B 138 (1984) 464 (Erratum).

[39] M. Ciccolini, A. Denner, S. Dittmaier, Phys. Rev. Lett. 99 (2007) 161803.

[40] M. Ciccolini, A. Denner, S. Dittmaier, Phys. Rev. D 77 (2008) 013002.

[41] K. Arnold, M. Bahr, G. Bozzi, F. Campanario, C. Englert, Comput. Phys. Commun. 180 (2009) 1661.

[42] P. Bolzoni, F. Maltoni, S.-O. Moch, M. Zaro, Phys. Rev. Lett. 105 (2010) 011801.

[43] S. Glashow, D.V. Nanopoulos, A. Yildiz, Phys. Rev. D 18 (1978) 1724.

[44] T. Han, S. Willenbrock, Phys. Lett. B 273 (1991) 167.

[45] O. Brein, A. Djouadi, R. Harlander, Phys. Lett. B 579 (2004) 149.

[46] M.L. Ciccolini, S. Dittmaier, M. Kramer, Phys. Rev. D 68 (2003) 073003.

[47] Z. Kunszt, Nucl. Phys. B 247 (1984) 339.

[48] W. Beenakker, et al., Phys. Rev. Lett. 87 (2001) 201805.

[49] W. Beenakker, et al., Nucl. Phys. B 653 (2003) 151.

[50] S. Dawson, L.H. Orr, L. Reina, D. Wackeroth, Phys. Rev. D 67 (2003) 071503.

[51] S. Dawson, C. Jackson, L.H. Orr, L. Reina, D. Wackeroth, Phys. Rev. D 68 (2003) 034022.

[52] S. Dittmaier, C. Mariotti, G. Passarino, R. Tanaka (Eds.), LHC Higgs Cross Section Working Group, Handbook of LHC Higgs cross sections: 1. Inclusive observables, CERN-2011-002, arXiv:1101.0593 [hep-ph], 2011.

[53] S. Dittmaier, C. Mariotti, G. Passarino, R. Tanaka (Eds.), LHC Higgs Cross Section Working Group, Handbook of LHC Higgs Cross Sections: 2. Differential Distributions, CERN-2012-002, arXiv:1201.3084 [hep-ph], 2012.

[54] A. Djouadi, J. Kalinowski, M. Spira, Comput. Phys. Commun. 108 (1998) 56.

[55] A. Bredenstein, A. Denner, S. Dittmaier, M.M. Weber, Phys. Rev. D 74 (2006) 013004.

[56] A. Bredenstein, A. Denner, S. Dittmaier, M.M. Weber, JHEP 0702 (2007) 080.

[57] S. Alioli, P. Nason, C. Oleari, E. Re, JHEP 0904 (2009) 002.

[58] P. Nason, C. Oleari, JHEP 1002 (2010) 037.

[59] M.L. Mangano, et al., JHEP 0307 (2003) 001.

[60] S. Frixione, B.R. Webber, JHEP 0206 (2002) 029;
S. Frixione, P. Nason, B.R. Webber, JHEP 0308 (2003) 007;
S. Frixione, E. Laenen, P. Motylinski, B.R. Webber, JHEP 0603 (2006) 092;
S. Frixione, E. Laenen, P. Motylinski, C. White, B.R. Webber, JHEP 0807 (2008) 029;
S. Frixione, F. Stoeckli, P. Torrielli, B.R. Webber, JHEP 1101 (2011) 053.

[61] B.P. Kersevan, E. Richter-Was, The Monte Carlo event generator AcerMC version 2.0 with interfaces to PYTHIA 6.2 and HERWIG 6.5, arXiv:hep-ph/0405247.

[62] T. Binoth, M. Ciccolini, N. Kauer, M. Krämer, JHEP 0612 (2006) 046.

[63] T. Melia, P. Nason, R. Rontsch, G. Zanderighi, JHEP 1111 (2011) 078.

[64] T. Binoth, N. Kauer, P. Mertsch, Gluon-induced QCD Corrections to $pp \to ZZ \to \ell\bar{\ell}\ell'\bar{\ell}'$, arXiv:0807.0024 [hep-ph].

[65] R.C. Gray, C. Kilic, M. Park, S. Somalwar, S. Thomas, Backgrounds to Higgs boson searches from $W\gamma^* \to l\nu l(l)$ asymmetric internal conversion, arXiv:1110.1368 [hep-ph].

[66] ATLAS Collaborations, New ATLAS event generator tunes to 2010 data, ATL-PHYS-PUB-2011-008, http://cdsweb.cern.ch/record/1345343, 2011.

[67] ATLAS Collaborations, ATLAS tunes of PYTHIA 6 and Pythia 8 for MC11, ATL-PHYS-PUB-2011-009, http://cdsweb.cern.ch/record/1363300, 2011.

[68] ATLAS Collaborations, Further ATLAS tunes of PYTHIA6 and Pythia 8, ATL-PHYS-PUB-2011-014, http://cdsweb.cern.ch/record/1400677, 2011.

[69] T. Sjöstrand, S. Mrenna, P. Skands, JHEP 0605 (2006) 026.

[70] J. Alwall, et al., JHEP 0709 (2007) 028.

[71] J. Alwall, M. Herquet, F. Maltoni, O. Mattelaer, T. Stelzer, JHEP 1106 (2011) 128.

[72] T. Sjöstrand, S. Mrenna, P. Skands, Comput. Phys. Commun. 178 (2008) 852.

[73] G. Corcella, I. Knowles, G. Marchesini, S. Moretti, K. Odagiri, et al., JHEP 0101 (2001) 010.

[74] T. Gleisberg, et al., JHEP 0902 (2009) 007.

[75] J.M. Butterworth, J.R. Forshaw, M.H. Seymour, Z. Phys. C 72 (1996) 637.

[76] S. Jadach, Z. Was, R. Decker, J.H. Kuhn, Comput. Phys. Commun. 76 (1993) 361.

[77] P. Golonka, Z. Was, Eur. Phys. J. C 45 (2006) 97.

[78] H.-L. Lai, et al., Phys. Rev. D 82 (2010) 074024.

[79] P.M. Nadolsky, et al., Phys. Rev. D 78 (2008) 013004.

[80] A. Sherstnev, R.S. Thorne, Eur. Phys. J. C 55 (2009) 553.

[81] ATLAS Collaboration, Eur. Phys. J. C 70 (2010) 823.

[82] S. Agostinelli, et al., Nucl. Instrum. Meth. A 506 (2003) 250.

[83] ATLAS Collaboration, Phys. Lett. B 710 (2012) 383.

[84] ATLAS Collaboration, Muon reconstruction efficiency in reprocessed 2010 LHC proton–proton collision data recorded with the ATLAS detector, ATLAS-CONF-2011-063, 2011, http://cdsweb.cern.ch/record/1345743.

[85] ATLAS Collaboration, Eur. Phys. J. C 72 (2012) 1909.

[86] ATLAS Collaboration, Improved electron reconstruction in ATLAS using the Gaussian Sum Filter-based model for bremsstrahlung, http://cdsweb.cern.ch/record/1449796.

[87] ATLAS Collaboration, Observation of an excess of events in the search for the Standard Model Higgs boson in the $H \to ZZ^{(*)} \to 4\ell$ channel with the ATLAS detector, ATLAS-CONF-2012-092, 2012, http://cdsweb.cern.ch/record/1460411.

[88] W. Lampl, S. Laplace, D. Lelas, P. Loch, H. Ma, S. Menke, S. Rajagopalan, D. Rousseau, S. Snyder, G. Unal, Calorimeter clustering algorithms: Description and performance, ATL-LARG-PUB-2008-002, 2008, http://cdsweb.cern.ch/record/1099735.

[89] M. Cacciari, G.P. Salam, Phys. Lett. B 659 (2008) 119.

[90] M. Cacciari, G.P. Salam, G. Soyez, Eur. Phys. J. C 72 (2012) 1896.

[91] ATLAS Collaboration, Phys. Lett. B 707 (2012) 438.

[92] ATLAS Collaboration, Improved luminosity determination in pp collisions at $\sqrt{s}$ = 7 TeV using the ATLAS detector at the LHC, ATLAS-CONF-2012-080, 2012, http://cdsweb.cern.ch/record/1460392.

[93] ATLAS Collaboration, Measurement of the total ZZ production cross section in the four-lepton channel using 5.8 fb^{-1} of ATLAS data at $\sqrt{s}$ = 8 TeV, ATLAS-CONF-2012-090, 2012, http://cdsweb.cern.ch/record/1460409.

[94] N. Kauer, G. Passarino, Inadequacy of zero-width approximation for a light Higgs boson signal, arXiv:1206.4803 [hep-ph].

[95] ATLAS Collaboration, Phys. Rev. Lett. 108 (2012) 111803.

[96] ATLAS Collaboration, Eur. Phys. J. C 72 (2012) 1849.

[97] ATLAS Collaboration, Phys. Rev. D 83 (2011) 052005.

[98] ATLAS Collaboration, Phys. Lett. B 705 (2011) 452.

[99] OPAL Collaboration, K. Ackerstaff, et al., Eur. Phys. J. C 4 (1998) 47.

[100] M. Vesterinen, T.R. Wyatt, Nucl. Instrum. Meth. A 602 (2009) 432.

[101] ATLAS Collaboration, Eur. Phys. J. C (2011), submitted for publication, arXiv:1112.6426 [hep-ex].

[102] M. Cacciari, G.P. Salam, G. Soyez, JHEP 0804 (2008) 063.

[103] L.J. Dixon, M.S. Siu, Phys. Rev. Lett. 90 (2003) 252001.

[104] J. Gaiser, Charmonium spectroscopy from radiative decays of the J/Ψ and Ψ', Ph.D. Thesis No. SLAC-R-255, 1982.

[105] S.N. Bernstein, Comm. Soc. Math. Kharkov 13 (1912) 1.

[106] ATLAS Collaboration, Phys. Lett. B 716 (2012) 62, in this issue.

[107] M. Dittmar, H. Dreiner, Phys. Rev. D 55 (1997) 167.

[108] ATLAS Collaboration, Commissioning of the ATLAS high-performance b-tagging algorithms in the 7 TeV collision data, ATLAS-CONF-2011-102, 2011, http://cdsweb.cern.ch/record/1369219.

[109] R.K. Ellis, et al., Nucl. Phys. B 297 (1988) 221.

[110] A.J. Barr, B. Gripaios, C.G. Lester, JHEP 0907 (2009) 072.

[111] ATLAS Collaboration, Phys. Rev. Lett. 108 (2012) 111802.

[112] ATLAS Collaboration, Eur. Phys. J. C 71 (2011) 1728.

[113] ATLAS Collaboration, Eur. Phys. J. C 72 (2012) 1844.

[114] ATLAS Collaboration, Measurement of the b-tag efficiency in a sample of jets containing muons with 5 fb^{-1} of data from the ATLAS detector, ATLAS-CONF-2012-043, 2012, http://cdsweb.cern.ch/record/1435197.

[115] J.M. Campbell, R.K. Ellis, C. Williams, JHEP 1107 (2011) 018.

[116] J. Campbell, R. Ellis, C. Williams, JHEP 1110 (2011) 005.

[117] I. Stewart, F. Tackmann, Phys. Rev. D 85 (2012) 034011.
[118] ATLAS Collaboration, CMS Collaboration, Procedure for the LHC Higgs boson search combination in Summer 2011, ATL-PHYS-PUB-2011-011, CERN-CMS-NOTE-2011-005, 2011, http://cdsweb.cern.ch/record/1375842.
[119] L. Moneta, K. Belasco, K.S. Cranmer, S. Kreiss, A. Lazzaro, et al., The RooStats Project, PoS ACAT2010 (2010) 057, arXiv:1009.1003 [physics.data-an].
[120] K. Cranmer, G. Lewis, L. Moneta, A. Shibata, W. Verkerke, HistFactory: A tool for creating statistical models for use with RooFit and RooStats, CERN-OPEN-2012-016, 2012, http://cdsweb.cern.ch/record/1456844.
[121] W. Verkerke, D. Kirkby, The RooFit toolkit for data modeling, Tech. Rep., SLAC, Stanford, CA, June 2003, arXiv:physics/0306116 [physics.data-an].
[122] G. Cowan, K. Cranmer, E. Gross, O. Vitells, Eur. Phys. J. C 71 (2011) 1554.
[123] A.L. Read, J. Phys. G 28 (2002) 2693.
[124] E. Gross, O. Vitells, Eur. Phys. J. C 70 (2010) 525.
[125] ATLAS Collaboration, Phys. Lett. B (2012), submitted for publication, arXiv: 1205.6744 [hep-ex].
[126] ATLAS Collaboration, Phys. Lett. B (2012), submitted for publication, arXiv: 1206.2443 [hep-ex].
[127] ATLAS Collaboration, Observation of an excess of events in the search for the Standard Model Higgs boson in the gamma–gamma channel with the ATLAS detector, ATLAS-CONF-2012-091, 2012, http://cdsweb.cern.ch/record/1460410.
[128] ATLAS Collaboration, Phys. Lett. B (2012), submitted for publication, arXiv: 1206.6074 [hep-ex].
[129] ATLAS Collaboration, JHEP (2012), in press, arXiv:1206.5971 [hep-ex].
[130] ATLAS Collaboration, Phys. Lett. B (2012), submitted for publication, arXiv: 1207.0210 [hep-ex].
[131] ATLAS Collaboration, Observation of an excess of events in the search for the Standard Model Higgs Boson in the $H \rightarrow WW^{(*)} \rightarrow \ell\nu\ell\nu$ channel with the ATLAS detector, ATLAS-CONF-2012-098, 2012, http://cdsweb.cern.ch/record/1462530.
[132] ATLAS Collaboration, Eur. Phys. J. C 71 (2011) 1630.
[133] ATLAS Collaboration, Luminosity determination in pp collisions at $\sqrt{s} = 7$ TeV using the ATLAS detector in 2011, ATLAS-CONF-2011-116, 2011, http://cdsweb.cern.ch/record/1376384.
[134] M. Botje, J. Butterworth, A. Cooper-Sarkar, A. de Roeck, J. Feltesse, et al., The PDF4LHC Working Group interim recommendations, arXiv:1101.0538 [hep-ph].
[135] A. Martin, W. Stirling, R. Thorne, G. Watt, Eur. Phys. J. C 63 (2009) 189.
[136] R.D. Ball, et al., Nucl. Phys. B 849 (2011) 296.
[137] J.M. Campbell, R.K. Ellis, G. Zanderighi, JHEP 0610 (2006) 028.
[138] ATLAS Collaboration, Observation of an excess of events in the search for the Standard Model Higgs boson with the ATLAS detector at the LHC, ATLAS-CONF-2012-093, 2012, http://cdsweb.cern.ch/record/1460439.
[139] ATLAS Collaboration, CMS Collaboration, Combined Standard Model Higgs boson searches with up to 2.3 fb^{-1} of pp, collisions at $\sqrt{s} = 7$ TeV at the LHC, ATLAS-CONF-2011-157, CMS-PAS-HIG-11-023, 2011, http://cdsweb.cern.ch/record/1399599.
[140] L.D. Landau, Dokl. Akad. Nauk USSR 60 (1948) 207.
[141] C.N. Yang, Phys. Rev. 77 (1950) 242.

ATLAS Collaboration

G. Aad [48], T. Abajyan [21], B. Abbott [111], J. Abdallah [12], S. Abdel Khalek [115], A.A. Abdelalim [49], O. Abdinov [11], R. Aben [105], B. Abi [112], M. Abolins [88], O.S. AbouZeid [158], H. Abramowicz [153], H. Abreu [136], B.S. Acharya [164a,164b], L. Adamczyk [38], D.L. Adams [25], T.N. Addy [56], J. Adelman [176], S. Adomeit [98], P. Adragna [75], T. Adye [129], S. Aefsky [23], J.A. Aguilar-Saavedra [124b,a], M. Agustoni [17], M. Aharrouche [81], S.P. Ahlen [22], F. Ahles [48], A. Ahmad [148], M. Ahsan [41], G. Aielli [133a,133b], T. Akdogan [19a], T.P.A. Åkesson [79], G. Akimoto [155], A.V. Akimov [94], M.S. Alam [2], M.A. Alam [76], J. Albert [169], S. Albrand [55], M. Aleksa [30], I.N. Aleksandrov [64], F. Alessandria [89a], C. Alexa [26a], G. Alexander [153], G. Alexandre [49], T. Alexopoulos [10], M. Alhroob [164a,164c], M. Aliev [16], G. Alimonti [89a], J. Alison [120], B.M.M. Allbrooke [18], P.P. Allport [73], S.E. Allwood-Spiers [53], J. Almond [82], A. Aloisio [102a,102b], R. Alon [172], A. Alonso [79], F. Alonso [70], A. Altheimer [35], B. Alvarez Gonzalez [88], M.G. Alviggi [102a,102b], K. Amako [65], C. Amelung [23], V.V. Ammosov [128,∗], S.P. Amor Dos Santos [124a], A. Amorim [124a,b], N. Amram [153], C. Anastopoulos [30], L.S. Ancu [17], N. Andari [115], T. Andeen [35], C.F. Anders [58b], G. Anders [58a], K.J. Anderson [31], A. Andreazza [89a,89b], V. Andrei [58a], M.-L. Andrieux [55], X.S. Anduaga [70], S. Angelidakis [9], P. Anger [44], A. Angerami [35], F. Anghinolfi [30], A. Anisenkov [107], N. Anjos [124a], A. Annovi [47], A. Antonaki [9], M. Antonelli [47], A. Antonov [96], J. Antos [144b], F. Anulli [132a], M. Aoki [101], S. Aoun [83], L. Aperio Bella [5], R. Apolle [118,c], G. Arabidze [88], I. Aracena [143], Y. Arai [65], A.T.H. Arce [45], S. Arfaoui [148], J.-F. Arguin [93], E. Arik [19a,∗], M. Arik [19a], A.J. Armbruster [87], O. Arnaez [81], V. Arnal [80], C. Arnault [115], A. Artamonov [95], G. Artoni [132a,132b], D. Arutinov [21], S. Asai [155], S. Ask [28], B. Åsman [146a,146b], L. Asquith [6], K. Assamagan [25], A. Astbury [169], M. Atkinson [165], B. Aubert [5], E. Auge [115], K. Augsten [127], M. Aurousseau [145a], G. Avolio [163], R. Avramidou [10], D. Axen [168], G. Azuelos [93,d], Y. Azuma [155], M.A. Baak [30], G. Baccaglioni [89a], C. Bacci [134a,134b], A.M. Bach [15], H. Bachacou [136], K. Bachas [30], M. Backes [49], M. Backhaus [21], J. Backus Mayes [143], E. Badescu [26a], P. Bagnaia [132a,132b], S. Bahinipati [3], Y. Bai [33a], D.C. Bailey [158], T. Bain [158], J.T. Baines [129], O.K. Baker [176], M.D. Baker [25], S. Baker [77], P. Balek [126], E. Banas [39], P. Banerjee [93], Sw. Banerjee [173], D. Banfi [30], A. Bangert [150], V. Bansal [169], H.S. Bansil [18], L. Barak [172], S.P. Baranov [94], A. Barbaro Galtieri [15], T. Barber [48], E.L. Barberio [86], D. Barberis [50a,50b], M. Barbero [21], D.Y. Bardin [64], T. Barillari [99], M. Barisonzi [175], T. Barklow [143], N. Barlow [28], B.M. Barnett [129], R.M. Barnett [15], A. Baroncelli [134a], G. Barone [49], A.J. Barr [118], F. Barreiro [80], J. Barreiro Guimarães da Costa [57], P. Barrillon [115], R. Bartoldus [143], A.E. Barton [71], V. Bartsch [149], A. Basye [165], R.L. Bates [53], L. Batkova [144a], J.R. Batley [28], A. Battaglia [17], M. Battistin [30], F. Bauer [136], H.S. Bawa [143,e], S. Beale [98], T. Beau [78], P.H. Beauchemin [161], R. Beccherle [50a], P. Bechtle [21], H.P. Beck [17], A.K. Becker [175], S. Becker [98], M. Beckingham [138], K.H. Becks [175], A.J. Beddall [19c], A. Beddall [19c], S. Bedikian [176], V.A. Bednyakov [64], C.P. Bee [83], L.J. Beemster [105], M. Begel [25], S. Behar Harpaz [152], P.K. Behera [62], M. Beimforde [99],

C. Belanger-Champagne [85], P.J. Bell [49], W.H. Bell [49], G. Bella [153], L. Bellagamba [20a], M. Bellomo [30], A. Belloni [57], O. Beloborodova [107,f], K. Belotskiy [96], O. Beltramello [30], O. Benary [153], D. Benchekroun [135a], K. Bendtz [146a,146b], N. Benekos [165], Y. Benhammou [153], E. Benhar Noccioli [49], J.A. Benitez Garcia [159b], D.P. Benjamin [45], M. Benoit [115], J.R. Bensinger [23], K. Benslama [130], S. Bentvelsen [105], D. Berge [30], E. Bergeaas Kuutmann [42], N. Berger [5], F. Berghaus [169], E. Berglund [105], J. Beringer [15], P. Bernat [77], R. Bernhard [48], C. Bernius [25], F.U. Bernlochner [169], T. Berry [76], C. Bertella [83], A. Bertin [20a,20b], F. Bertolucci [122a,122b], M.I. Besana [89a,89b], G.J. Besjes [104], N. Besson [136], S. Bethke [99], W. Bhimji [46], R.M. Bianchi [30], M. Bianco [72a,72b], O. Biebel [98], S.P. Bieniek [77], K. Bierwagen [54], J. Biesiada [15], M. Biglietti [134a], H. Bilokon [47], M. Bindi [20a,20b], S. Binet [115], A. Bingul [19c], C. Bini [132a,132b], C. Biscarat [178], B. Bittner [99], K.M. Black [22], R.E. Blair [6], J.-B. Blanchard [136], G. Blanchot [30], T. Blazek [144a], I. Bloch [42], C. Blocker [23], J. Blocki [39], A. Blondel [49], W. Blum [81], U. Blumenschein [54], G.J. Bobbink [105], V.B. Bobrovnikov [107], S.S. Bocchetta [79], A. Bocci [45], C.R. Boddy [118], M. Boehler [48], J. Boek [175], N. Boelaert [36], J.A. Bogaerts [30], A. Bogdanchikov [107], A. Bogouch [90,*], C. Bohm [146a], J. Bohm [125], V. Boisvert [76], T. Bold [38], V. Boldea [26a], N.M. Bolnet [136], M. Bomben [78], M. Bona [75], M. Boonekamp [136], S. Bordoni [78], C. Borer [17], A. Borisov [128], G. Borissov [71], I. Borjanovic [13a], M. Borri [82], S. Borroni [87], V. Bortolotto [134a,134b], K. Bos [105], D. Boscherini [20a], M. Bosman [12], H. Boterenbrood [105], J. Bouchami [93], J. Boudreau [123], E.V. Bouhova-Thacker [71], D. Boumediene [34], C. Bourdarios [115], N. Bousson [83], A. Boveia [31], J. Boyd [30], I.R. Boyko [64], I. Bozovic-Jelisavcic [13b], J. Bracinik [18], P. Branchini [134a], G.W. Brandenburg [57], A. Brandt [8], G. Brandt [118], O. Brandt [54], U. Bratzler [156], B. Brau [84], J.E. Brau [114], H.M. Braun [175,*], S.F. Brazzale [164a,164c], B. Brelier [158], J. Bremer [30], K. Brendlinger [120], R. Brenner [166], S. Bressler [172], D. Britton [53], F.M. Brochu [28], I. Brock [21], R. Brock [88], F. Broggi [89a], C. Bromberg [88], J. Bronner [99], G. Brooijmans [35], T. Brooks [76], W.K. Brooks [32b], G. Brown [82], H. Brown [8], P.A. Bruckman de Renstrom [39], D. Bruncko [144b], R. Bruneliere [48], S. Brunet [60], A. Bruni [20a], G. Bruni [20a], M. Bruschi [20a], T. Buanes [14], Q. Buat [55], F. Bucci [49], J. Buchanan [118], P. Buchholz [141], R.M. Buckingham [118], A.G. Buckley [46], S.I. Buda [26a], I.A. Budagov [64], B. Budick [108], V. Büscher [81], L. Bugge [117], O. Bulekov [96], A.C. Bundock [73], M. Bunse [43], T. Buran [117], H. Burckhart [30], S. Burdin [73], T. Burgess [14], S. Burke [129], E. Busato [34], P. Bussey [53], C.P. Buszello [166], B. Butler [143], J.M. Butler [22], C.M. Buttar [53], J.M. Butterworth [77], W. Buttinger [28], S. Cabrera Urbán [167], D. Caforio [20a,20b], O. Cakir [4a], P. Calafiura [15], G. Calderini [78], P. Calfayan [98], R. Calkins [106], L.P. Caloba [24a], R. Caloi [132a,132b], D. Calvet [34], S. Calvet [34], R. Camacho Toro [34], P. Camarri [133a,133b], D. Cameron [117], L.M. Caminada [15], R. Caminal Armadans [12], S. Campana [30], M. Campanelli [77], V. Canale [102a,102b], F. Canelli [31,g], A. Canepa [159a], J. Cantero [80], R. Cantrill [76], L. Capasso [102a,102b], M.D.M. Capeans Garrido [30], I. Caprini [26a], M. Caprini [26a], D. Capriotti [99], M. Capua [37a,37b], R. Caputo [81], R. Cardarelli [133a], T. Carli [30], G. Carlino [102a], L. Carminati [89a,89b], B. Caron [85], S. Caron [104], E. Carquin [32b], G.D. Carrillo-Montoya [173], A.A. Carter [75], J.R. Carter [28], J. Carvalho [124a,h], D. Casadei [108], M.P. Casado [12], M. Cascella [122a,122b], C. Caso [50a,50b,*], A.M. Castaneda Hernandez [173,i], E. Castaneda-Miranda [173], V. Castillo Gimenez [167], N.F. Castro [124a], G. Cataldi [72a], P. Catastini [57], A. Catinaccio [30], J.R. Catmore [30], A. Cattai [30], G. Cattani [133a,133b], S. Caughron [88], V. Cavaliere [165], P. Cavalleri [78], D. Cavalli [89a], M. Cavalli-Sforza [12], V. Cavasinni [122a,122b], F. Ceradini [134a,134b], A.S. Cerqueira [24b], A. Cerri [30], L. Cerrito [75], F. Cerutti [47], S.A. Cetin [19b], A. Chafaq [135a], D. Chakraborty [106], I. Chalupkova [126], K. Chan [3], P. Chang [165], B. Chapleau [85], J.D. Chapman [28], J.W. Chapman [87], E. Chareyre [78], D.G. Charlton [18], V. Chavda [82], C.A. Chavez Barajas [30], S. Cheatham [85], S. Chekanov [6], S.V. Chekulaev [159a], G.A. Chelkov [64], M.A. Chelstowska [104], C. Chen [63], H. Chen [25], S. Chen [33c], X. Chen [173], Y. Chen [35], Y. Cheng [31], A. Cheplakov [64], R. Cherkaoui El Moursli [135e], V. Chernyatin [25], E. Cheu [7], S.L. Cheung [158], L. Chevalier [136], G. Chiefari [102a,102b], L. Chikovani [51a,*], J.T. Childers [30], A. Chilingarov [71], G. Chiodini [72a], A.S. Chisholm [18], R.T. Chislett [77], A. Chitan [26a], M.V. Chizhov [64], G. Choudalakis [31], S. Chouridou [137], I.A. Christidi [77], A. Christov [48], D. Chromek-Burckhart [30], M.L. Chu [151], J. Chudoba [125], G. Ciapetti [132a,132b], A.K. Ciftci [4a], R. Ciftci [4a], D. Cinca [34], V. Cindro [74], C. Ciocca [20a,20b], A. Ciocio [15], M. Cirilli [87], P. Cirkovic [13b], Z.H. Citron [172], M. Citterio [89a], M. Ciubancan [26a], A. Clark [49], P.J. Clark [46], R.N. Clarke [15], W. Cleland [123], J.C. Clemens [83], B. Clement [55], C. Clement [146a,146b], Y. Coadou [83], M. Cobal [164a,164c], A. Coccaro [138], J. Cochran [63], L. Coffey [23], J.G. Cogan [143], J. Coggeshall [165], E. Cogneras [178], J. Colas [5], S. Cole [106], A.P. Colijn [105], N.J. Collins [18], C. Collins-Tooth [53], J. Collot [55], T. Colombo [119a,119b], G. Colon [84], G. Compostella [99], P. Conde Muiño [124a], E. Coniavitis [166], M.C. Conidi [12], S.M. Consonni [89a,89b], V. Consorti [48],

S. Constantinescu [26a], C. Conta [119a,119b], G. Conti [57], F. Conventi [102a,j], M. Cooke [15], B.D. Cooper [77], A.M. Cooper-Sarkar [118], N.J. Cooper-Smith [76], K. Copic [15], T. Cornelissen [175], M. Corradi [20a], F. Corriveau [85,k], A. Cortes-Gonzalez [165], G. Cortiana [99], G. Costa [89a], M.J. Costa [167], D. Costanzo [139], D. Côté [30], L. Courneyea [169], G. Cowan [76], C. Cowden [28], B.E. Cox [82], K. Cranmer [108], F. Crescioli [122a,122b], M. Cristinziani [21], G. Crosetti [37a,37b], S. Crépé-Renaudin [55], C.-M. Cuciuc [26a], C. Cuenca Almenar [176], T. Cuhadar Donszelmann [139], M. Curatolo [47], C.J. Curtis [18], C. Cuthbert [150], P. Cwetanski [60], H. Czirr [141], P. Czodrowski [44], Z. Czyczula [176], S. D'Auria [53], M. D'Onofrio [73], A. D'Orazio [132a,132b], M.J. Da Cunha Sargedas De Sousa [124a], C. Da Via [82], W. Dabrowski [38], A. Dafinca [118], T. Dai [87], C. Dallapiccola [84], M. Dam [36], M. Dameri [50a,50b], D.S. Damiani [137], H.O. Danielsson [30], V. Dao [49], G. Darbo [50a], G.L. Darlea [26b], J.A. Dassoulas [42], W. Davey [21], T. Davidek [126], N. Davidson [86], R. Davidson [71], E. Davies [118,c], M. Davies [93], O. Davignon [78], A.R. Davison [77], Y. Davygora [58a], E. Dawe [142], I. Dawson [139], R.K. Daya-Ishmukhametova [23], K. De [8], R. de Asmundis [102a], S. De Castro [20a,20b], S. De Cecco [78], J. de Graat [98], N. De Groot [104], P. de Jong [105], C. De La Taille [115], H. De la Torre [80], F. De Lorenzi [63], L. de Mora [71], L. De Nooij [105], D. De Pedis [132a], A. De Salvo [132a], U. De Sanctis [164a,164c], A. De Santo [149], J.B. De Vivie De Regie [115], G. De Zorzi [132a,132b], W.J. Dearnaley [71], R. Debbe [25], C. Debenedetti [46], B. Dechenaux [55], D.V. Dedovich [64], J. Degenhardt [120], C. Del Papa [164a,164c], J. Del Peso [80], T. Del Prete [122a,122b], T. Delemontex [55], M. Deliyergiyev [74], A. Dell'Acqua [30], L. Dell'Asta [22], M. Della Pietra [102a,j], D. della Volpe [102a,102b], M. Delmastro [5], P. Delpierre [83], P.A. Delsart [55], C. Deluca [105], S. Demers [176], M. Demichev [64], B. Demirkoz [12,l], J. Deng [163], S.P. Denisov [128], D. Derendarz [39], J.E. Derkaoui [135d], F. Derue [78], P. Dervan [73], K. Desch [21], E. Devetak [148], P.O. Deviveiros [105], A. Dewhurst [129], B. DeWilde [148], S. Dhaliwal [158], R. Dhullipudi [25,m], A. Di Ciaccio [133a,133b], L. Di Ciaccio [5], C. Di Donato [102a,102b], A. Di Girolamo [30], B. Di Girolamo [30], S. Di Luise [134a,134b], A. Di Mattia [173], B. Di Micco [30], R. Di Nardo [47], A. Di Simone [133a,133b], R. Di Sipio [20a,20b], M.A. Diaz [32a], E.B. Diehl [87], J. Dietrich [42], T.A. Dietzsch [58a], S. Diglio [86], K. Dindar Yagci [40], J. Dingfelder [21], F. Dinut [26a], C. Dionisi [132a,132b], P. Dita [26a], S. Dita [26a], F. Dittus [30], F. Djama [83], T. Djobava [51b], M.A.B. do Vale [24c], A. Do Valle Wemans [124a,n], T.K.O. Doan [5], M. Dobbs [85], R. Dobinson [30,∗], D. Dobos [30], E. Dobson [30,o], J. Dodd [35], C. Doglioni [49], T. Doherty [53], Y. Doi [65,∗], J. Dolejsi [126], I. Dolenc [74], Z. Dolezal [126], B.A. Dolgoshein [96,∗], T. Dohmae [155], M. Donadelli [24d], J. Donini [34], J. Dopke [30], A. Doria [102a], A. Dos Anjos [173], A. Dotti [122a,122b], M.T. Dova [70], J.D. Dowell [18], A.D. Doxiadis [105], A.T. Doyle [53], N. Dressnandt [120], M. Dris [10], J. Dubbert [99], S. Dube [15], E. Duchovni [172], G. Duckeck [98], D. Duda [175], A. Dudarev [30], F. Dudziak [63], M. Dührssen [30], I.P. Duerdoth [82], L. Duflot [115], M.-A. Dufour [85], L. Duguid [76], M. Dunford [58a], H. Duran Yildiz [4a], R. Duxfield [139], M. Dwuznik [38], F. Dydak [30], M. Düren [52], W.L. Ebenstein [45], J. Ebke [98], S. Eckweiler [81], K. Edmonds [81], W. Edson [2], C.A. Edwards [76], N.C. Edwards [53], W. Ehrenfeld [42], T. Eifert [143], G. Eigen [14], K. Einsweiler [15], E. Eisenhandler [75], T. Ekelof [166], M. El Kacimi [135c], M. Ellert [166], S. Elles [5], F. Ellinghaus [81], K. Ellis [75], N. Ellis [30], J. Elmsheuser [98], M. Elsing [30], D. Emeliyanov [129], R. Engelmann [148], A. Engl [98], B. Epp [61], J. Erdmann [54], A. Ereditato [17], D. Eriksson [146a], J. Ernst [2], M. Ernst [25], J. Ernwein [136], D. Errede [165], S. Errede [165], E. Ertel [81], M. Escalier [115], H. Esch [43], C. Escobar [123], X. Espinal Curull [12], B. Esposito [47], F. Etienne [83], A.I. Etienvre [136], E. Etzion [153], D. Evangelakou [54], H. Evans [60], L. Fabbri [20a,20b], C. Fabre [30], R.M. Fakhrutdinov [128], S. Falciano [132a], Y. Fang [173], M. Fanti [89a,89b], A. Farbin [8], A. Farilla [134a], J. Farley [148], T. Farooque [158], S. Farrell [163], S.M. Farrington [170], P. Farthouat [30], F. Fassi [167], P. Fassnacht [30], D. Fassouliotis [9], B. Fatholahzadeh [158], A. Favareto [89a,89b], L. Fayard [115], S. Fazio [37a,37b], R. Febbraro [34], P. Federic [144a], O.L. Fedin [121], W. Fedorko [88], M. Fehling-Kaschek [48], L. Feligioni [83], D. Fellmann [6], C. Feng [33d], E.J. Feng [6], A.B. Fenyuk [128], J. Ferencei [144b], W. Fernando [6], S. Ferrag [53], J. Ferrando [53], V. Ferrara [42], A. Ferrari [166], P. Ferrari [105], R. Ferrari [119a], D.E. Ferreira de Lima [53], A. Ferrer [167], D. Ferrere [49], C. Ferretti [87], A. Ferretto Parodi [50a,50b], M. Fiascaris [31], F. Fiedler [81], A. Filipčič [74], F. Filthaut [104], M. Fincke-Keeler [169], M.C.N. Fiolhais [124a,h], L. Fiorini [167], A. Firan [40], G. Fischer [42], M.J. Fisher [109], M. Flechl [48], I. Fleck [141], J. Fleckner [81], P. Fleischmann [174], S. Fleischmann [175], T. Flick [175], A. Floderus [79], L.R. Flores Castillo [173], M.J. Flowerdew [99], T. Fonseca Martin [17], A. Formica [136], A. Forti [82], D. Fortin [159a], D. Fournier [115], A.J. Fowler [45], H. Fox [71], P. Francavilla [12], M. Franchini [20a,20b], S. Franchino [119a,119b], D. Francis [30], T. Frank [172], M. Franklin [57], S. Franz [30], M. Fraternali [119a,119b], S. Fratina [120], S.T. French [28], C. Friedrich [42], F. Friedrich [44], R. Froeschl [30], D. Froidevaux [30], J.A. Frost [28], C. Fukunaga [156], E. Fullana Torregrosa [30],

B.G. Fulsom [143], J. Fuster [167], C. Gabaldon [30], O. Gabizon [172], S. Gadatsch [105], T. Gadfort [25], S. Gadomski [49], G. Gagliardi [50a,50b], P. Gagnon [60], C. Galea [98], B. Galhardo [124a], E.J. Gallas [118], V. Gallo [17], B.J. Gallop [129], P. Gallus [125], K.K. Gan [109], Y.S. Gao [143,e], A. Gaponenko [15], F. Garberson [176], M. Garcia-Sciveres [15], C. García [167], J.E. García Navarro [167], R.W. Gardner [31], N. Garelli [30], H. Garitaonandia [105], V. Garonne [30], C. Gatti [47], G. Gaudio [119a], B. Gaur [141], L. Gauthier [136], P. Gauzzi [132a,132b], I.L. Gavrilenko [94], C. Gay [168], G. Gaycken [21], E.N. Gazis [10], P. Ge [33d], Z. Gecse [168], C.N.P. Gee [129], D.A.A. Geerts [105], Ch. Geich-Gimbel [21], K. Gellerstedt [146a,146b], C. Gemme [50a], A. Gemmell [53], M.H. Genest [55], S. Gentile [132a,132b], M. George [54], S. George [76], P. Gerlach [175], A. Gershon [153], C. Geweniger [58a], H. Ghazlane [135b], N. Ghodbane [34], B. Giacobbe [20a], S. Giagu [132a,132b], V. Giakoumopoulou [9], V. Giangiobbe [12], F. Gianotti [30], B. Gibbard [25], A. Gibson [158], S.M. Gibson [30], M. Gilchriese [15], O. Gildemeister [30], D. Gillberg [29], A.R. Gillman [129], D.M. Gingrich [3,d], J. Ginzburg [153], N. Giokaris [9], M.P. Giordani [164c], R. Giordano [102a,102b], F.M. Giorgi [16], P. Giovannini [99], P.F. Giraud [136], D. Giugni [89a], M. Giunta [93], P. Giusti [20a], B.K. Gjelsten [117], L.K. Gladilin [97], C. Glasman [80], J. Glatzer [21], A. Glazov [42], K.W. Glitza [175], G.L. Glonti [64], J.R. Goddard [75], J. Godfrey [142], J. Godlewski [30], M. Goebel [42], T. Göpfert [44], C. Goeringer [81], C. Gössling [43], S. Goldfarb [87], T. Golling [176], A. Gomes [124a,b], L.S. Gomez Fajardo [42], R. Gonçalo [76], J. Goncalves Pinto Firmino Da Costa [42], L. Gonella [21], S. González de la Hoz [167], G. Gonzalez Parra [12], M.L. Gonzalez Silva [27], S. Gonzalez-Sevilla [49], J.J. Goodson [148], L. Goossens [30], P.A. Gorbounov [95], H.A. Gordon [25], I. Gorelov [103], G. Gorfine [175], B. Gorini [30], E. Gorini [72a,72b], A. Gorišek [74], E. Gornicki [39], B. Gosdzik [42], A.T. Goshaw [6], M. Gosselink [105], M.I. Gostkin [64], I. Gough Eschrich [163], M. Gouighri [135a], D. Goujdami [135c], M.P. Goulette [49], A.G. Goussiou [138], C. Goy [5], S. Gozpinar [23], I. Grabowska-Bold [38], P. Grafström [20a,20b], K.-J. Grahn [42], E. Gramstad [117], F. Grancagnolo [72a], S. Grancagnolo [16], V. Grassi [148], V. Gratchev [121], N. Grau [35], H.M. Gray [30], J.A. Gray [148], E. Graziani [134a], O.G. Grebenyuk [121], T. Greenshaw [73], Z.D. Greenwood [25,m], K. Gregersen [36], I.M. Gregor [42], P. Grenier [143], J. Griffiths [8], N. Grigalashvili [64], A.A. Grillo [137], S. Grinstein [12], Ph. Gris [34], Y.V. Grishkevich [97], J.-F. Grivaz [115], E. Gross [172], J. Grosse-Knetter [54], J. Groth-Jensen [172], K. Grybel [141], D. Guest [176], C. Guicheney [34], T. Guillemin [115], S. Guindon [54], U. Gul [53], J. Gunther [125], B. Guo [158], J. Guo [35], P. Gutierrez [111], N. Guttman [153], O. Gutzwiller [173], C. Guyot [136], C. Gwenlan [118], C.B. Gwilliam [73], A. Haas [143], S. Haas [30], C. Haber [15], H.K. Hadavand [8], D.R. Hadley [18], P. Haefner [21], F. Hahn [30], S. Haider [30], Z. Hajduk [39], H. Hakobyan [177], D. Hall [118], J. Haller [54], K. Hamacher [175], P. Hamal [113], K. Hamano [86], M. Hamer [54], A. Hamilton [145b,p], S. Hamilton [161], L. Han [33b], K. Hanagaki [116], K. Hanawa [160], M. Hance [15], C. Handel [81], P. Hanke [58a], J.R. Hansen [36], J.B. Hansen [36], J.D. Hansen [36], P.H. Hansen [36], P. Hansson [143], K. Hara [160], A.S. Hard [173], G.A. Hare [137], T. Harenberg [175], S. Harkusha [90], D. Harper [87], R.D. Harrington [46], O.M. Harris [138], J. Hartert [48], F. Hartjes [105], T. Haruyama [65], A. Harvey [56], S. Hasegawa [101], Y. Hasegawa [140], S. Hassani [136], S. Haug [17], M. Hauschild [30], R. Hauser [88], M. Havranek [21], C.M. Hawkes [18], R.J. Hawkings [30], A.D. Hawkins [79], T. Hayakawa [66], T. Hayashi [160], D. Hayden [76], C.P. Hays [118], H.S. Hayward [73], S.J. Haywood [129], S.J. Head [18], V. Hedberg [79], L. Heelan [8], S. Heim [88], B. Heinemann [15], S. Heisterkamp [36], L. Helary [22], C. Heller [98], M. Heller [30], S. Hellman [146a,146b], D. Hellmich [21], C. Helsens [12], R.C.W. Henderson [71], M. Henke [58a], A. Henrichs [54], A.M. Henriques Correia [30], S. Henrot-Versille [115], C. Hensel [54], T. Henß [175], C.M. Hernandez [8], Y. Hernández Jiménez [167], R. Herrberg [16], G. Herten [48], R. Hertenberger [98], L. Hervas [30], G.G. Hesketh [77], N.P. Hessey [105], E. Higón-Rodriguez [167], J.C. Hill [28], K.H. Hiller [42], S. Hillert [21], S.J. Hillier [18], I. Hinchliffe [15], E. Hines [120], M. Hirose [116], F. Hirsch [43], D. Hirschbuehl [175], J. Hobbs [148], N. Hod [153], M.C. Hodgkinson [139], P. Hodgson [139], A. Hoecker [30], M.R. Hoeferkamp [103], J. Hoffman [40], D. Hoffmann [83], M. Hohlfeld [81], M. Holder [141], S.O. Holmgren [146a], T. Holy [127], J.L. Holzbauer [88], T.M. Hong [120], L. Hooft van Huysduynen [108], S. Horner [48], J.-Y. Hostachy [55], S. Hou [151], A. Hoummada [135a], J. Howard [118], J. Howarth [82], I. Hristova [16], J. Hrivnac [115], T. Hryn'ova [5], P.J. Hsu [81], S.-C. Hsu [15], D. Hu [35], Z. Hubacek [127], F. Hubaut [83], F. Huegging [21], A. Huettmann [42], T.B. Huffman [118], E.W. Hughes [35], G. Hughes [71], M. Huhtinen [30], M. Hurwitz [15], N. Huseynov [64,q], J. Huston [88], J. Huth [57], G. Iacobucci [49], G. Iakovidis [10], M. Ibbotson [82], I. Ibragimov [141], L. Iconomidou-Fayard [115], J. Idarraga [115], P. Iengo [102a], O. Igonkina [105], Y. Ikegami [65], M. Ikeno [65], D. Iliadis [154], N. Ilic [158], T. Ince [99], J. Inigo-Golfin [30], P. Ioannou [9], M. Iodice [134a], K. Iordanidou [9], V. Ippolito [132a,132b], A. Irles Quiles [167], C. Isaksson [166], M. Ishino [67], M. Ishitsuka [157], R. Ishmukhametov [109], C. Issever [118], S. Istin [19a], A.V. Ivashin [128], W. Iwanski [39], H. Iwasaki [65], J.M. Izen [41], V. Izzo [102a], B. Jackson [120], J.N. Jackson [73], P. Jackson [1], M.R. Jaekel [30], V. Jain [60], K. Jakobs [48],

S. Jakobsen [36], T. Jakoubek [125], J. Jakubek [127], D.O. Jamin [151], D.K. Jana [111], E. Jansen [77], H. Jansen [30], A. Jantsch [99], M. Janus [48], G. Jarlskog [79], L. Jeanty [57], I. Jen-La Plante [31], D. Jennens [86], P. Jenni [30], A.E. Loevschall-Jensen [36], P. Jež [36], S. Jézéquel [5], M.K. Jha [20a], H. Ji [173], W. Ji [81], J. Jia [148], Y. Jiang [33b], M. Jimenez Belenguer [42], S. Jin [33a], O. Jinnouchi [157], M.D. Joergensen [36], D. Joffe [40], M. Johansen [146a,146b], K.E. Johansson [146a], P. Johansson [139], S. Johnert [42], K.A. Johns [7], K. Jon-And [146a,146b], G. Jones [170], R.W.L. Jones [71], T.J. Jones [73], C. Joram [30], P.M. Jorge [124a], K.D. Joshi [82], J. Jovicevic [147], T. Jovin [13b], X. Ju [173], C.A. Jung [43], R.M. Jungst [30], V. Juranek [125], P. Jussel [61], A. Juste Rozas [12], S. Kabana [17], M. Kaci [167], A. Kaczmarska [39], P. Kadlecik [36], M. Kado [115], H. Kagan [109], M. Kagan [57], E. Kajomovitz [152], S. Kalinin [175], L.V. Kalinovskaya [64], S. Kama [40], N. Kanaya [155], M. Kaneda [30], S. Kaneti [28], T. Kanno [157], V.A. Kantserov [96], J. Kanzaki [65], B. Kaplan [108], A. Kapliy [31], J. Kaplon [30], D. Kar [53], M. Karagounis [21], K. Karakostas [10], M. Karnevskiy [42], V. Kartvelishvili [71], A.N. Karyukhin [128], L. Kashif [173], G. Kasieczka [58b], R.D. Kass [109], A. Kastanas [14], M. Kataoka [5], Y. Kataoka [155], E. Katsoufis [10], J. Katzy [42], V. Kaushik [7], K. Kawagoe [69], T. Kawamoto [155], G. Kawamura [81], M.S. Kayl [105], S. Kazama [155], V.A. Kazanin [107], M.Y. Kazarinov [64], R. Keeler [169], P.T. Keener [120], R. Kehoe [40], M. Keil [54], G.D. Kekelidze [64], J.S. Keller [138], M. Kenyon [53], O. Kepka [125], N. Kerschen [30], B.P. Kerševan [74], S. Kersten [175], K. Kessoku [155], J. Keung [158], F. Khalil-zada [11], H. Khandanyan [146a,146b], A. Khanov [112], D. Kharchenko [64], A. Khodinov [96], A. Khomich [58a], T.J. Khoo [28], G. Khoriauli [21], A. Khoroshilov [175], V. Khovanskiy [95], E. Khramov [64], J. Khubua [51b], H. Kim [146a,146b], S.H. Kim [160], N. Kimura [171], O. Kind [16], B.T. King [73], M. King [66], R.S.B. King [118], J. Kirk [129], A.E. Kiryunin [99], T. Kishimoto [66], D. Kisielewska [38], T. Kitamura [66], T. Kittelmann [123], K. Kiuchi [160], E. Kladiva [144b], M. Klein [73], U. Klein [73], K. Kleinknecht [81], M. Klemetti [85], A. Klier [172], P. Klimek [146a,146b], A. Klimentov [25], R. Klingenberg [43], J.A. Klinger [82], E.B. Klinkby [36], T. Klioutchnikova [30], P.F. Klok [104], S. Klous [105], E.-E. Kluge [58a], T. Kluge [73], P. Kluit [105], S. Kluth [99], E. Kneringer [61], E.B.F.G. Knoops [83], A. Knue [54], B.R. Ko [45], T. Kobayashi [155], M. Kobel [44], M. Kocian [143], P. Kodys [126], K. Köneke [30], A.C. König [104], S. Koenig [81], L. Köpke [81], F. Koetsveld [104], P. Koevesarki [21], T. Koffas [29], E. Koffeman [105], L.A. Kogan [118], S. Kohlmann [175], F. Kohn [54], Z. Kohout [127], T. Kohriki [65], T. Koi [143], G.M. Kolachev [107,*], H. Kolanoski [16], V. Kolesnikov [64], I. Koletsou [89a], J. Koll [88], A.A. Komar [94], Y. Komori [155], T. Kondo [65], T. Kono [42,r], A.I. Kononov [48], R. Konoplich [108,s], N. Konstantinidis [77], R. Kopeliansky [152], S. Koperny [38], K. Korcyl [39], K. Kordas [154], A. Korn [118], A. Korol [107], I. Korolkov [12], E.V. Korolkova [139], V.A. Korotkov [128], O. Kortner [99], S. Kortner [99], V.V. Kostyukhin [21], S. Kotov [99], V.M. Kotov [64], A. Kotwal [45], C. Kourkoumelis [9], V. Kouskoura [154], A. Koutsman [159a], R. Kowalewski [169], T.Z. Kowalski [38], W. Kozanecki [136], A.S. Kozhin [128], V. Kral [127], V.A. Kramarenko [97], G. Kramberger [74], M.W. Krasny [78], A. Krasznahorkay [108], J.K. Kraus [21], S. Kreiss [108], F. Krejci [127], J. Kretzschmar [73], N. Krieger [54], P. Krieger [158], K. Kroeninger [54], H. Kroha [99], J. Kroll [120], J. Kroseberg [21], J. Krstic [13a], U. Kruchonak [64], H. Krüger [21], T. Kruker [17], N. Krumnack [63], Z.V. Krumshteyn [64], A. Kruse [173], T. Kubota [86], S. Kuday [4a], S. Kuehn [48], A. Kugel [58c], T. Kuhl [42], D. Kuhn [61], V. Kukhtin [64], Y. Kulchitsky [90], S. Kuleshov [32b], C. Kummer [98], M. Kuna [78], J. Kunkle [120], A. Kupco [125], H. Kurashige [66], M. Kurata [160], Y.A. Kurochkin [90], V. Kus [125], E.S. Kuwertz [147], M. Kuze [157], J. Kvita [142], R. Kwee [16], A. La Rosa [49], L. La Rotonda [37a,37b], L. Labarga [80], J. Labbe [5], S. Lablak [135a], C. Lacasta [167], F. Lacava [132a,132b], J. Lacey [29], H. Lacker [16], D. Lacour [78], V.R. Lacuesta [167], E. Ladygin [64], R. Lafaye [5], B. Laforge [78], T. Lagouri [176], S. Lai [48], E. Laisne [55], M. Lamanna [30], L. Lambourne [77], C.L. Lampen [7], W. Lampl [7], E. Lancon [136], U. Landgraf [48], M.P.J. Landon [75], V.S. Lang [58a], C. Lange [42], A.J. Lankford [163], F. Lanni [25], K. Lantzsch [175], S. Laplace [78], C. Lapoire [21], J.F. Laporte [136], T. Lari [89a], A. Larner [118], M. Lassnig [30], P. Laurelli [47], V. Lavorini [37a,37b], W. Lavrijsen [15], P. Laycock [73], T. Lazovich [57], O. Le Dortz [78], E. Le Guirriec [83], E. Le Menedeu [12], T. LeCompte [6], F. Ledroit-Guillon [55], H. Lee [105], J.S.H. Lee [116], S.C. Lee [151], L. Lee [176], M. Lefebvre [169], M. Legendre [136], F. Legger [98], C. Leggett [15], M. Lehmacher [21], G. Lehmann Miotto [30], X. Lei [7], M.A.L. Leite [24d], R. Leitner [126], D. Lellouch [172], B. Lemmer [54], V. Lendermann [58a], K.J.C. Leney [145b], T. Lenz [105], G. Lenzen [175], B. Lenzi [30], K. Leonhardt [44], S. Leontsinis [10], F. Lepold [58a], C. Leroy [93], J.-R. Lessard [169], C.G. Lester [28], C.M. Lester [120], J. Levêque [5], D. Levin [87], L.J. Levinson [172], A. Lewis [118], G.H. Lewis [108], A.M. Leyko [21], M. Leyton [16], B. Li [83], H. Li [148], H.L. Li [31], S. Li [33b,t], X. Li [87], Z. Liang [118,u], H. Liao [34], B. Liberti [133a], P. Lichard [30], M. Lichtnecker [98], K. Lie [165], W. Liebig [14], C. Limbach [21], A. Limosani [86], M. Limper [62], S.C. Lin [151,v], F. Linde [105], J.T. Linnemann [88], E. Lipeles [120], A. Lipniacka [14], T.M. Liss [165], D. Lissauer [25], A. Lister [49], A.M. Litke [137], C. Liu [29], D. Liu [151], H. Liu [87], J.B. Liu [87], K. Liu [33b,w], L. Liu [87], M. Liu [33b], Y. Liu [33b], M. Livan [119a,119b], S.S.A. Livermore [118],

A. Lleres [55], J. Llorente Merino [80], S.L. Lloyd [75], E. Lobodzinska [42], P. Loch [7], W.S. Lockman [137], T. Loddenkoetter [21], F.K. Loebinger [82], A. Loginov [176], C.W. Loh [168], T. Lohse [16], K. Lohwasser [48], M. Lokajicek [125], V.P. Lombardo [5], J.D. Long [87], R.E. Long [71], L. Lopes [124a], D. Lopez Mateos [57], J. Lorenz [98], N. Lorenzo Martinez [115], M. Losada [162], P. Loscutoff [15], F. Lo Sterzo [132a,132b], M.J. Losty [159a,∗], X. Lou [41], A. Lounis [115], K.F. Loureiro [162], J. Love [6], P.A. Love [71], A.J. Lowe [143,e], F. Lu [33a], H.J. Lubatti [138], C. Luci [132a,132b], A. Lucotte [55], A. Ludwig [44], D. Ludwig [42], I. Ludwig [48], J. Ludwig [48], F. Luehring [60], G. Luijckx [105], W. Lukas [61], L. Luminari [132a], E. Lund [117], B. Lund-Jensen [147], B. Lundberg [79], J. Lundberg [146a,146b], O. Lundberg [146a,146b], J. Lundquist [36], M. Lungwitz [81], D. Lynn [25], E. Lytken [79], H. Ma [25], L.L. Ma [173], G. Maccarrone [47], A. Macchiolo [99], B. Maček [74], J. Machado Miguens [124a], R. Mackeprang [36], R.J. Madaras [15], H.J. Maddocks [71], W.F. Mader [44], R. Maenner [58c], T. Maeno [25], P. Mättig [175], S. Mättig [81], L. Magnoni [163], E. Magradze [54], K. Mahboubi [48], J. Mahlstedt [105], S. Mahmoud [73], G. Mahout [18], C. Maiani [136], C. Maidantchik [24a], A. Maio [124a,b], S. Majewski [25], Y. Makida [65], N. Makovec [115], P. Mal [136], B. Malaescu [30], Pa. Malecki [39], P. Malecki [39], V.P. Maleev [121], F. Malek [55], U. Mallik [62], D. Malon [6], C. Malone [143], S. Maltezos [10], V. Malyshev [107], S. Malyukov [30], R. Mameghani [98], J. Mamuzic [13b], A. Manabe [65], L. Mandelli [89a], I. Mandić [74], R. Mandrysch [16], J. Maneira [124a], A. Manfredini [99], P.S. Mangeard [88], L. Manhaes de Andrade Filho [24b], J.A. Manjarres Ramos [136], A. Mann [54], P.M. Manning [137], A. Manousakis-Katsikakis [9], B. Mansoulie [136], A. Mapelli [30], L. Mapelli [30], L. March [167], J.F. Marchand [29], F. Marchese [133a,133b], G. Marchiori [78], M. Marcisovsky [125], C.P. Marino [169], F. Marroquim [24a], Z. Marshall [30], F.K. Martens [158], L.F. Marti [17], S. Marti-Garcia [167], B. Martin [30], B. Martin [88], J.P. Martin [93], T.A. Martin [18], V.J. Martin [46], B. Martin dit Latour [49], S. Martin-Haugh [149], M. Martinez [12], V. Martinez Outschoorn [57], A.C. Martyniuk [169], M. Marx [82], F. Marzano [132a], A. Marzin [111], L. Masetti [81], T. Mashimo [155], R. Mashinistov [94], J. Masik [82], A.L. Maslennikov [107], I. Massa [20a,20b], G. Massaro [105], N. Massol [5], P. Mastrandrea [148], A. Mastroberardino [37a,37b], T. Masubuchi [155], P. Matricon [115], H. Matsunaga [155], T. Matsushita [66], C. Mattravers [118,c], J. Maurer [83], S.J. Maxfield [73], A. Mayne [139], R. Mazini [151], M. Mazur [21], L. Mazzaferro [133a,133b], M. Mazzanti [89a], J. Mc Donald [85], S.P. Mc Kee [87], A. McCarn [165], R.L. McCarthy [148], T.G. McCarthy [29], N.A. McCubbin [129], K.W. McFarlane [56,∗], J.A. Mcfayden [139], G. Mchedlidze [51b], T. Mclaughlan [18], S.J. McMahon [129], R.A. McPherson [169,k], A. Meade [84], J. Mechnich [105], M. Mechtel [175], M. Medinnis [42], R. Meera-Lebbai [111], T. Meguro [116], R. Mehdiyev [93], S. Mehlhase [36], A. Mehta [73], K. Meier [58a], B. Meirose [79], C. Melachrinos [31], B.R. Mellado Garcia [173], F. Meloni [89a,89b], L. Mendoza Navas [162], Z. Meng [151,x], A. Mengarelli [20a,20b], S. Menke [99], E. Meoni [161], K.M. Mercurio [57], P. Mermod [49], L. Merola [102a,102b], C. Meroni [89a], F.S. Merritt [31], H. Merritt [109], A. Messina [30,y], J. Metcalfe [25], A.S. Mete [163], C. Meyer [81], C. Meyer [31], J.-P. Meyer [136], J. Meyer [174], J. Meyer [54], T.C. Meyer [30], S. Michal [30], L. Micu [26a], R.P. Middleton [129], S. Migas [73], L. Mijović [136], G. Mikenberg [172], M. Mikestikova [125], M. Mikuž [74], D.W. Miller [31], R.J. Miller [88], W.J. Mills [168], C. Mills [57], A. Milov [172], D.A. Milstead [146a,146b], D. Milstein [172], A.A. Minaenko [128], M. Miñano Moya [167], I.A. Minashvili [64], A.I. Mincer [108], B. Mindur [38], M. Mineev [64], Y. Ming [173], L.M. Mir [12], G. Mirabelli [132a], J. Mitrevski [137], V.A. Mitsou [167], S. Mitsui [65], P.S. Miyagawa [139], J.U. Mjörnmark [79], T. Moa [146a,146b], V. Moeller [28], K. Mönig [42], N. Möser [21], S. Mohapatra [148], W. Mohr [48], R. Moles-Valls [167], A. Molfetas [30], J. Monk [77], E. Monnier [83], J. Montejo Berlingen [12], F. Monticelli [70], S. Monzani [20a,20b], R.W. Moore [3], G.F. Moorhead [86], C. Mora Herrera [49], A. Moraes [53], N. Morange [136], J. Morel [54], G. Morello [37a,37b], D. Moreno [81], M. Moreno Llácer [167], P. Morettini [50a], M. Morgenstern [44], M. Morii [57], A.K. Morley [30], G. Mornacchi [30], J.D. Morris [75], L. Morvaj [101], H.G. Moser [99], M. Mosidze [51b], J. Moss [109], R. Mount [143], E. Mountricha [10,z], S.V. Mouraviev [94,∗], E.J.W. Moyse [84], F. Mueller [58a], J. Mueller [123], K. Mueller [21], T.A. Müller [98], T. Mueller [81], D. Muenstermann [30], Y. Munwes [153], W.J. Murray [129], I. Mussche [105], E. Musto [102a,102b], A.G. Myagkov [128], M. Myska [125], O. Nackenhorst [54], J. Nadal [12], K. Nagai [160], R. Nagai [157], K. Nagano [65], A. Nagarkar [109], Y. Nagasaka [59], M. Nagel [99], A.M. Nairz [30], Y. Nakahama [30], K. Nakamura [155], T. Nakamura [155], I. Nakano [110], G. Nanava [21], A. Napier [161], R. Narayan [58b], M. Nash [77,c], T. Nattermann [21], T. Naumann [42], G. Navarro [162], H.A. Neal [87], P.Yu. Nechaeva [94], T.J. Neep [82], A. Negri [119a,119b], G. Negri [30], M. Negrini [20a], S. Nektarijevic [49], A. Nelson [163], T.K. Nelson [143], S. Nemecek [125], P. Nemethy [108], A.A. Nepomuceno [24a], M. Nessi [30,aa], M.S. Neubauer [165], M. Neumann [175], A. Neusiedl [81], R.M. Neves [108], P. Nevski [25], F.M. Newcomer [120], P.R. Newman [18], V. Nguyen Thi Hong [136], R.B. Nickerson [118],

R. Nicolaidou [136], B. Nicquevert [30], F. Niedercorn [115], J. Nielsen [137], N. Nikiforou [35], A. Nikiforov [16],
V. Nikolaenko [128], I. Nikolic-Audit [78], K. Nikolics [49], K. Nikolopoulos [18], H. Nilsen [48], P. Nilsson [8],
Y. Ninomiya [155], A. Nisati [132a], R. Nisius [99], T. Nobe [157], L. Nodulman [6], M. Nomachi [116], I. Nomidis [154],
S. Norberg [111], M. Nordberg [30], P.R. Norton [129], J. Novakova [126], M. Nozaki [65], L. Nozka [113],
I.M. Nugent [159a], A.-E. Nuncio-Quiroz [21], G. Nunes Hanninger [86], T. Nunnemann [98], E. Nurse [77],
B.J. O'Brien [46], D.C. O'Neil [142], V. O'Shea [53], L.B. Oakes [98], F.G. Oakham [29,d], H. Oberlack [99], J. Ocariz [78],
A. Ochi [66], S. Oda [69], S. Odaka [65], J. Odier [83], H. Ogren [60], A. Oh [82], S.H. Oh [45], C.C. Ohm [30], T. Ohshima [101],
W. Okamura [116], H. Okawa [25], Y. Okumura [31], T. Okuyama [155], A. Olariu [26a], A.G. Olchevski [64],
S.A. Olivares Pino [32a], M. Oliveira [124a,h], D. Oliveira Damazio [25], E. Oliver Garcia [167], D. Olivito [120],
A. Olszewski [39], J. Olszowska [39], A. Onofre [124a,ab], P.U.E. Onyisi [31], C.J. Oram [159a], M.J. Oreglia [31],
Y. Oren [153], D. Orestano [134a,134b], N. Orlando [72a,72b], I. Orlov [107], C. Oropeza Barrera [53], R.S. Orr [158],
B. Osculati [50a,50b], R. Ospanov [120], C. Osuna [12], G. Otero y Garzon [27], J.P. Ottersbach [105], M. Ouchrif [135d],
E.A. Ouellette [169], F. Ould-Saada [117], A. Ouraou [136], Q. Ouyang [33a], A. Ovcharova [15], M. Owen [82],
S. Owen [139], V.E. Ozcan [19a], N. Ozturk [8], A. Pacheco Pages [12], C. Padilla Aranda [12], S. Pagan Griso [15],
E. Paganis [139], C. Pahl [99], F. Paige [25], P. Pais [84], K. Pajchel [117], G. Palacino [159b], C.P. Paleari [7], S. Palestini [30],
D. Pallin [34], A. Palma [124a], J.D. Palmer [18], Y.B. Pan [173], E. Panagiotopoulou [10], J.G. Panduro Vazquez [76],
P. Pani [105], N. Panikashvili [87], S. Panitkin [25], D. Pantea [26a], A. Papadelis [146a], Th.D. Papadopoulou [10],
A. Paramonov [6], D. Paredes Hernandez [34], W. Park [25,ac], M.A. Parker [28], F. Parodi [50a,50b], J.A. Parsons [35],
U. Parzefall [48], S. Pashapour [54], E. Pasqualucci [132a], S. Passaggio [50a], A. Passeri [134a], F. Pastore [134a,134b,*],
Fr. Pastore [76], G. Pásztor [49,ad], S. Pataraia [175], N. Patel [150], J.R. Pater [82], S. Patricelli [102a,102b], T. Pauly [30],
M. Pecsy [144a], S. Pedraza Lopez [167], M.I. Pedraza Morales [173], S.V. Peleganchuk [107], D. Pelikan [166],
H. Peng [33b], B. Penning [31], A. Penson [35], J. Penwell [60], M. Perantoni [24a], K. Perez [35,ae],
T. Perez Cavalcanti [42], E. Perez Codina [159a], M.T. Pérez García-Estañ [167], V. Perez Reale [35], L. Perini [89a,89b],
H. Pernegger [30], R. Perrino [72a], P. Perrodo [5], V.D. Peshekhonov [64], K. Peters [30], B.A. Petersen [30],
J. Petersen [30], T.C. Petersen [36], E. Petit [5], A. Petridis [154], C. Petridou [154], E. Petrolo [132a], F. Petrucci [134a,134b],
D. Petschull [42], M. Petteni [142], R. Pezoa [32b], A. Phan [86], P.W. Phillips [129], G. Piacquadio [30], A. Picazio [49],
E. Piccaro [75], M. Piccinini [20a,20b], S.M. Piec [42], R. Piegaia [27], D.T. Pignotti [109], J.E. Pilcher [31],
A.D. Pilkington [82], J. Pina [124a,b], M. Pinamonti [164a,164c], A. Pinder [118], J.L. Pinfold [3], B. Pinto [124a],
C. Pizio [89a,89b], M. Plamondon [169], M.-A. Pleier [25], E. Plotnikova [64], A. Poblaguev [25], S. Poddar [58a],
F. Podlyski [34], L. Poggioli [115], D. Pohl [21], M. Pohl [49], G. Polesello [119a], A. Policicchio [37a,37b], R. Polifka [158],
A. Polini [20a], J. Poll [75], V. Polychronakos [25], D. Pomeroy [23], K. Pommès [30], L. Pontecorvo [132a], B.G. Pope [88],
G.A. Popeneciu [26a], D.S. Popovic [13a], A. Poppleton [30], X. Portell Bueso [30], G.E. Pospelov [99], S. Pospisil [127],
I.N. Potrap [99], C.J. Potter [149], C.T. Potter [114], G. Poulard [30], J. Poveda [60], V. Pozdnyakov [64], R. Prabhu [77],
P. Pralavorio [83], A. Pranko [15], S. Prasad [30], R. Pravahan [25], S. Prell [63], K. Pretzl [17], D. Price [60], J. Price [73],
L.E. Price [6], D. Prieur [123], M. Primavera [72a], K. Prokofiev [108], F. Prokoshin [32b], S. Protopopescu [25],
J. Proudfoot [6], X. Prudent [44], M. Przybycien [38], H. Przysiezniak [5], S. Psoroulas [21], E. Ptacek [114],
E. Pueschel [84], J. Purdham [87], M. Purohit [25,ac], P. Puzo [115], Y. Pylypchenko [62], J. Qian [87], A. Quadt [54],
D.R. Quarrie [15], W.B. Quayle [173], F. Quinonez [32a], M. Raas [104], S. Raddum [117], V. Radeka [25], V. Radescu [42],
P. Radloff [114], T. Rador [19a], F. Ragusa [89a,89b], G. Rahal [178], A.M. Rahimi [109], D. Rahm [25], S. Rajagopalan [25],
M. Rammensee [48], M. Rammes [141], A.S. Randle-Conde [40], K. Randrianarivony [29], F. Rauscher [98],
T.C. Rave [48], M. Raymond [30], A.L. Read [117], D.M. Rebuzzi [119a,119b], A. Redelbach [174], G. Redlinger [25],
R. Reece [120], K. Reeves [41], E. Reinherz-Aronis [153], A. Reinsch [114], I. Reisinger [43], C. Rembser [30], Z.L. Ren [151],
A. Renaud [115], M. Rescigno [132a], S. Resconi [89a], B. Resende [136], P. Reznicek [98], R. Rezvani [158], R. Richter [99],
E. Richter-Was [5,af], M. Ridel [78], M. Rijpstra [105], M. Rijssenbeek [148], A. Rimoldi [119a,119b], L. Rinaldi [20a],
R.R. Rios [40], I. Riu [12], G. Rivoltella [89a,89b], F. Rizatdinova [112], E. Rizvi [75], S.H. Robertson [85,k],
A. Robichaud-Veronneau [118], D. Robinson [28], J.E.M. Robinson [82], A. Robson [53], J.G. Rocha de Lima [106],
C. Roda [122a,122b], D. Roda Dos Santos [30], A. Roe [54], S. Roe [30], O. Røhne [117], S. Rolli [161], A. Romaniouk [96],
M. Romano [20a,20b], G. Romeo [27], E. Romero Adam [167], N. Rompotis [138], L. Roos [78], E. Ros [167], S. Rosati [132a],
K. Rosbach [49], A. Rose [149], M. Rose [76], G.A. Rosenbaum [158], E.I. Rosenberg [63], P.L. Rosendahl [14],
O. Rosenthal [141], L. Rosselet [49], V. Rossetti [12], E. Rossi [132a,132b], L.P. Rossi [50a], M. Rotaru [26a], I. Roth [172],
J. Rothberg [138], D. Rousseau [115], C.R. Royon [136], A. Rozanov [83], Y. Rozen [152], X. Ruan [33a,ag], F. Rubbo [12],
I. Rubinskiy [42], N. Ruckstuhl [105], V.I. Rud [97], C. Rudolph [44], G. Rudolph [61], F. Rühr [7], A. Ruiz-Martinez [63],

L. Rumyantsev [64], Z. Rurikova [48], N.A. Rusakovich [64], J.P. Rutherfoord [7], P. Ruzicka [125], Y.F. Ryabov [121], M. Rybar [126], G. Rybkin [115], N.C. Ryder [118], A.F. Saavedra [150], I. Sadeh [153], H.F.-W. Sadrozinski [137], R. Sadykov [64], F. Safai Tehrani [132a], H. Sakamoto [155], G. Salamanna [75], A. Salamon [133a], M. Saleem [111], D. Salek [30], D. Salihagic [99], A. Salnikov [143], J. Salt [167], B.M. Salvachua Ferrando [6], D. Salvatore [37a,37b], F. Salvatore [149], A. Salvucci [104], A. Salzburger [30], D. Sampsonidis [154], B.H. Samset [117], A. Sanchez [102a,102b], V. Sanchez Martinez [167], H. Sandaker [14], H.G. Sander [81], M.P. Sanders [98], M. Sandhoff [175], T. Sandoval [28], C. Sandoval [162], R. Sandstroem [99], D.P.C. Sankey [129], A. Sansoni [47], C. Santamarina Rios [85], C. Santoni [34], R. Santonico [133a,133b], H. Santos [124a], J.G. Saraiva [124a], T. Sarangi [173], E. Sarkisyan-Grinbaum [8], F. Sarri [122a,122b], G. Sartisohn [175], O. Sasaki [65], Y. Sasaki [155], N. Sasao [67], I. Satsounkevitch [90], G. Sauvage [5,*], E. Sauvan [5], J.B. Sauvan [115], P. Savard [158,d], V. Savinov [123], D.O. Savu [30], L. Sawyer [25,m], D.H. Saxon [53], J. Saxon [120], C. Sbarra [20a], A. Sbrizzi [20a,20b], D.A. Scannicchio [163], M. Scarcella [150], J. Schaarschmidt [115], P. Schacht [99], D. Schaefer [120], U. Schäfer [81], A. Schaelicke [46], S. Schaepe [21], S. Schaetzel [58b], A.C. Schaffer [115], D. Schaile [98], R.D. Schamberger [148], A.G. Schamov [107], V. Scharf [58a], V.A. Schegelsky [121], D. Scheirich [87], M. Schernau [163], M.I. Scherzer [35], C. Schiavi [50a,50b], J. Schieck [98], M. Schioppa [37a,37b], S. Schlenker [30], P. Schmid [30], E. Schmidt [48], K. Schmieden [21], C. Schmitt [81], S. Schmitt [58b], M. Schmitz [21], B. Schneider [17], U. Schnoor [44], L. Schoeffel [136], A. Schoening [58b], A.L.S. Schorlemmer [54], M. Schott [30], D. Schouten [159a], J. Schovancova [125], M. Schram [85], C. Schroeder [81], N. Schroer [58c], M.J. Schultens [21], J. Schultes [175], H.-C. Schultz-Coulon [58a], H. Schulz [16], M. Schumacher [48], B.A. Schumm [137], Ph. Schune [136], C. Schwanenberger [82], A. Schwartzman [143], Ph. Schwegler [99], Ph. Schwemling [78], R. Schwienhorst [88], R. Schwierz [44], J. Schwindling [136], T. Schwindt [21], M. Schwoerer [5], G. Sciolla [23], W.G. Scott [129], J. Searcy [114], G. Sedov [42], E. Sedykh [121], S.C. Seidel [103], A. Seiden [137], F. Seifert [44], J.M. Seixas [24a], G. Sekhniaidze [102a], S.J. Sekula [40], K.E. Selbach [46], D.M. Seliverstov [121], B. Sellden [146a], G. Sellers [73], M. Seman [144b], N. Semprini-Cesari [20a,20b], C. Serfon [98], L. Serin [115], L. Serkin [54], R. Seuster [159a], H. Severini [111], A. Sfyrla [30], E. Shabalina [54], M. Shamim [114], L.Y. Shan [33a], J.T. Shank [22], Q.T. Shao [86], M. Shapiro [15], P.B. Shatalov [95], K. Shaw [164a,164c], D. Sherman [176], P. Sherwood [77], S. Shimizu [101], M. Shimojima [100], T. Shin [56], M. Shiyakova [64], A. Shmeleva [94], M.J. Shochet [31], D. Short [118], S. Shrestha [63], E. Shulga [96], M.A. Shupe [7], P. Sicho [125], A. Sidoti [132a], F. Siegert [48], Dj. Sijacki [13a], O. Silbert [172], J. Silva [124a], Y. Silver [153], D. Silverstein [143], S.B. Silverstein [146a], V. Simak [127], O. Simard [136], Lj. Simic [13a], S. Simion [115], E. Simioni [81], B. Simmons [77], R. Simoniello [89a,89b], M. Simonyan [36], P. Sinervo [158], N.B. Sinev [114], V. Sipica [141], G. Siragusa [174], A. Sircar [25], A.N. Sisakyan [64,*], S.Yu. Sivoklokov [97], J. Sjölin [146a,146b], T.B. Sjursen [14], L.A. Skinnari [15], H.P. Skottowe [57], K. Skovpen [107], P. Skubic [111], M. Slater [18], T. Slavicek [127], K. Sliwa [161], V. Smakhtin [172], B.H. Smart [46], L. Smestad [117], S.Yu. Smirnov [96], Y. Smirnov [96], L.N. Smirnova [97], O. Smirnova [79], B.C. Smith [57], D. Smith [143], K.M. Smith [53], M. Smizanska [71], K. Smolek [127], A.A. Snesarev [94], S.W. Snow [82], J. Snow [111], S. Snyder [25], R. Sobie [169,k], J. Sodomka [127], A. Soffer [153], C.A. Solans [167], M. Solar [127], J. Solc [127], E.Yu. Soldatov [96], U. Soldevila [167], E. Solfaroli Camillocci [132a,132b], A.A. Solodkov [128], O.V. Solovyanov [128], V. Solovyev [121], N. Soni [1], V. Sopko [127], B. Sopko [127], M. Sosebee [8], R. Soualah [164a,164c], A. Soukharev [107], S. Spagnolo [72a,72b], F. Spanò [76], W.R. Spearman [57], R. Spighi [20a], G. Spigo [30], R. Spiwoks [30], M. Spousta [126,ah], T. Spreitzer [158], B. Spurlock [8], R.D. St. Denis [53], J. Stahlman [120], R. Stamen [58a], E. Stanecka [39], R.W. Stanek [6], C. Stanescu [134a], M. Stanescu-Bellu [42], M.M. Stanitzki [42], S. Stapnes [117], E.A. Starchenko [128], J. Stark [55], P. Staroba [125], P. Starovoitov [42], R. Staszewski [39], A. Staude [98], P. Stavina [144a,*], G. Steele [53], P. Steinbach [44], P. Steinberg [25], I. Stekl [127], B. Stelzer [142], H.J. Stelzer [88], O. Stelzer-Chilton [159a], H. Stenzel [52], S. Stern [99], G.A. Stewart [30], J.A. Stillings [21], M.C. Stockton [85], K. Stoerig [48], G. Stoicea [26a], S. Stonjek [99], P. Strachota [126], A.R. Stradling [8], A. Straessner [44], J. Strandberg [147], S. Strandberg [146a,146b], A. Strandlie [117], M. Strang [109], E. Strauss [143], M. Strauss [111], P. Strizenec [144b], R. Ströhmer [174], D.M. Strom [114], J.A. Strong [76,*], R. Stroynowski [40], B. Stugu [14], I. Stumer [25,*], J. Stupak [148], P. Sturm [175], N.A. Styles [42], D.A. Soh [151,u], D. Su [143], HS. Subramania [3], R. Subramaniam [25], A. Succurro [12], Y. Sugaya [116], C. Suhr [106], M. Suk [126], V.V. Sulin [94], S. Sultansoy [4d], T. Sumida [67], X. Sun [55], J.E. Sundermann [48], K. Suruliz [139], G. Susinno [37a,37b], M.R. Sutton [149], Y. Suzuki [65], Y. Suzuki [66], M. Svatos [125], S. Swedish [168], I. Sykora [144a], T. Sykora [126], J. Sánchez [167], D. Ta [105], K. Tackmann [42], A. Taffard [163], R. Tafirout [159a], N. Taiblum [153], Y. Takahashi [101], H. Takai [25], R. Takashima [68], H. Takeda [66], T. Takeshita [140], Y. Takubo [65], M. Talby [83], A. Talyshev [107,f], M.C. Tamsett [25], K.G. Tan [86], J. Tanaka [155], R. Tanaka [115], S. Tanaka [131], S. Tanaka [65], A.J. Tanasijczuk [142],

K. Tani [66], N. Tannoury [83], S. Tapprogge [81], D. Tardif [158], S. Tarem [152], F. Tarrade [29], G.F. Tartarelli [89a], P. Tas [126], M. Tasevsky [125], E. Tassi [37a,37b], M. Tatarkhanov [15], Y. Tayalati [135d], C. Taylor [77], F.E. Taylor [92], G.N. Taylor [86], W. Taylor [159b], M. Teinturier [115], F.A. Teischinger [30], M. Teixeira Dias Castanheira [75], P. Teixeira-Dias [76], K.K. Temming [48], H. Ten Kate [30], P.K. Teng [151], S. Terada [65], K. Terashi [155], J. Terron [80], M. Testa [47], R.J. Teuscher [158,k], J. Therhaag [21], T. Theveneaux-Pelzer [78], S. Thoma [48], J.P. Thomas [18], E.N. Thompson [35], P.D. Thompson [18], P.D. Thompson [158], A.S. Thompson [53], L.A. Thomsen [36], E. Thomson [120], M. Thomson [28], W.M. Thong [86], R.P. Thun [87], F. Tian [35], M.J. Tibbetts [15], T. Tic [125], V.O. Tikhomirov [94], Y.A. Tikhonov [107,f], S. Timoshenko [96], E. Tiouchichine [83], P. Tipton [176], S. Tisserant [83], T. Todorov [5], S. Todorova-Nova [161], B. Toggerson [163], J. Tojo [69], S. Tokár [144a], K. Tokushuku [65], K. Tollefson [88], M. Tomoto [101], L. Tompkins [31], K. Toms [103], A. Tonoyan [14], C. Topfel [17], N.D. Topilin [64], I. Torchiani [30], E. Torrence [114], H. Torres [78], E. Torró Pastor [167], J. Toth [83,ad], F. Touchard [83], D.R. Tovey [139], T. Trefzger [174], L. Tremblet [30], A. Tricoli [30], I.M. Trigger [159a], G. Trilling [15], S. Trincaz-Duvoid [78], M.F. Tripiana [70], N. Triplett [25], W. Trischuk [158], B. Trocmé [55], C. Troncon [89a], M. Trottier-McDonald [142], M. Trzebinski [39], A. Trzupek [39], C. Tsarouchas [30], J.C.-L. Tseng [118], M. Tsiakiris [105], P.V. Tsiareshka [90], D. Tsionou [5,ai], G. Tsipolitis [10], S. Tsiskaridze [12], V. Tsiskaridze [48], E.G. Tskhadadze [51a], I.I. Tsukerman [95], V. Tsulaia [15], J.-W. Tsung [21], S. Tsuno [65], D. Tsybychev [148], A. Tua [139], A. Tudorache [26a], V. Tudorache [26a], J.M. Tuggle [31], M. Turala [39], D. Turecek [127], I. Turk Cakir [4e], E. Turlay [105], R. Turra [89a,89b], P.M. Tuts [35], A. Tykhonov [74], M. Tylmad [146a,146b], M. Tyndel [129], G. Tzanakos [9], K. Uchida [21], I. Ueda [155], R. Ueno [29], M. Ugland [14], M. Uhlenbrock [21], M. Uhrmacher [54], F. Ukegawa [160], G. Unal [30], A. Undrus [25], G. Unel [163], Y. Unno [65], D. Urbaniec [35], P. Urquijo [21], G. Usai [8], M. Uslenghi [119a,119b], L. Vacavant [83], V. Vacek [127], B. Vachon [85], S. Vahsen [15], J. Valenta [125], S. Valentinetti [20a,20b], A. Valero [167], S. Valkar [126], E. Valladolid Gallego [167], S. Vallecorsa [152], J.A. Valls Ferrer [167], R. Van Berg [120], P.C. Van Der Deijl [105], R. van der Geer [105], H. van der Graaf [105], R. Van Der Leeuw [105], E. van der Poel [105], D. van der Ster [30], N. van Eldik [30], P. van Gemmeren [6], I. van Vulpen [105], M. Vanadia [99], W. Vandelli [30], R. Vanguri [120], A. Vaniachine [6], P. Vankov [42], F. Vannucci [78], R. Vari [132a], T. Varol [84], D. Varouchas [15], A. Vartapetian [8], K.E. Varvell [150], V.I. Vassilakopoulos [56], F. Vazeille [34], T. Vazquez Schroeder [54], G. Vegni [89a,89b], J.J. Veillet [115], F. Veloso [124a], R. Veness [30], S. Veneziano [132a], A. Ventura [72a,72b], D. Ventura [84], M. Venturi [48], N. Venturi [158], V. Vercesi [119a], M. Verducci [138], W. Verkerke [105], J.C. Vermeulen [105], A. Vest [44], M.C. Vetterli [142,d], I. Vichou [165], T. Vickey [145b,aj], O.E. Vickey Boeriu [145b], G.H.A. Viehhauser [118], S. Viel [168], M. Villa [20a,20b], M. Villaplana Perez [167], E. Vilucchi [47], M.G. Vincter [29], E. Vinek [30], V.B. Vinogradov [64], M. Virchaux [136,*], J. Virzi [15], O. Vitells [172], M. Viti [42], I. Vivarelli [48], F. Vives Vaque [3], S. Vlachos [10], D. Vladoiu [98], M. Vlasak [127], A. Vogel [21], P. Vokac [127], G. Volpi [47], M. Volpi [86], G. Volpini [89a], H. von der Schmitt [99], H. von Radziewski [48], E. von Toerne [21], V. Vorobel [126], V. Vorwerk [12], M. Vos [167], R. Voss [30], T.T. Voss [175], J.H. Vossebeld [73], N. Vranjes [136], M. Vranjes Milosavljevic [105], V. Vrba [125], M. Vreeswijk [105], T. Vu Anh [48], R. Vuillermet [30], I. Vukotic [31], W. Wagner [175], P. Wagner [120], H. Wahlen [175], S. Wahrmund [44], J. Wakabayashi [101], S. Walch [87], J. Walder [71], R. Walker [98], W. Walkowiak [141], R. Wall [176], P. Waller [73], B. Walsh [176], C. Wang [45], F. Wang [173], H. Wang [173], H. Wang [33b,ak], J. Wang [151], J. Wang [55], R. Wang [103], S.M. Wang [151], T. Wang [21], A. Warburton [85], C.P. Ward [28], D.R. Wardrope [77], M. Warsinsky [48], A. Washbrook [46], C. Wasicki [42], I. Watanabe [66], P.M. Watkins [18], A.T. Watson [18], I.J. Watson [150], M.F. Watson [18], G. Watts [138], S. Watts [82], A.T. Waugh [150], B.M. Waugh [77], M.S. Weber [17], P. Weber [54], J.S. Webster [31], A.R. Weidberg [118], P. Weigell [99], J. Weingarten [54], C. Weiser [48], P.S. Wells [30], T. Wenaus [25], D. Wendland [16], Z. Weng [151,u], T. Wengler [30], S. Wenig [30], N. Wermes [21], M. Werner [48], P. Werner [30], M. Werth [163], M. Wessels [58a], J. Wetter [161], C. Weydert [55], K. Whalen [29], S.J. Wheeler-Ellis [163], A. White [8], M.J. White [86], S. White [122a,122b], S.R. Whitehead [118], D. Whiteson [163], D. Whittington [60], F. Wicek [115], D. Wicke [175], F.J. Wickens [129], W. Wiedenmann [173], M. Wielers [129], P. Wienemann [21], C. Wiglesworth [75], L.A.M. Wiik-Fuchs [48], P.A. Wijeratne [77], A. Wildauer [99], M.A. Wildt [42,r], I. Wilhelm [126], H.G. Wilkens [30], J.Z. Will [98], E. Williams [35], H.H. Williams [120], W. Willis [35], S. Willocq [84], J.A. Wilson [18], M.G. Wilson [143], A. Wilson [87], I. Wingerter-Seez [5], S. Winkelmann [48], F. Winklmeier [30], M. Wittgen [143], S.J. Wollstadt [81], M.W. Wolter [39], H. Wolters [124a,h], W.C. Wong [41], G. Wooden [87], B.K. Wosiek [39], J. Wotschack [30], M.J. Woudstra [82], K.W. Wozniak [39], K. Wraight [53], M. Wright [53], B. Wrona [73], S.L. Wu [173], X. Wu [49], Y. Wu [33b,al], E. Wulf [35], B.M. Wynne [46], S. Xella [36], M. Xiao [136], S. Xie [48], C. Xu [33b,z], D. Xu [139], B. Yabsley [150], S. Yacoob [145a,am], M. Yamada [65], H. Yamaguchi [155], Y. Yamaguchi [155], A. Yamamoto [65],

K. Yamamoto [63], S. Yamamoto [155], T. Yamamura [155], T. Yamanaka [155], T. Yamazaki [155], Y. Yamazaki [66], Z. Yan [22], H. Yang [87], H. Yang [173], U.K. Yang [82], Y. Yang [109], Z. Yang [146a,146b], S. Yanush [91], L. Yao [33a], Y. Yao [15], Y. Yasu [65], G.V. Ybeles Smit [130], J. Ye [40], S. Ye [25], M. Yilmaz [4c], R. Yoosoofmiya [123], K. Yorita [171], R. Yoshida [6], K. Yoshihara [155], C. Young [143], C.J. Young [118], S. Youssef [22], D. Yu [25], J. Yu [8], J. Yu [112], L. Yuan [66], A. Yurkewicz [106], M. Byszewski [30], B. Zabinski [39], R. Zaidan [62], A.M. Zaitsev [128], Z. Zajacova [30], L. Zanello [132a,132b], D. Zanzi [99], A. Zaytsev [25], C. Zeitnitz [175], M. Zeman [125], A. Zemla [39], C. Zendler [21], O. Zenin [128], T. Ženiš [144a], Z. Zinonos [122a,122b], D. Zerwas [115], G. Zevi della Porta [57], D. Zhang [33b,ak], H. Zhang [88], J. Zhang [6], X. Zhang [33d], Z. Zhang [115], L. Zhao [108], Z. Zhao [33b], A. Zhemchugov [64], J. Zhong [118], B. Zhou [87], N. Zhou [163], Y. Zhou [151], C.G. Zhu [33d], H. Zhu [42], J. Zhu [87], Y. Zhu [33b], X. Zhuang [98], V. Zhuravlov [99], D. Zieminska [60], N.I. Zimin [64], R. Zimmermann [21], S. Zimmermann [21], S. Zimmermann [48], M. Ziolkowski [141], R. Zitoun [5], L. Živković [35], V.V. Zmouchko [128,*], G. Zobernig [173], A. Zoccoli [20a,20b], M. zur Nedden [16], V. Zutshi [106], L. Zwalinski [30]

[1] School of Chemistry and Physics, University of Adelaide, Adelaide, Australia
[2] Physics Department, SUNY Albany, Albany, NY, United States
[3] Department of Physics, University of Alberta, Edmonton, AB, Canada
[4] (a) Department of Physics, Ankara University, Ankara; (b) Department of Physics, Dumlupinar University, Kutahya; (c) Department of Physics, Gazi University, Ankara; (d) Division of Physics, TOBB University of Economics and Technology, Ankara; (e) Turkish Atomic Energy Authority, Ankara, Turkey
[5] LAPP, CNRS/IN2P3 and Université de Savoie, Annecy-le-Vieux, France
[6] High Energy Physics Division, Argonne National Laboratory, Argonne, IL, United States
[7] Department of Physics, University of Arizona, Tucson, AZ, United States
[8] Department of Physics, The University of Texas at Arlington, Arlington, TX, United States
[9] Physics Department, University of Athens, Athens, Greece
[10] Physics Department, National Technical University of Athens, Zografou, Greece
[11] Institute of Physics, Azerbaijan Academy of Sciences, Baku, Azerbaijan
[12] Institut de Física d'Altes Energies and Departament de Física de la Universitat Autònoma de Barcelona and ICREA, Barcelona, Spain
[13] (a) Institute of Physics, University of Belgrade, Belgrade; (b) Vinca Institute of Nuclear Sciences, University of Belgrade, Belgrade, Serbia
[14] Department for Physics and Technology, University of Bergen, Bergen, Norway
[15] Physics Division, Lawrence Berkeley National Laboratory and University of California, Berkeley, CA, United States
[16] Department of Physics, Humboldt University, Berlin, Germany
[17] Albert Einstein Center for Fundamental Physics and Laboratory for High Energy Physics, University of Bern, Bern, Switzerland
[18] School of Physics and Astronomy, University of Birmingham, Birmingham, United Kingdom
[19] (a) Department of Physics, Bogazici University, Istanbul; (b) Division of Physics, Dogus University, Istanbul; (c) Department of Physics Engineering, Gaziantep University, Gaziantep; (d) Department of Physics, Istanbul Technical University, Istanbul, Turkey
[20] (a) INFN Sezione di Bologna; (b) Dipartimento di Fisica, Università di Bologna, Bologna, Italy
[21] Physikalisches Institut, University of Bonn, Bonn, Germany
[22] Department of Physics, Boston University, Boston, MA, United States
[23] Department of Physics, Brandeis University, Waltham, MA, United States
[24] (a) Universidade Federal do Rio De Janeiro COPPE/EE/IF, Rio de Janeiro; (b) Federal University of Juiz de Fora (UFJF), Juiz de Fora; (c) Federal University of Sao Joao del Rei (UFSJ), Sao Joao del Rei; (d) Instituto de Fisica, Universidade de Sao Paulo, Sao Paulo, Brazil
[25] Physics Department, Brookhaven National Laboratory, Upton, NY, United States
[26] (a) National Institute of Physics and Nuclear Engineering, Bucharest; (b) University Politehnica Bucharest, Bucharest; (c) West University in Timisoara, Timisoara, Romania
[27] Departamento de Física, Universidad de Buenos Aires, Buenos Aires, Argentina
[28] Cavendish Laboratory, University of Cambridge, Cambridge, United Kingdom
[29] Department of Physics, Carleton University, Ottawa, ON, Canada
[30] CERN, Geneva, Switzerland
[31] Enrico Fermi Institute, University of Chicago, Chicago, IL, United States
[32] (a) Departamento de Física, Pontificia Universidad Católica de Chile, Santiago; (b) Departamento de Física, Universidad Técnica Federico Santa María, Valparaíso, Chile
[33] (a) Institute of High Energy Physics, Chinese Academy of Sciences, Beijing; (b) Department of Modern Physics, University of Science and Technology of China, Anhui; (c) Department of Physics, Nanjing University, Jiangsu; (d) School of Physics, Shandong University, Shandong, China
[34] Laboratoire de Physique Corpusculaire, Clermont Université and Université Blaise Pascal and CNRS/IN2P3, Clermont-Ferrand, France
[35] Nevis Laboratory, Columbia University, Irvington, NY, United States
[36] Niels Bohr Institute, University of Copenhagen, Kobenhavn, Denmark
[37] (a) INFN Gruppo Collegato di Cosenza; (b) Dipartimento di Fisica, Università della Calabria, Arcavata di Rende, Italy
[38] AGH University of Science and Technology, Faculty of Physics and Applied Computer Science, Krakow, Poland
[39] The Henryk Niewodniczanski Institute of Nuclear Physics, Polish Academy of Sciences, Krakow, Poland
[40] Physics Department, Southern Methodist University, Dallas, TX, United States
[41] Physics Department, University of Texas at Dallas, Richardson, TX, United States
[42] DESY, Hamburg and Zeuthen, Germany
[43] Institut für Experimentelle Physik IV, Technische Universität Dortmund, Dortmund, Germany
[44] Institut für Kern- und Teilchenphysik, Technical University Dresden, Dresden, Germany
[45] Department of Physics, Duke University, Durham, NC, United States
[46] SUPA – School of Physics and Astronomy, University of Edinburgh, Edinburgh, United Kingdom
[47] INFN Laboratori Nazionali di Frascati, Frascati, Italy
[48] Fakultät für Mathematik und Physik, Albert-Ludwigs-Universität, Freiburg, Germany
[49] Section de Physique, Université de Genève, Geneva, Switzerland
[50] (a) INFN Sezione di Genova; (b) Dipartimento di Fisica, Università di Genova, Genova, Italy
[51] (a) E. Andronikashvili Institute of Physics, Tbilisi State University, Tbilisi; (b) High Energy Physics Institute, Tbilisi State University, Tbilisi, Georgia
[52] II Physikalisches Institut, Justus-Liebig-Universität Giessen, Giessen, Germany
[53] SUPA – School of Physics and Astronomy, University of Glasgow, Glasgow, United Kingdom
[54] II Physikalisches Institut, Georg-August-Universität, Göttingen, Germany
[55] Laboratoire de Physique Subatomique et de Cosmologie, Université Joseph Fourier and CNRS/IN2P3 and Institut National Polytechnique de Grenoble, Grenoble, France
[56] Department of Physics, Hampton University, Hampton, VA, United States

[57] Laboratory for Particle Physics and Cosmology, Harvard University, Cambridge, MA, United States

[58] [a] Kirchhoff-Institut für Physik, Ruprecht-Karls-Universität Heidelberg, Heidelberg; [b] Physikalisches Institut, Ruprecht-Karls-Universität Heidelberg, Heidelberg; [c] ZITI Institut für technische Informatik, Ruprecht-Karls-Universität Heidelberg, Mannheim, Germany

[59] Faculty of Applied Information Science, Hiroshima Institute of Technology, Hiroshima, Japan

[60] Department of Physics, Indiana University, Bloomington, IN, United States

[61] Institut für Astro- und Teilchenphysik, Leopold-Franzens-Universität, Innsbruck, Austria

[62] University of Iowa, Iowa City, IA, United States

[63] Department of Physics and Astronomy, Iowa State University, Ames, IA, United States

[64] Joint Institute for Nuclear Research, JINR Dubna, Dubna, Russia

[65] KEK, High Energy Accelerator Research Organization, Tsukuba, Japan

[66] Graduate School of Science, Kobe University, Kobe, Japan

[67] Faculty of Science, Kyoto University, Kyoto, Japan

[68] Kyoto University of Education, Kyoto, Japan

[69] Department of Physics, Kyushu University, Fukuoka, Japan

[70] Instituto de Física La Plata, Universidad Nacional de La Plata and CONICET, La Plata, Argentina

[71] Physics Department, Lancaster University, Lancaster, United Kingdom

[72] [a] INFN Sezione di Lecce; [b] Dipartimento di Matematica e Fisica, Università del Salento, Lecce, Italy

[73] Oliver Lodge Laboratory, University of Liverpool, Liverpool, United Kingdom

[74] Department of Physics, Jožef Stefan Institute and University of Ljubljana, Ljubljana, Slovenia

[75] School of Physics and Astronomy, Queen Mary University of London, London, United Kingdom

[76] Department of Physics, Royal Holloway University of London, Surrey, United Kingdom

[77] Department of Physics and Astronomy, University College London, London, United Kingdom

[78] Laboratoire de Physique Nucléaire et de Hautes Energies, UPMC and Université Paris-Diderot and CNRS/IN2P3, Paris, France

[79] Fysiska institutionen, Lunds universitet, Lund, Sweden

[80] Departamento de Fisica Teorica C-15, Universidad Autonoma de Madrid, Madrid, Spain

[81] Institut für Physik, Universität Mainz, Mainz, Germany

[82] School of Physics and Astronomy, University of Manchester, Manchester, United Kingdom

[83] CPPM, Aix-Marseille Université and CNRS/IN2P3, Marseille, France

[84] Department of Physics, University of Massachusetts, Amherst, MA, United States

[85] Department of Physics, McGill University, Montreal, QC, Canada

[86] School of Physics, University of Melbourne, Victoria, Australia

[87] Department of Physics, The University of Michigan, Ann Arbor, MI, United States

[88] Department of Physics and Astronomy, Michigan State University, East Lansing, MI, United States

[89] [a] INFN Sezione di Milano; [b] Dipartimento di Fisica, Università di Milano, Milano, Italy

[90] B.I. Stepanov Institute of Physics, National Academy of Sciences of Belarus, Minsk, Belarus

[91] National Scientific and Educational Centre for Particle and High Energy Physics, Minsk, Belarus

[92] Department of Physics, Massachusetts Institute of Technology, Cambridge, MA, United States

[93] Group of Particle Physics, University of Montreal, Montreal, QC, Canada

[94] P.N. Lebedev Institute of Physics, Academy of Sciences, Moscow, Russia

[95] Institute for Theoretical and Experimental Physics (ITEP), Moscow, Russia

[96] Moscow Engineering and Physics Institute (MEPhI), Moscow, Russia

[97] Skobeltsyn Institute of Nuclear Physics, Lomonosov Moscow State University, Moscow, Russia

[98] Fakultät für Physik, Ludwig-Maximilians-Universität München, München, Germany

[99] Max-Planck-Institut für Physik (Werner-Heisenberg-Institut), München, Germany

[100] Nagasaki Institute of Applied Science, Nagasaki, Japan

[101] Graduate School of Science and Kobayashi-Maskawa Institute, Nagoya University, Nagoya, Japan

[102] [a] INFN Sezione di Napoli; [b] Dipartimento di Scienze Fisiche, Università di Napoli, Napoli, Italy

[103] Department of Physics and Astronomy, University of New Mexico, Albuquerque, NM, United States

[104] Institute for Mathematics, Astrophysics and Particle Physics, Radboud University Nijmegen/Nikhef, Nijmegen, Netherlands

[105] Nikhef National Institute for Subatomic Physics and University of Amsterdam, Amsterdam, Netherlands

[106] Department of Physics, Northern Illinois University, DeKalb, IL, United States

[107] Budker Institute of Nuclear Physics, SB RAS, Novosibirsk, Russia

[108] Department of Physics, New York University, New York, NY, United States

[109] Ohio State University, Columbus, OH, United States

[110] Faculty of Science, Okayama University, Okayama, Japan

[111] Homer L. Dodge Department of Physics and Astronomy, University of Oklahoma, Norman, OK, United States

[112] Department of Physics, Oklahoma State University, Stillwater, OK, United States

[113] Palacký University, RCPTM, Olomouc, Czech Republic

[114] Center for High Energy Physics, University of Oregon, Eugene, OR, United States

[115] LAL, Université Paris-Sud and CNRS/IN2P3, Orsay, France

[116] Graduate School of Science, Osaka University, Osaka, Japan

[117] Department of Physics, University of Oslo, Oslo, Norway

[118] Department of Physics, Oxford University, Oxford, United Kingdom

[119] [a] INFN Sezione di Pavia; [b] Dipartimento di Fisica, Università di Pavia, Pavia, Italy

[120] Department of Physics, University of Pennsylvania, Philadelphia PA, United States

[121] Petersburg Nuclear Physics Institute, Gatchina, Russia

[122] [a] INFN Sezione di Pisa; [b] Dipartimento di Fisica E. Fermi, Università di Pisa, Pisa, Italy

[123] Department of Physics and Astronomy, University of Pittsburgh, Pittsburgh, PA, United States

[124] [a] Laboratorio de Instrumentacao e Fisica Experimental de Particulas – LIP, Lisboa, Portugal; [b] Departamento de Fisica Teorica y del Cosmos and CAFPE, Universidad de Granada, Granada, Spain

[125] Institute of Physics, Academy of Sciences of the Czech Republic, Praha, Czech Republic

[126] Faculty of Mathematics and Physics, Charles University in Prague, Praha, Czech Republic

[127] Czech Technical University in Prague, Praha, Czech Republic

[128] State Research Center Institute for High Energy Physics, Protvino, Russia

[129] Particle Physics Department, Rutherford Appleton Laboratory, Didcot, United Kingdom

[130] Physics Department, University of Regina, Regina, SK, Canada

[131] Ritsumeikan University, Kusatsu, Shiga, Japan

[132] [a] INFN Sezione di Roma I; [b] Dipartimento di Fisica, Università La Sapienza, Roma, Italy

[133] [a] INFN Sezione di Roma Tor Vergata; [b] Dipartimento di Fisica, Università di Roma Tor Vergata, Roma, Italy

134 *(a) INFN Sezione di Roma Tre; (b) Dipartimento di Fisica, Università Roma Tre, Roma, Italy*

135 *(a) Faculté des Sciences Ain Chock, Réseau Universitaire de Physique des Hautes Energies – Université Hassan II, Casablanca; (b) Centre National de l'Energie des Sciences Techniques Nucleaires, Rabat; (c) Faculté des Sciences Semlalia, Université Cadi Ayyad, LPHEA-Marrakech; (d) Faculté des Sciences, Université Mohamed Premier and LPTPM, Oujda; (e) Faculté des sciences, Université Mohammed V-Agdal, Rabat, Morocco*

136 *DSM/IRFU (Institut de Recherches sur les Lois Fondamentales de l'Univers), CEA Saclay (Commissariat a l'Energie Atomique), Gif-sur-Yvette, France*

137 *Santa Cruz Institute for Particle Physics, University of California Santa Cruz, Santa Cruz, CA, United States*

138 *Department of Physics, University of Washington, Seattle, WA, United States*

139 *Department of Physics and Astronomy, University of Sheffield, Sheffield, United Kingdom*

140 *Department of Physics, Shinshu University, Nagano, Japan*

141 *Fachbereich Physik, Universität Siegen, Siegen, Germany*

142 *Department of Physics, Simon Fraser University, Burnaby, BC, Canada*

143 *SLAC National Accelerator Laboratory, Stanford, CA, United States*

144 *(a) Faculty of Mathematics, Physics & Informatics, Comenius University, Bratislava, Slovak Republic; (b) Department of Subnuclear Physics, Institute of Experimental Physics of the Slovak Academy of Sciences, Kosice, Slovak Republic*

145 *(a) Department of Physics, University of Johannesburg, Johannesburg; (b) School of Physics, University of the Witwatersrand, Johannesburg, South Africa*

146 *(a) Department of Physics, Stockholm University; (b) The Oskar Klein Centre, Stockholm, Sweden*

147 *Physics Department, Royal Institute of Technology, Stockholm, Sweden*

148 *Departments of Physics & Astronomy and Chemistry, Stony Brook University, Stony Brook, NY, United States*

149 *Department of Physics and Astronomy, University of Sussex, Brighton, United Kingdom*

150 *School of Physics, University of Sydney, Sydney, Australia*

151 *Institute of Physics, Academia Sinica, Taipei, Taiwan*

152 *Department of Physics, Technion: Israel Institute of Technology, Haifa, Israel*

153 *Raymond and Beverly Sackler School of Physics and Astronomy, Tel Aviv University, Tel Aviv, Israel*

154 *Department of Physics, Aristotle University of Thessaloniki, Thessaloniki, Greece*

155 *International Center for Elementary Particle Physics and Department of Physics, The University of Tokyo, Tokyo, Japan*

156 *Graduate School of Science and Technology, Tokyo Metropolitan University, Tokyo, Japan*

157 *Department of Physics, Tokyo Institute of Technology, Tokyo, Japan*

158 *Department of Physics, University of Toronto, Toronto, ON, Canada*

159 *(a) TRIUMF, Vancouver, BC; (b) Department of Physics and Astronomy, York University, Toronto, ON, Canada*

160 *Faculty of Pure and Applied Sciences, University of Tsukuba, Tsukuba, Japan*

161 *Department of Physics and Astronomy, Tufts University, Medford, MA, United States*

162 *Centro de Investigaciones, Universidad Antonio Narino, Bogota, Colombia*

163 *Department of Physics and Astronomy, University of California Irvine, Irvine, CA, United States*

164 *(a) INFN Gruppo Collegato di Udine; (b) ICTP, Trieste; (c) Dipartimento di Chimica, Fisica e Ambiente, Università di Udine, Udine, Italy*

165 *Department of Physics, University of Illinois, Urbana, IL, United States*

166 *Department of Physics and Astronomy, University of Uppsala, Uppsala, Sweden*

167 *Instituto de Física Corpuscular (IFIC) and Departamento de Física Atómica, Molecular y Nuclear and Departamento de Ingeniería Electrónica and Instituto de Microelectrónica de Barcelona (IMB-CNM), University of Valencia and CSIC, Valencia, Spain*

168 *Department of Physics, University of British Columbia, Vancouver, BC, Canada*

169 *Department of Physics and Astronomy, University of Victoria, Victoria, BC, Canada*

170 *Department of Physics, University of Warwick, Coventry, United Kingdom*

171 *Waseda University, Tokyo, Japan*

172 *Department of Particle Physics, The Weizmann Institute of Science, Rehovot, Israel*

173 *Department of Physics, University of Wisconsin, Madison, WI, United States*

174 *Fakultät für Physik und Astronomie, Julius-Maximilians-Universität, Würzburg, Germany*

175 *Fachbereich C Physik, Bergische Universität Wuppertal, Wuppertal, Germany*

176 *Department of Physics, Yale University, New Haven, CT, United States*

177 *Yerevan Physics Institute, Yerevan, Armenia*

178 *Centre de Calcul de l'Institut National de Physique Nucléaire et de Physique des Particules (IN2P3), Villeurbanne, France*

[a] Also at Laboratorio de Instrumentacao e Fisica Experimental de Particulas – LIP, Lisboa, Portugal.
[b] Also at Faculdade de Ciencias and CFNUL, Universidade de Lisboa, Lisboa, Portugal.
[c] Also at Particle Physics Department, Rutherford Appleton Laboratory, Didcot, United Kingdom.
[d] Also at TRIUMF, Vancouver, BC, Canada.
[e] Also at Department of Physics, California State University, Fresno, CA, United States.
[f] Also at Novosibirsk State University, Novosibirsk, Russia.
[g] Also at Fermilab, Batavia, IL, United States.
[h] Also at Department of Physics, University of Coimbra, Coimbra, Portugal.
[i] Also at Department of Physics, UASLP, San Luis Potosi, Mexico.
[j] Also at Università di Napoli Parthenope, Napoli, Italy.
[k] Also at Institute of Particle Physics (IPP), Canada.
[l] Also at Department of Physics, Middle East Technical University, Ankara, Turkey.
[m] Also at Louisiana Tech University, Ruston, LA, United States.
[n] Also at Dep Fisica and CEFITEC of Faculdade de Ciencias e Tecnologia, Universidade Nova de Lisboa, Caparica, Portugal.
[o] Also at Department of Physics and Astronomy, University College London, London, United Kingdom.
[p] Also at Department of Physics, University of Cape Town, Cape Town, South Africa.
[q] Also at Institute of Physics, Azerbaijan Academy of Sciences, Baku, Azerbaijan.
[r] Also at Institut für Experimentalphysik, Universität Hamburg, Hamburg, Germany.
[s] Also at Manhattan College, New York, NY, United States.
[t] Also at CPPM, Aix-Marseille Université and CNRS/IN2P3, Marseille, France.
[u] Also at School of Physics and Engineering, Sun Yat-sen University, Guanzhou, China.
[v] Also at Academia Sinica Grid Computing, Institute of Physics, Academia Sinica, Taipei, Taiwan.
[w] Also at Laboratoire de Physique Nucléaire et de Hautes Energies, UPMC and Université Paris-Diderot and CNRS/IN2P3, Paris, France.
[x] Also at School of Physics, Shandong University, Shandong, China.
[y] Also at Dipartimento di Fisica, Università La Sapienza, Roma, Italy.
[z] Also at DSM/IRFU (Institut de Recherches sur les Lois Fondamentales de l'Univers), CEA Saclay (Commissariat a l'Energie Atomique), Gif-sur-Yvette, France.
[aa] Also at Section de Physique, Université de Genève, Geneva, Switzerland.

[ab] Also at Departamento de Fisica, Universidade de Minho, Braga, Portugal.
[ac] Also at Department of Physics and Astronomy, University of South Carolina, Columbia, SC, United States.
[ad] Also at Institute for Particle and Nuclear Physics, Wigner Research Centre for Physics, Budapest, Hungary.
[ae] Also at California Institute of Technology, Pasadena, CA, United States.
[af] Also at Institute of Physics, Jagiellonian University, Krakow, Poland.
[ag] Also at LAL, Université Paris-Sud and CNRS/IN2P3, Orsay, France.
[ah] Also at Nevis Laboratory, Columbia University, Irvington, NY, United States.
[ai] Also at Department of Physics and Astronomy, University of Sheffield, Sheffield, United Kingdom.
[aj] Also at Department of Physics, Oxford University, Oxford, United Kingdom.
[ak] Also at Institute of Physics, Academia Sinica, Taipei, Taiwan.
[al] Also at Department of Physics, The University of Michigan, Ann Arbor, MI, United States.
[am] Also at Discipline of Physics, University of KwaZulu-Natal, Durban, South Africa.
[*] Deceased.